UNIVERSITY OF CALIFORNIA, SAN DIEGO

New Peptide and Indole Alkaloid Based Marine Natural Products and a Novel Tool for Stereoassignment of Amino Acids

A Thesis Submitted in partial satisfaction of the requirements for the degree Master of Science

in

Chemistry

by

Mariam Nader Salib

Committee in charge:

Professor Tadeusz F. Molinski, Chair
Professor Michael D. Burkart
Professor Dionicio R. Siegel

2018

The Thesis of Mariam Nader Salib is approved, and it is acceptable in quality and form for publication on microfilm and electronically:

Chair

University of California, San Diego

2018

DEDICATION

To my incredible parents Nader and Nabila for giving me the opportunity to pursue my education and passion for chemistry: I would not have made it this far in my life without you. You have been there for me through it all.

Thank you.

TABLE OF CONTENTS

LIST OF FIGURES

LIST OF TABLES

LIST OF SCHEMES

LIST OF ABBREVIATIONS

NMR: Nuclear Magnetic Resonance
COSY: Correlation Spectroscopy
HSQC: Heteronuclear Single-Quantum Correlation Spectroscopy
HMBC: Heteronuclear Multiple-Bond Correlation Spectroscopy
NOESY: Nuclear Overhauser Effect Spectroscopy
TOCSY: Total Correlation Spectroscopy
FDAA: 1-fluoro-2,4-dinitrophenyl-5-L-alaninamide
FDLA: 1-fluoro-2,4-dinitrophenyl-5-L-leucinamide
FDVA: 1-fluoro-2,4-dinitrophenyl-5-L-valinamide
FDFA: 1-fluoro-2,4-dinitrophenyl-5-L-phenylalaninamide
FDPA: 1-fluoro-2,4-dinitrophenyl-5-L-propinamide
FDTA: 1-fluoro-2,4-dinitrophenyl-5-L-tryptophanamide
L-Val-DAA: (5-(((*S*)-1-amino-1-oxopropan-2-yl)amino)-2,4-dinitrophenyl)-L-valine
L-Ala-DTA: (5-(((*S*)-1-amino-3-(1*H*-indol-3-yl)-1oxopropan-2-yl)amino)-2,4-dinitrophenyl)-L-alanine
Ala: Alanine
Nva: Norvaline
Val: Valine
Leu: Leucine
Ile: Isoleucine
Met: Methionine
Phe: Phenylalanine
Tyr: Tyrosine
Pro: Proline
Ser: Serine
allo-Thr: *allo*-Threonine
Asn: Asparagine
Glu: Glutamic Acid
Asp: Aspartic Acid
Lys: Lysine
Orn: Ornithine
His: Histidine
Arg: Arginine
Cit: Citrulline
N-Me-Ala: *N*-Methylalanine
N-Me-Asp: *N*-Methylaspartic acid
Iso-Ser: Isoserine
allo-Ile: *allo*-Isoleucine

ACKNOWLEDGMENTS

Primarily, I would like to thank Dr. Ted Molinski for his innumerable help and support while completing my research. I would also like to acknowledge Matthew Jamison for mentoring and training me in the isolation and structural elucidation of marine natural products. I am grateful to Brendan Duggen and Anthony Mrse for advice on NMR measurements, and Yongxuan Su for HRMS (UCSD) measurements. I am also thankful to Zhixin Cao for his assistance with the preliminary isolation of *trans*-Herbindole A and Trikentramides E-I.

I would also like to thank my former lab mate Christopher Gartshore for his lightheartedness and his invaluable advice. I would like to thank my dear friend Bashayer Althufairi for making me laugh and helping me forget my problems even for a few minutes. I would like to thank my brothers Peter and Basim and my sister Nancy for being there for me when I needed them the most. Lastly, I would love to thank my best friend and sister Sarra – my travel companion through life – who has listened to all my complaints and given me innumerable advice. I could not have asked for a better friend.

Chapter 2, in part, is a reprint of the material as it appears in "Cyclic Hexapeptide Dimers, Antatollamides A and B, from the Ascidian *Didemnum Molle*. A Tryptophan-Derived Auxiliary for L- and D-Amino Acid Assignments" published in the Journal of Organic Chemistry, 2017, *82*, 10181-10187 by Salib, Mariam N.; Molinski, Tadeusz F. The thesis author was the primary investigator and author of this paper.

Chapter 3, in total, is a reprint of the material as it appears in "Six Trikentrin-like Cyclopentanoindoles from *Trikentrion flabelliforme*. Absolute Structural Assignment by NMR and ECD" published in the Journal of Organic Chemistry, 2018, *83*, 1278-1286 by Salib, Mariam N.; Molinski, Tadeusz F. The thesis author was the primary investigator and author of this paper.

ABSTRACT OF THE THESIS

New Peptide and Indole Alkaloid Based Marine Natural Products and a Novel Tool for Stereoassignment of Amino Acids

by

Mariam Nader Salib

Master of Science in Chemistry

University of California, San Diego, 2018

Professor Tadeusz F. Molinski, Chair

Two dimerized cyclic hexapeptides, antatollamides A (**146**) and B (**147**) were isolated from the colonial ascidian *Didemnum molle* collected in Pohnpei. The amino acid compositions and sequences were determined by interpretation of MS, 1D and 2D NMR data. Raney Ni reduction of antatollamide A cleaved the dimer to the corresponding monomeric cyclic hexapeptide with replacement of Cys by Ala. The amino acid configuration of **146** was established, after total hydrolysis, by derivatization with a new chiral reagent, (5-fluoro-2,4-dinitrophenyl)-N_{α}-L-tryptophanamide (FDTA), prepared from L-tryptophanamide, followed by LCMS analysis; all

amino acids were L-configured except for D-Ala. The FDTA reagent was developed as an alternate reagent to Marfey's reagent for the determination of the absolute configuration of amino acids. The improved resolution observed with FDTA is attributed to discrete π-cation interactions of the electron rich indole ring in Trp with the ammonium counterion in buffer.

Additionally, six new cyclopentano[*g*]indoles, *trans*-herbindole A (**147**) and trikentramides E-I (**155-159**), were isolated from a West Australian sponge, *Trikentrion flabelliforme* Hentschel, 1912 and their structures elucidated by integrated spectroscopic analysis. The compounds are analogs of previously described trikentrins, herbindoles and trikentramides from related Axinellid sponges. The assignment of absolute configuration of the new compounds was carried out largely by ECD – specifically, deconvolution of their Cotton effects by exploiting van't Hoff's principle of optical superposition – and by chemical interconversion of *trans*-herbindole A to trikentramide G and trikentramide G to trikentramides E, H and I.

CHAPTER ONE. INTRODUCTION

1.1 Marine Natural Products

Marine invertebrates are well-known sources of diverse natural products many with profound biological activities that present a significant source of drug leads in the pharmaceutical industry. For example, the potent antineoplastic agelastatins isolated from the sponges *Agelas dendromorpha* by Pietra and coworkers from the Coral Sea,[1] by Al-Mourabit's group from a specimen of *A. dendromorpha* collected in New Caledonia,[2] and from *Cymbastela* sp. gathered from the Indian Ocean by Molinski and colleagues.[3] Agelastatin A is moderately cytotoxic against various cancer cell lines[1,4a] and is suspected of causing an arrest in the G2-phase of the cell cycle.[4b]

The antiproliferative aplidine (plitidepsin), discovered from a temperate Atlantic species of *Aplidium*, is another natural product that is now in phase II and III trials for treatment of multiple myeloma and T-cell lymphoma.[5] The potential for new drug candidates has stimulated the interest of the entire scientific community and promoted the search for novel terrestrial and marine natural products in the hopes of discovering metabolites with a wide range of bioactivities.

Traditionally, microorganisms and terrestrial plants were the major source of new drug leads; however, recently marine invertebrates comprising tunicates, sponges and soft corals have attracted interest due to the structural diversity of both the species and marine natural products that is superior to terrestrial organisms.[6,7] The largely unexplored marine environment may provide structurally 'novel' natural products that may possess 'new' modes of action crucial to combating microbial resistance and treating life-threatening illnesses such as HIV and cancer.[8] Advances made in the last decade including the development of sampling devices to obtain inaccessible marine specimens, nanoscale NMR for structural elucidation, new reaction methodology for total

synthesis and in biotechnology for biosynthesis have been instrumental to the successful development of these often complex natural products as novel therapeutics.

1.2 Natural Products from the ascidian *Didemnum molle*

Various species of free-living cyanobacteria or those in symbiotic associations with ascidians are the sources of the unique family of cyanobactins or the ribosomal RNA-derived peptides.[9] The low molecular weight cyclic peptides are characterized by the presence of thiazole, thiazoline, oxazole and oxazoline rings in series with proteinogenic and nonproteinogenic amino acids. Cyanobactins are biosynthesized via amide coupling of the free amine of the N-terminal amino acid to the α-carbonyl group of the C-terminal amino acid. Proteolytic cleavage at the N- and C- terminus, macrocyclization followed by post-translational modifications such as heterocyclization and oxidation of cysteine, serine and threonine leads to the diverse family of cyanobactins.

The presence of "small, hypervariable cassettes" within the conserved biosynthetic pathway contributes to the chemical diversity observed within the cyanobactin family and may explain the presence of the exceptionally diverse families within the cyanobactins.[10] For example, the *pat* gene cluster consists of seven genes comprising *Pat*A - *Pat*G, five of which are essential for patallemide biosynthesis. The variable *Pat*E gene among each cluster encodes the amino acid sequences for two cyclic peptides such as the patellamides, ulithiacyclamides, and lissoclindamides. In some instances, the *Pat*E gene or specifically *Pat*E3, encodes the same primary sequence of amino acids for two peptides, which may then undergo post-translational modification to alter the stereochemistry and oxidation states. Additionally, Tianero and coworkers discovered that the biosynthetic diversity observed for the patellamides and trunkamides may arise

from the "relaxed substrate specificity" of the late-stage *tru* and *pat* enzymes that may catalyze "structurally divergent substrates" to produce a wide-range of diverse compounds.[11] Lin and coworkers further demonstrated that the chemical diversity observed within the cyanobactin family may also arise from the transfer of various enzymatic functions in identical biosynthetic pathways among the host and symbiont organism thereby expanding the range of post-translational chemistry possible.[12] The diverse cyanobactins appear to arise due to substrate changes and enzymatic exchanges that is reminiscent of medicinal chemistry in a diversity-generating biosynthetic model that enables both the host and symbiotic organism to adapt to environmental changes.

D. molle, a common Indo-Pacific colonial tunicate known for its symbiotic relationship with the cyanobacterium *Prochloron*, is the source of prenylated azole-containing peptides and ribosomal RNA-derived peptides. *D. molle* is a rich source of structurally diverse and bioactive cyclic peptides such as the comoramides and mayotamides,[13] didmolamides,[14] cyclodidemnamide,[15] and mollamides.[16] Comoramides A (**1**) and B (**2**) and the cyclic heptapeptides mayotamides A (**3**) and B (**4**) were isolated from a specimen of *D. molle* collected in the lagoon of Mayotte by Kashman and coworkers (Figure 1.1).[13] The prenylated comoramides A and B are identical except for the 5-methyloxazoline ring present in **1** that is replaced with a free threonine in **2** leading to the hypothesis that **2** may be the biogenic precursor of **1**. Mayotamides A and B possess the same amino acid sequence except for the replacement of isoleucine in **3** with valine in **4**. Interestingly, special care had to be taken with the isolation of "highly air- and acid-sensitive" **3** and **4** to prevent the air oxidation of the methionine methyl group.

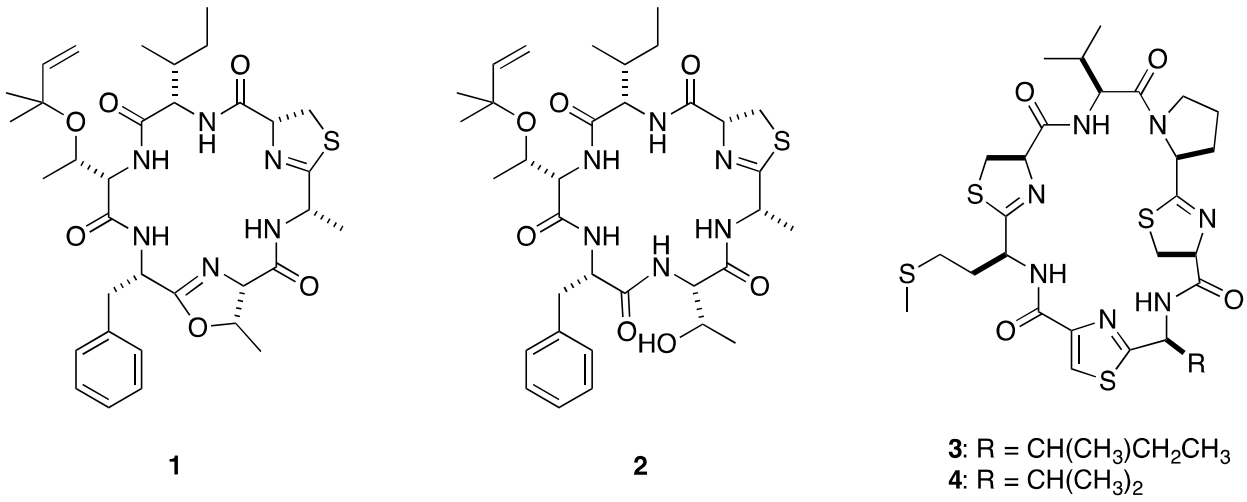

Figure 1.1: Structures of comoramides A (**1**) and B (**2**), and mayotamides A (**3**) and B (**4**).

Rudi and coworkers[14] also reported the isolation of the cyclic hexapeptides didmolamides A (**5**) and B (**6**) from a specimen of *D. molle* collected in Madagascar (Figure 1.2). As observed with comoramides A and B, didmolamides A and B are identical bar for the replacement of the 5-methyloxazoline ring in **5** with threonine in **6** indicating that threonine is the likely biogenic predecessor of the methyloxazoline ring via dehydration as in **1** and **2**.

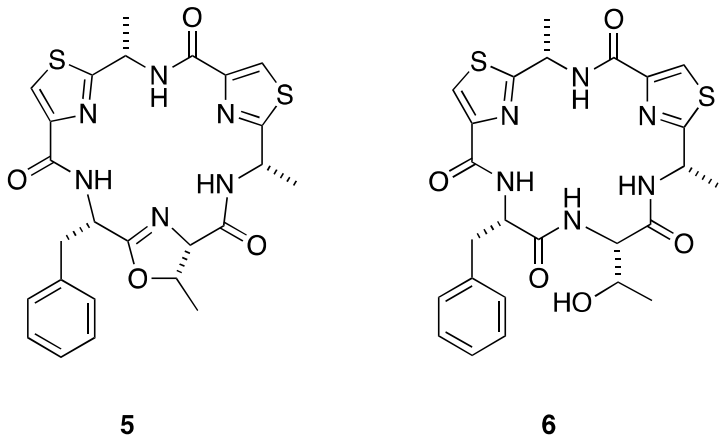

Figure 1.2: Structures of didmolamides A (**5**) and B (**6**).

Toske and Fenical[15] also reported the isolation of the cyclic heptapeptide cyclodidemnamide (**7**) from the marine ascidian *D. molle* collected in the Philippine Islands (Figure 1.3). The absolute configuration of cyclodidemnamide was determined after the hydrolysis

of the peptide, derivatization of the individual amino acids with pentafluoropropionic anhydride followed by GC-MS analysis to give the absolute assignment as depicted with **7**. Yet, Boden and coworkers[17] discovered during the total synthesis of cyclodidemnamide that the assignment of C-15-(*S*)-Val stereocenter didn't correlate with the synthetic-**7**'s NMR data. Consequently, the authors reassigned the C-15 center as (*R*)-Val as depicted in **8**, and confirmed the assignment with the total synthesis of **8** starting with the (R)-Val enantiomer. The characterization data of the synthetic **8** were identical with those reported for the natural product originally isolated from *D. molle* leading Boden et. al. to conclude that during the hydrolysis of the original cyclodidemnamide, the thiazole-valine unit underwent epimerization as previously observed with thiazole and thiazoline based amino acids under acidic and basic conditions.[18]

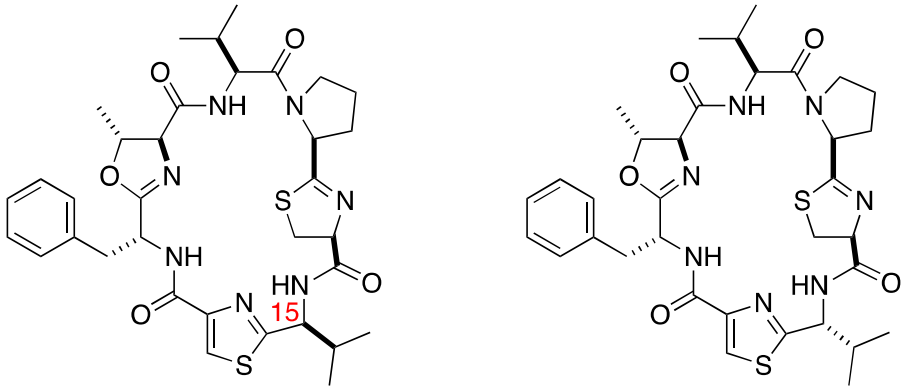

7: Original **8**: Corrected

Figure 1.3: The original (**7**) and corrected (**8**) structures of cyclodidemnamide.

Additionally, a cluster of cytotoxic cyclic hexa- and hepta- peptides known as the mollamides have been isolated from *D. molle*. The mollamides are a rare collection of cyclopeptides containing a reversed prenyl unit attached to an L-Ser or L-Thr residue (Figures 1.4 and 1.5). The first cyclic heptapeptide mollamide (**9**) was isolated by Carrol and coworkers from a sample of *D. molle* collected from the Great Barrier Reef, Australia.[16a] Mollamides B (**10**) and C (**11**) as well as keenamide A (**12**) were also isolated from *D. molle* collected in Manado Bay,

Indonesia.[16b] Mollamide C and keenamide A share an identical structure with the replacement of a thiazole unit in **11** with a thiazoline in **12**. Interestingly, Keenamide A has previously been isolated from the motaspidean mollusk *Pleurobranchus forskalii* collected in Manado, Indonesia that is known to feed on the ascidian *D. molle*.[19]

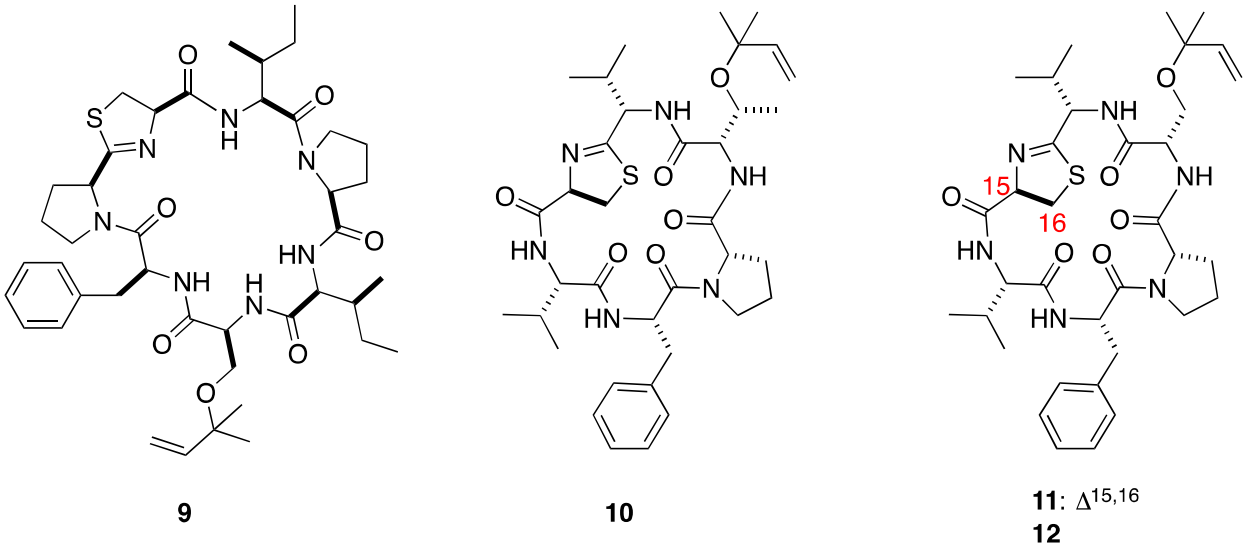

Figure 1.4: Structures of mollamide (**9**), mollamides B (**10**) and C (**11**), and keenamide A (**12**).

Mollamides E (**13**) and F (**14**) were isolated by Ireland and Wagoner from a species of *D. molle* collected in New Britain, Papua New Guinea (Figure 1.5).[16c] While mollamide E contains the inverted prenyl group attached to L-Thr, it's replaced by L-Ile in mollamide F. Interestingly, both the Ser-Pro peptide bond in mollamide E and the Pro2-Pro1 segment in mollamide F adopt the *cis* geometry based on the large chemical shift differences between C_β and C_γ.

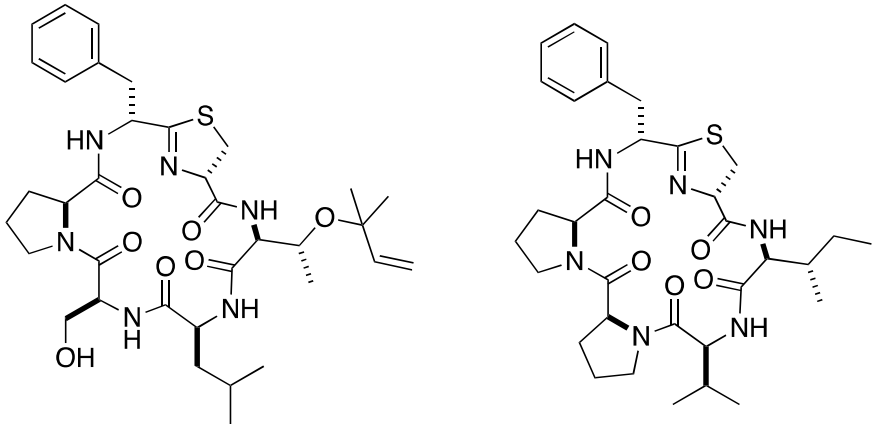

13 **14**

Figure 1.5: Structures of mollamides E (**13**) and F (**14**).

The structures of the peptides were elucidated through exhaustive 1D and 2D NMR analysis and chemical degradation to the individual amino acids. The assignment of the absolute configuration of the amino acids was determined directly by chiral HPLC of the hydrolyzed amino acids or after derivatization of the amino acids with pentafluoropropionic anhydride or 1-fluoro-2,4-dinitrophenyl-5-L-alaninamide (FDAA). Direct comparison to authentic or derivatized amino acids gave the amino acid configurations. Although, the relative structure of mollamide was determined by NMR analysis, it was confirmed through X-ray crystallography. The absolute structure was obtained after hydrolysis and derivatization with FDAA.

1.2.1 Similar Peptides from Other Sponges

The heptapeptides lissoclinamides 1-10 (**15**-**24**), ulicyclamide (**25**)[20], and the octapeptides patellamides A-G (**26**-**32**)[20b,c,21] and ulithiacyclamides (**33**-**37**)[21d,22] are examples of cyanobactins isolated from the ascidian *Lissoclinum patella* (Figure 1.6) in which threonine and two cysteines are cyclized to oxazoline and thiazoline or thiazole, respectively. Patellamide G and ulithiacyclamide E-G contain free threonine while the ulithiacyclamides contain two additional

cysteines as a disulfide bridge. The biosynthesis of the biologically active and diverse peptides has been attributed to the obligate symbiont *Prochloron* spp as supported by the work of Schmidt and coworkers who sequenced, isolated and expressed the patellamides A and C gene cluster.[23]

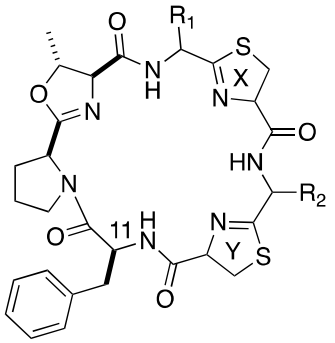

15 Lissoclinamide 1 R_1=L-Val, R_2=D-Ile, X=Y=Thiazole
16 Lissoclinamide 2 R_1=D-Ile, R_2=D-Ala, X=Thiazoline, Y=Thiazole
17 Lissoclinamide 3 R_1=D-Ile, R_2=L-Ala, X=Thiazoline, Y=Thiazole
18 Lissoclinamide 4 R_1=L-Val, R_2=D-Phe, X=Thiazoline, Y=Thiazole
19 Lissoclinamide 5 R_1=L-Val, R_2=D-Phe, X=Y=Thiazole
20 Lissoclinamide 6 R_1=D-Val, R_2=D-Phe, X=Thiazoline, Y=Thiazole
21 Lissoclinamide 7 R_1=D-Val, R_2=D-Phe, X=Y=Thiazole
22 Lissoclinamide 8 R_1=Val, R_2=Phe, X=Thiazoline, Y=Thiazole
23 Lissoclinamide 9 R_1=L-Ile, R_2=D-Val, X=Thiazoline, Y=Thiazole, 11-(*R*)
24 Lissoclinamide 10 R_1=R_2=L-Ile, X=Y=Thiazoline, 11-(*R*)
25 Ulicyclamide R_1=L-Ile, R_2=D-Ala, X=Y=Thiazole

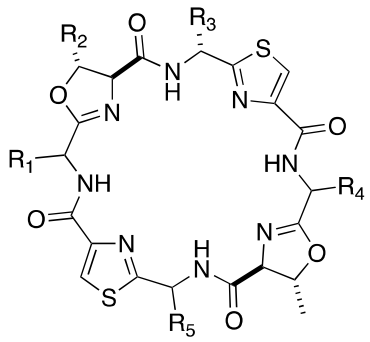

26 Patellamide A R_1=R_4=L-Ile, R_2=, R_3=R_5=D-Val
27 Patellamide B R_1=L-Leu, R_2=Me, R_3=Me, R_4=L-Ile, R_5=D-Phe
28 Patellamide C R_1=L-Val, R_2=Me, R_3=Me, R_4=L-Ile, R_5=D-Phe
29 Patellamide D R_1=R_4=D-Ile, R_2=Me, R_3=Me, R_5=D-Phe
30 Patellamide E R_1=L-Val, R_2=Me, R_3=D-Val, R_4=D-Ile, R_5=D-Phe
31 Patellamide F R_1=R_4=L-Val, R_2=Me, R_3=D-Val, R_5=D-Phe

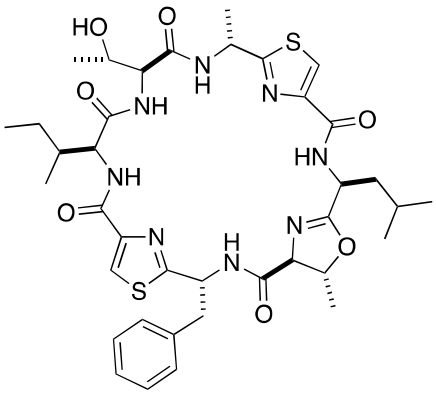

32 Patellamide G

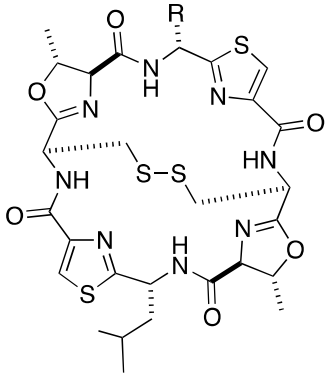

33 Ulithiacyclamide R=Leu
34 Ulithiacyclamide B R=Phe

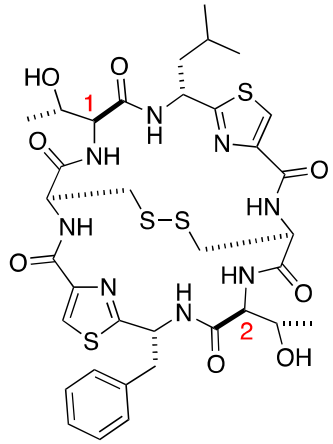

35 Ulithiacyclamide E
36 Ulithiacyclamide F: Oxazoline at 2
37 Ulithiacyclamide G: Oxazoline at 1

Figure 1.6: Structures of lissoclinamide 1-10 (**15-24**), ulicyclamide (**25**), patellamide A-G (**26-32**), and the ulithiacyclamides (**33-37**).

Additional cyanobactins include the heptapeptides axinastatin 1-5 isolated from *Axinella* sp. by Pettit and coworkers,[24] stylissamide A-H isolated from *Stylissa caribica*,[25] and hymenamides A-F and octapeptides hymenamides G-K isolated from *D. molle* and *Hymeniacidon* sp. (Figure 1.7).[26] The cyclic peptides comprise proteinogenic amino acids occasionally containing free serine and threonine. Interestingly, the proline amino acids appear conserved in cyclic peptides lacking heterocyclized amino acids.[9] The hexapeptides bistratamide A-J, and octapeptides haliclonamide A-E were isolated from *Lissoclinum bistratum* and *Haliclona* sp., respectively. Unlike the axinastatin, stylissamides, and hymenamides, the bistratamides and haliclonamides contain oxidized serine, threonine and cysteine as thiazoline, oxazoline and oxazole.

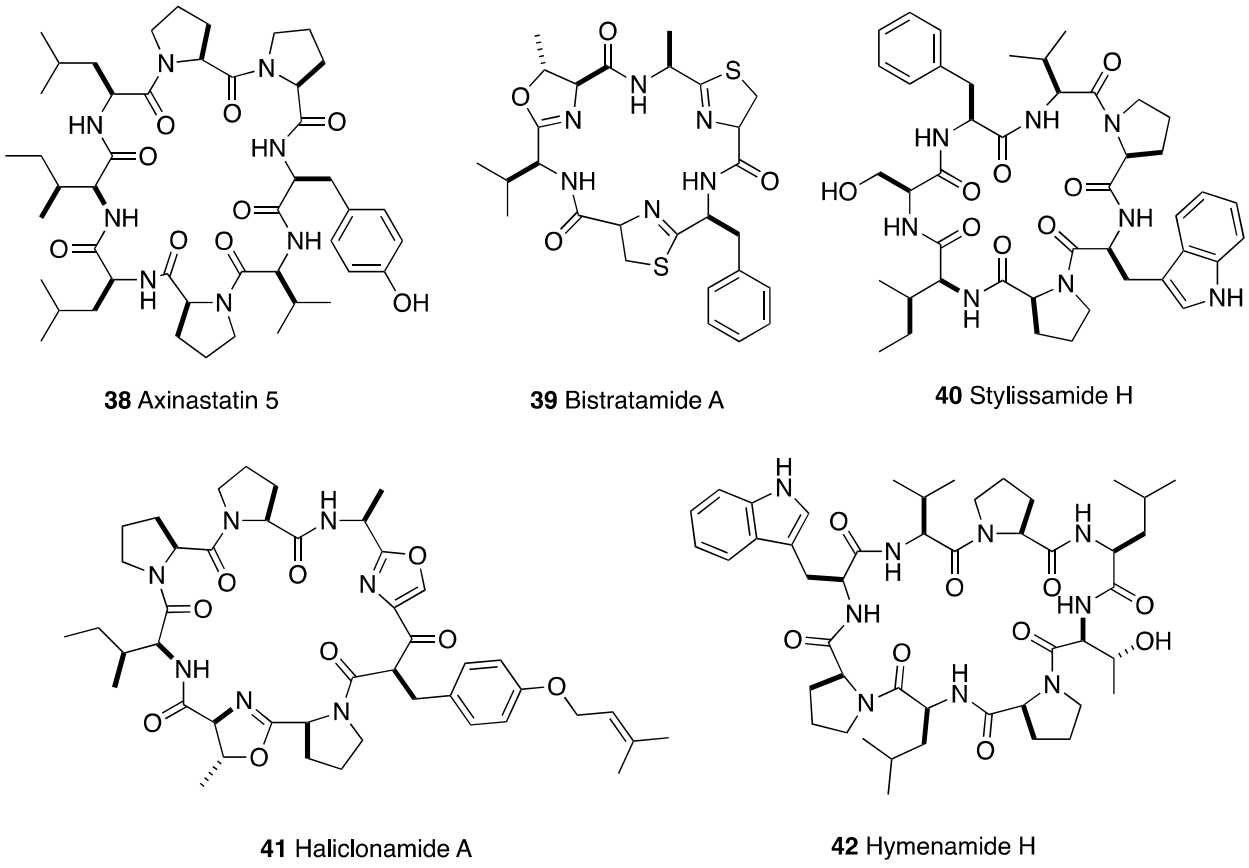

Figure 1.7: The structures of various cyanobactins including axinastatin 5 (**38**), bistratamide A (**39**), stylissamide H (**40**), haliclonamide A (**41**) and hymenamide H (**42**).

Remarkably, while the various specimens of the ascidian *D. molle* were collected from numerous locations throughout the world, the similarities of the thiazole-, oxazole- and thiazoline-containing peptides as well as the peculiar reverse-prenylated ethers of threonine or serine residues imply that the biosynthesis of these metabolites is shared by a common symbiotic organism. Müller et. al. isolated *Prochloron* cells from *D. molle* and *D. fulgens* and demonstrated that the absence of the *Prochloron* organism eliminated the strong cytotoxic activity of the methanol extracts of the sponge against L5178y mouse lymphoma cells.[27] The biosynthetic genes responsible for the synthesis of several cyanobactins have been identified and described from the cyanobacteria *Prochloron*, *Trichodesmium*, *Microcystis*, *Nostoc*, *Lyngbya*, and *Anabaena*.[9]

Additionally, Schmidt and coworkers identified the patellamide biosynthetic gene cluster in the obligate cyanobacteria *Prochloron* spp. that is responsible for the synthesis of the patellamides.[23] They also discovered PatD2, which is similar to hydrolases involved in the cyclization of cysteine and threonine residues to form thiazoline and oxazoline amino acids, respectively. Furthermore, the authors were able to obtain patellamides A and C after expressing the entire pathway in *Escherichia coli*. Moreover, Donia et. al. analyzed 46 prochloron-containing didemnid ascidians, and discovered a diverse library of patellamides.[10] Subsequently, Donia and coworkers engineered a *patEdm* gene and isolated a novel cyclic peptide, eptidemnamide, that is similar to the anticoagulant eptifibatide with replacement of the disulfide bridge with an amide. The aforementioned research supports the hypothesis that the cyanobactins are likely biosynthesized by an obligate or symbiotic organism in association with the host ascidian.

1.2.2 Biological Roles

A broad range of bioactivities have been observed for the structurally diverse cyanobactins. Comoramides A (**1**) and B (**2**), and mayotamides A (**3**) and B (**4**) exhibited mild cytotoxicity

against several cultured tumor cell lines including A549, HT29 and MEL-28 with IC_{50} values of 5-10 μg/mL.[13] Cyclodidemnamide (**8**) displayed weak cytotoxicity against HCT116 (human colon tumor cells) with an ED_{50} of 16 μg/mL.[15] The cyclic heptapeptide mollamide (**9**) inhibited RNA synthesis at an IC_{50} of 1 μg/mL and displayed moderate cytotoxic activity against several cultured cell lines including P388 (murine leukemia at 1 μg/mL), A549 (human lung carcinoma at 2.5 μg/mL), HT29 (human colon carcinoma), and CV1 (monkey kidney fibroblast).[16a] Similarly, mollamide B (**10**) demonstrated cytotoxicity against various cultured cancer cell lines including H460 (non-small cell lung), MCF7 (breast), and SF268 (CNS) as well as significant growth inhibition of the aforementioned cell lines.[16b] In contrast, *in vitro* disk diffusion assay revealed that mollamide C (**11**) displayed no selectivity against solid tumors. Interestingly, both mollamide B (**10**) and F (**14**) are structurally analogous to dolastatin 3 and similarly displayed anti-HIV activity.[16b,c] Mollamide B exhibited an EC_{50} of 48.7 μg/mL against HIV-1 in human PMB cells while mollamide F inhibited HIV integrase activity.

The structural similarities of the lissoclinamides 4-5 (**18**-**19**) and 7-8 (**21**-**22**) provided insight into the structure-activity relationship of these four peptides.[28] The four lissoclinamides share the same amino acid sequence with minor differences in the stereochemistry and the presence of thiazole in the place of thiazoline. Interestingly, the authors discovered that lissoclinamide 7, which contains two thiazole rings, is a more potent *in vitro* cytotoxic agent than didemnin B against the cultured cell lines MRC5CV1 (human fibroblast) and T24 (bladder carcinoma) with an IC_{50} of 0.04 μg/mL in comparison to the IC_{50} of 0.046 μg/mL for didemnin B after the exposure of cultured tumor cells to the compounds for 1 hour. The findings appear to imply that the overall conformation of the compound plays a more important role in the function of the molecule than the simple presence of the heterocycles.

Although, patellamides B and C (**27**-**28**) reduced drug resistance by ~ tenfold against vinblast-resistant CCRF-CEM human leukemic lymphoblasts with an IC_{50} of 12 nM, patellamides A (**26**) and G (**32**) and ulithiacyclamides E-G (**35**-**37**) are inactive modulators of drug resistance.[21d] Additionally, the lissoclinamides, ulicyclamide, patellamides and ulithiacyclamides exhibited cytotoxicity against various cultured cancer cell lines. Furthermore, the cytostatic axinastatins 2-4 strongly inhibited the cell growth of cultured cell lines including P388 (lymphocytic leukemia), OVCAR-3 (ovarian), SF-295 (CNS), A498 (renal), NCI-H460 (lung-NSC), KM20L2 (colon) and SK-MEL-5 (melanoma) at GI_{50} values less than 0.4 μg/mL.[24b,c] As evidenced by the above-mentioned cytotoxic activities, the structurally distinct cyanobactins display a broad range of bioactivities that is dependent on the chemical structure of the individual peptides that further influences their selectivity in activity. Moreover, not all cyanobactins demonstrate cytotoxicity and that may be due to the limited testing of these molecules. The emergence of structurally diverse peptides with differing bioactivities is an evolving coping mechanism that both the host and symbiotic organism utilize to survive environmental changes as well as predators. Advantageously, the bioactive cyanobactins serve as drug leads and potential therapeutics.

1.3 Development of Marfey's Reagent and its Variants – FDAA

An important aspect of structure elucidation of natural products deals with determining the absolute configuration of all the stereocenters in a molecule. In the case of peptides or amino acid containing natural products, the stereochemistry is determined by the well-known Marfey's method that relies on the different retention times of diastereoisomers to differentiate derivatized amino acids. By comparison with standards, the absolute configuration of each amino acid is

determined. The method of Marfey's reagent relies on HPLC, GC or LC-MS, requires small quantities of hydrolysate and provides relatively quick results.

Marfey's reagent, 1-fluoro-2,4-dinitrophenyl-5-L-alaninamide (FDAA), was originally developed by Peter Marfey in 1984.[29] It's synthesized via the S_NAr coupling of L-alaninamide with 1,5-difluoro-2,4-dinitrobenzene in acetone at room temperature in 76% yield (Scheme 1.1). The decidedly stable FDAA displays strong UV absorption at 340 nm due to the highly absorbing benzene chromophore. The reactive aromatic fluoride in FDAA reacts via nucleophilic substitutions with the free amino group of proteinogenic and non-proteinogenic amino acids to form diastereoisomers. FDAA allows for the separation and quantitation of said diastereoisomers by HPLC at the nanomole range as observed by the linear relationship between %D-area and %D-isomer in solution.

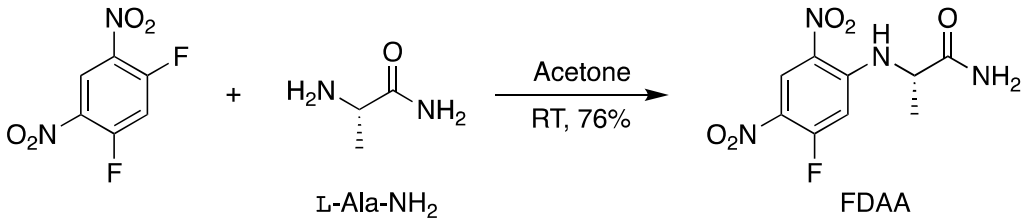

Scheme 1.1: The synthesis of FDAA via S_NAr coupling.

The Marfey's reagent provides good resolution for neutral amino acids and shows improved resolution and increased the retention times as the alkyl sidechain length of the amino acids increases. However, while the method affords good resolution for the L- and D-diastereoisomers of non-polar amino acids, it provides relatively poor resolution for some hydroxyl- and *N*-Me- amino acids as well as mixed results with some non-proteinogenic amino acids.[30] For example, the separation times of Asp and Glu are small relative to the retention times of the neutral amino acids Met, Phe and Ala due to the ionization of the sidechains of the amino

acids. Asn and Gln display even poorer resolution due to the relatively short retention times while Ser shows the worst resolving power due to the presence of the hydroxyl group.

Fujii and coworkers proposed a mechanism of separation for L- and D-Val-DAA.[30b] The authors observed that generally the L-diastereoisomers elute first with the exception of Orn, His, Cit and *N*-Me Asp, and proposed that the structures of L- and D-Val-DAA are planar with a three-ring system similar to anthracene based on analysis of NOESY data as depicted in Figure 1.8. Strong NOEs were observed between the α-protons of valine, the L-alaninamide of DAA and H-6 of the benzene ring whereas none were observed among H-6 and the protons of the isopropyl group of valine or the methyl of L-alaninamide. Consequently, the authors proposed D-Val-DAA possesses a *cis* (Z)-type arrangement that has the two hydrophobic groups, the isopropyl of the valine and the methyl of L-alaninamide, on the same plane of the dinitrobenzene while L-Val-DAA occupies a *trans* (E)-type arrangement. DAA derivatives of the *cis*-type arrangement interact more strongly with the ODA silica gel and have longer retention time than the *trans*-type arrangement. In most amino acids, the sidechain substituent is more hydrophobic than the carboxyl group with the D-amino acid possessing the *cis*-type arrangement leading to the L-amino acid eluting first and implying that the retention time and elution order are dependent on the difference in the hydrophobicity of α-carboxyl group and sidechain of the amino acid.

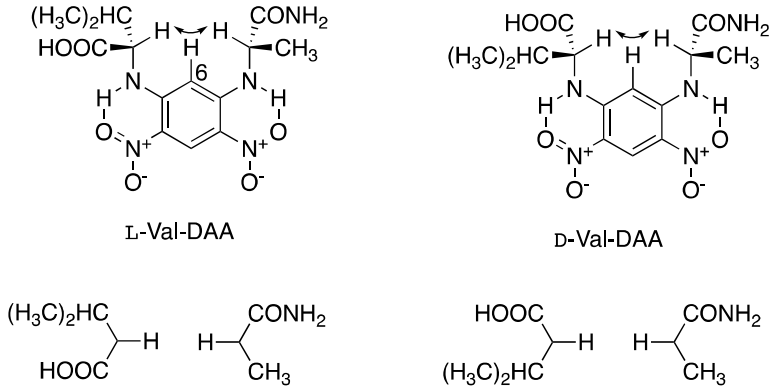

Figure 1.8: Proposed structure of L- and D-Val-DAA with NOE.

It has been observed that the resolution is improved by changing the α-amino chiral auxiliary group in the derivatizing reagent from L-alaninamide to L-leucinamide (FDLA), L-valinamide (FDVA), L-phenylalaninamide (FDFA) or L-prolinamide (FDPA, Figure 1.9).[30a,31] The increased hydrophobicity of the α-amino chiral auxiliary increases the retention times and enables the resolution of 19 diastereoisomers of neutral, acidic, basic or aromatic DL-proteinogenic amino acids as compared to FDAA. L-Valinamide and L-leucinamide variants increased the Δt_R significantly compared to the original Marfey's reagent and the other variants.

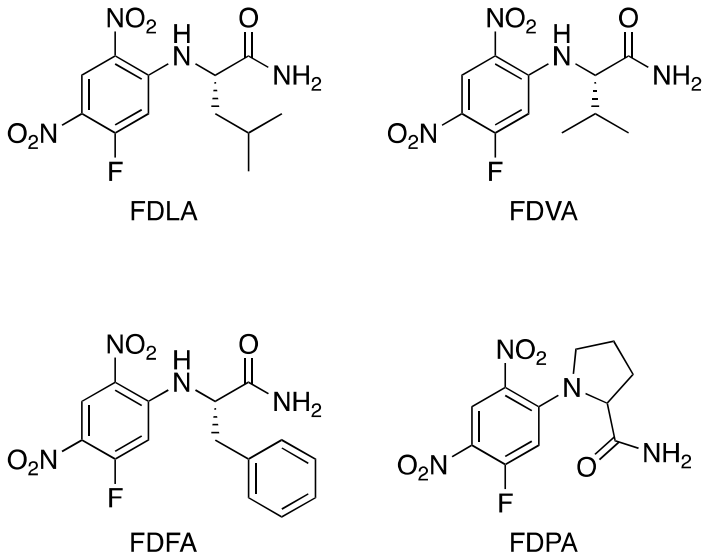

Figure 1.9: Structures of L-leucinamide, L-valinamide, L-phenylalaninamide and L-prolinamide variants of Marfey's reagent.

1.4 Natural Products from the Sponges *Trikentrion flabelliform* and *Trikentrion loeve*

The majority of marine indole alkaloids are derived from secondary metabolism of tryptophan. The indigo derivative, 'Tyrian purple' (**43**, 6,6'-dibromoindigotin), from the hypobranchial gland of various marine mollusks primarily *Murex* and *Thais*, has been known since ancient times:[32] contemporary studies revealed its structure through X-ray crystallography (Figure 1.10).[33] Still rarer are simple indoles that lack carbon substitution at C-3; their structures imply

biosynthesis that diverges substantially from tryptophan metabolism. In a study by Brennan and Erickson, one of the first investigations of red algae, 10 achiral polyhalogenated indoles were reported from *Rhodophyllis membranacea* Harvey, and more recent studies of *R. membranacea* have delivered another 18 new analogs including **44**-**46**.[34] Interestingly, all the polyhalogenated indoles possess antifungal activities.

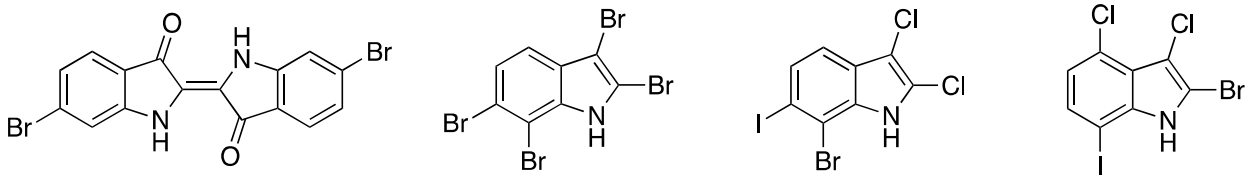

43 Tyrian Purple **44** **45** **46**

Figure 1.10: Structures of Tyrian Purple (**43**), and polyhalogenated indoles **44**-**46**.

Among the more curious natural indoles are unique, optically active cyclopenta[*g*]indoles from two Axinellid sponges (Figure 1.11). Capon and MacLeod described (+)-*cis*- and (+)-*trans*-trikentrins A (**47**, **48**), (–)-*trans*-trikentrin B (**50**) and an inseparable mixture of *cis*- and iso-*trans*-trikentrin B (**49** and **51**, respectively) from *Trikentrion flabelliforme* Hentschel, 1912, collected in Darwin, Australia.[35] All the compounds exhibited antimicrobial activities against the gram-positive bacteria *Bacillus subtillis* as determined by a disc diffusion assay.

Additionally, Scheuer and coworkers characterized the trikentrin homologs, (–)-herbindoles A-C (**52**-**54**), from a specimen of *Axinella* sp. collected in Exmouth Gulf, Western Australia.[36] The latter compounds are antipodal in configuration to the *cis*-trikentrins as established through independent total syntheses of *ent*-(–)-**47**, (+)-**48**,[37] and *ent*-(+)-**52**–**53** by Natsume and coworkers,[38] and of (+)-**50** by Kanematsu and coworkers.[39] The herbindoles displayed cytotoxic activity against KB cells (nasopharyngeal carcinoma) at IC_{50} values of 5 μg/mL, >10 μg/mL, and 10 μg/mL for herbindoles A (**52**), B (**53**), and C (**54**), respectively, and were found to deter feeding against wrasses, triggerfishes and sergeant majors at 48.1 ± 10% relative to 80.8 ± 6.4% for the

control when tested with squid. Lastly, (+)-Trikentramides A-D (**55-58**), isolated and characterized by Quinn and coworkers from a specimen of *T. flabelliforme* collected at Port Hedland (500 km from Exmouth), are isatin and oxindole analogs of (+)-*cis*- and (+)-*trans*-trikentrins A.[40]

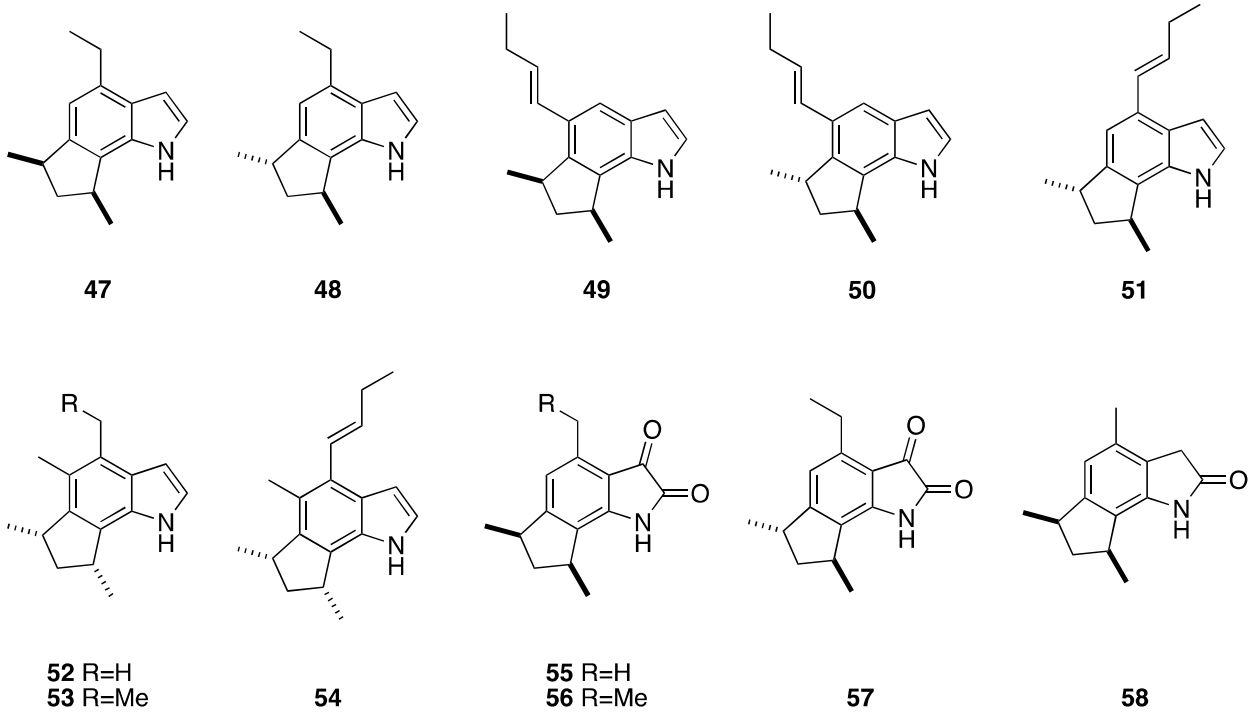

Figure 1.11. The structures of the trikentrins A-B (**47-51**), herbindoles A-C (**52-54**) and trikentramides A-D (**55-58**).

Clardy and co-workers reported the isolation of the unusual pyrrole trikentramine (**59**) from the sponge *Trikentron loeve* Carter from the Senegalese coast whose structure was identified via NMR analysis and X-ray crystallography (Figure 1.12).[41] Loukaci and Guyot also studied *T. loeve* collected along the coast of Senegal and discovered the unusual anti-HIV, red pigment Trikendiol (**60**), which is likely the oxidized product of trikentramine.[42] In all likelihood, the biosynthesis of the polyhalogenated indoles in red alga is linked to the enduring natural history of indole, indoxyl, indigo dye, and other indigoid compounds from plants of the genus *Indigofera* and, as shown through genetic and ecological studies, bacterial biosynthesis.[43] On the other hand, the origin of

the sponge-derived 1,3-dimethylcyclopenta[*g*]indoles must differ considerably from the latter. To date, no hypotheses for the origin of **47**–**60** have been advanced.

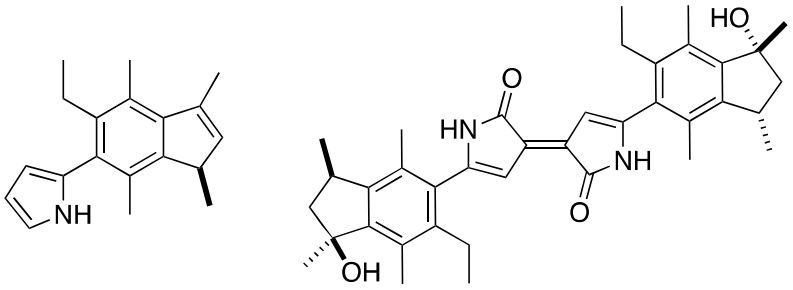

59 **60**

Figure 1.12: The structures of trikentramine (**59**) and trikendiol (**60**).

1.4.1 Enantioselective Syntheses of Trikentrins and Herbindoles

Quite a few total syntheses of the trikentrins and herbindoles have been reported since the late 1980s;[44] yet, only a few syntheses including those reported by Natsume, Kanematsu and Sato were asymmetric and those syntheses will be reviewed here. Natsume and coworkers reported the first asymmetric syntheses of various trikentrins and herbindoles utilizing indolization of pyrroles starting from suitable reactants with the appropriate substituents contingent on the structure of the natural product.[37,38] Kanematsu and colleagues employed an intramolecular Diels-Alder reaction of allenic dienamides to build the indole ring in their synthesis of (+)-*cis*-trikentrin B.[39] Sato and coworkers used a transition-metal-catalyzed intramolecular [2+2+2] cyclization of ynamide with diynes to construct the indole and achieve the synthesis of (−)-herbindoles A-C.[45]

In 1989, Muratake and Natsume utilized the indolization of pyrroles to enantioselectively synthesize (−)-*cis*- and (−)-*trans*- trikentrin A (**47**-**48**) as depicted in Scheme 1.2.[37a] Oxidative cleavage of (*R*)-(+)-pulegone with $KMnO_4$ gave the (*R*)-3-methyladipic acid. Esterification and

Dieckmann condensation of the acid formed an inseparable mixture of the cyclopentanones **61**-**62**. α-Methylation followed by decarboxylation yielded another inseparable mixture of the dimethylcyclopentanones **63**-**66**. Trimethylsilylation of the ketones **63**-**66** followed by condensation of the silyl ethers **67**-**68** with the endoperoxide **69** of 1-benzenesulfonylpyrrole afforded the chiral 3,5-dimethyl-2-pyrrolylcyclopentanones as two groups of mixtures of **70** (4 isomers) and **71**-**72** (1:4) in 19% and 37%, respectively. Silva et. al. proposed a mechanism for the condensation of the silyl enol ethers **67**-**68** with the endoperoxide **69**.[44] Silyl enol ether attack on an *in-situ* pre-formed organotin intermediate is followed by aromatization via elimination and loss of SnO_2 to result in a mixture **71**-**72**. Treatment of **71**-**72** with the azo-enolate 2-butanone *N,N*-dimethylhydrazone (**73**) enabled the elongation of the sidechain by four carbons and gave **74** in 61% yield. Indole cyclization was achieved by reaction of the pyrrole **74** with sulfuric acid, in which hydrolysis of the hydrozone, intramolecular attack of the pyrrole onto the carbonyl group followed by aromatization through dehydration gave the indole **76** in 73% yield. Alkaline Hydrolysis with KOH gave (−)-*cis*-trikentrin A (**47**) and (−)-*trans*-trikentrin A (**48**) in 52% and 37%, respectively.

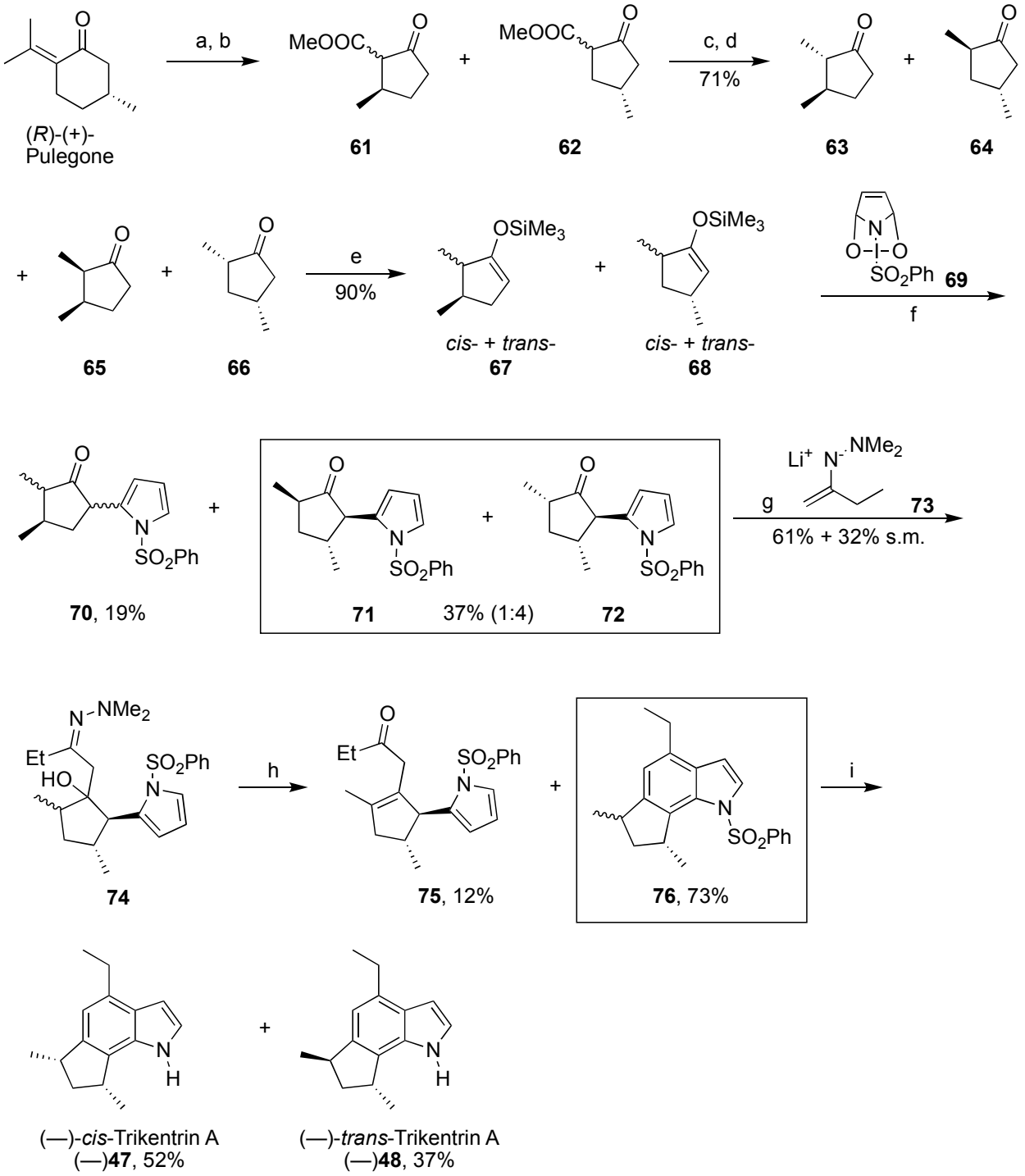

Scheme 1.2: The asymmetric synthesis of (–)-*cis*-Trikentrin A [(–)-**47**] and (–)-*trans*-Trikentrin A [(-)-**48**] by Muratake and Natsume (1989). Reagents and conditions: (a) $KMnO_4$; (b) (i) H^+, MeOH; (ii) $NaNH_2$; (c) (i) NaOMe, MeOH, -18 ºC, 1 hr.; (ii) MeI, -18 ºC, 14.5 hr.; (d) 47% HBr, 120 ºC, 6 hr.; (e) LDA, THF, TMSCl, -80 ºC, 15 min.; (f) $SnCl_2$, EtOAc, -40 ºC to -47 ºC, 1 hr. to rt, 1.5 hr.; (g) toluene/Et_2O (1:1), -75 ºC to -65 ºC, 1 hr.; (h) 6.5% H_2SO_4, 2-propanol, reflux, 14 hr.; (i) 20% KOH in DME/MeOH/H_2O (1:1:1), 85–90 ºC, 6.5 hr.

Natsume's group also published the asymmetric syntheses of (+)-*cis*-, (+)-*trans*-, and *iso*-*trans*- trikentrin B and (+)-herbindoles A-C.[37c] The starting material for all the syntheses was (3*R*,5*S*)-3,5-dimethyl-1-cyclopentenyl methanol (**77**), which was prepared in eight steps from the ester **87** (Scheme 1.3). A Diels-Alder condensation of cyclopentadiene with the ester **87** gave the Diels-Alder adduct **88**. Transesterification of **88** with dilute base resulted in the carboxylic acid that was transformed into the *tert*-butyl ester **89** in 60% yield. Substitution of the bromide atom with the benzyloxy group followed to give **90** in 87%. Oxidation of **90** with catalytic OsO_4 in the presence of trimethylamine *N*-oxide gave the diol **91** that was further oxidized with sodium metaperiodate to give the dialdehyde as an intermediate. The dialdehyde was immediately treated with ethanethiol and boron trifluoride to produce the bisdithioacetal **92** in 76%. Reductive desulfurization of **92** with Raney Nickel followed by treatment with potassium *tert*-butoxide afforded the α,β-unsaturated ester **93** in 76%. DIBAL reduction of the ester **94** gave the carbinol **77** in 96% yield. The transesterification of the *tert*-butoxy ester **93** to the methoxy ester **94** was necessary to eliminate the undesired reduction of the double bond that was occurring concurrently with the reduction of the ester.

In the synthesis of (+)-*cis*- and (+)-*trans*- trikentrin B, the first step involved the Claisen rearrangement of the alcohol **77** with the olefin **78** to form the unsaturated ester **79** in 87% yield. Condensation of **79** with 3-formyl-1-(phenylsulfonyl)pyrrole (**80**) in the presence of LDA gave **81** in quantitative yield. Oxidative cleavage of the exocyclic double bond of **81** with OsO_4 and sodium periodate unmasked the ketone group that was directly treated with *p*-toluenesulfonic acid to construct the indole in an acid-catalyzed cyclization and aromatization. Separation of the indole mixture **82** by HPLC followed by reduction of the ester to the alcohol gave **83** and **84** in 73% and 17% yield, respectively. Oxidation of the primary alcohol to the aldehyde with MnO_2 followed by

nucleophilic addition to the aldehyde with *n*-propylmagnesium bromide gave each respective secondary alcohol. Dehydration of the resulting secondary alcohols with *p*-toluenesulfonic acid and deprotection of the N-phenylsulfonyl group with KOH resulted in (+)-*cis*- and (+)-*trans*-trikentrin B as identified by MS, ^{1}H and ^{13}C NMR, IR and $[\alpha]_D$.

Scheme 1.3: The asymmetric synthesis of (+)-*cis*-Trikentrin B [(+)-**49**] and (+)-*trans*-Trikentrin B [(-)-**50**] by Natsume and coworkers (1993). Reagents and conditions: (a) *t*-BuCOOH, $MeC(OEt)_3$, toluene, sealed tube, 150 ºC, 8 hr.; (b) (i) LDA, THF, -68 ºC, 40 min.; (ii) -78 ºC, 40 min.; (c) (i) OsO_4, $NaIO_4$, THF, H_2O, rt, 18 hr.; (ii) PTSA, PhSH, reflux, 4 hr.; (d) $LiAlH_4$, THF, -20 ºC, 10 min. to 0 ºC, 2 hr.; (e) MnO_2, CH_2Cl_2, rt, 1.5 hr.; (f) *n*-PrMgBr, THF, -20 C, 20 min.; (g) C_6H_6, PTSA, reflux, 0.5 hr.; (h) KOH, DME/MeOH/H_2O (1:1:1), reflux, 3 hr. Box: (i) (i) NaOH, DME, MeOH, 0 ºC, 1 hr.; (ii) CH_2Cl_2, H_2SO_4, isobutene, -20 ºC, 2 hr to rt, 48 hr.; (j) (i) NaH, benzylic alcohol, THF, 0 ºC, 20 min.; (ii) 0 ºC, 3 hr.; (k) OsO_4, triethylamine *N*-oxide, rt, 15 hr.; (l) (i) $NaIO_4$, THF, H_2O, 0 ºC, 1 hr.; (ii) CH_2Cl_2, EtSH, $BF_3 \bullet Et_2O$, 0 ºC, 18 hr.; (m) (i) Raney nickel W-2, DME, reflux, 2 hr.; (ii) THF, *t*-BuOK, 0 ºC, 1 hr.; (n) H_2SO_4, MeOH, reflux, 3 hr.; (o) DIBAL, hexane, -65 ºC.

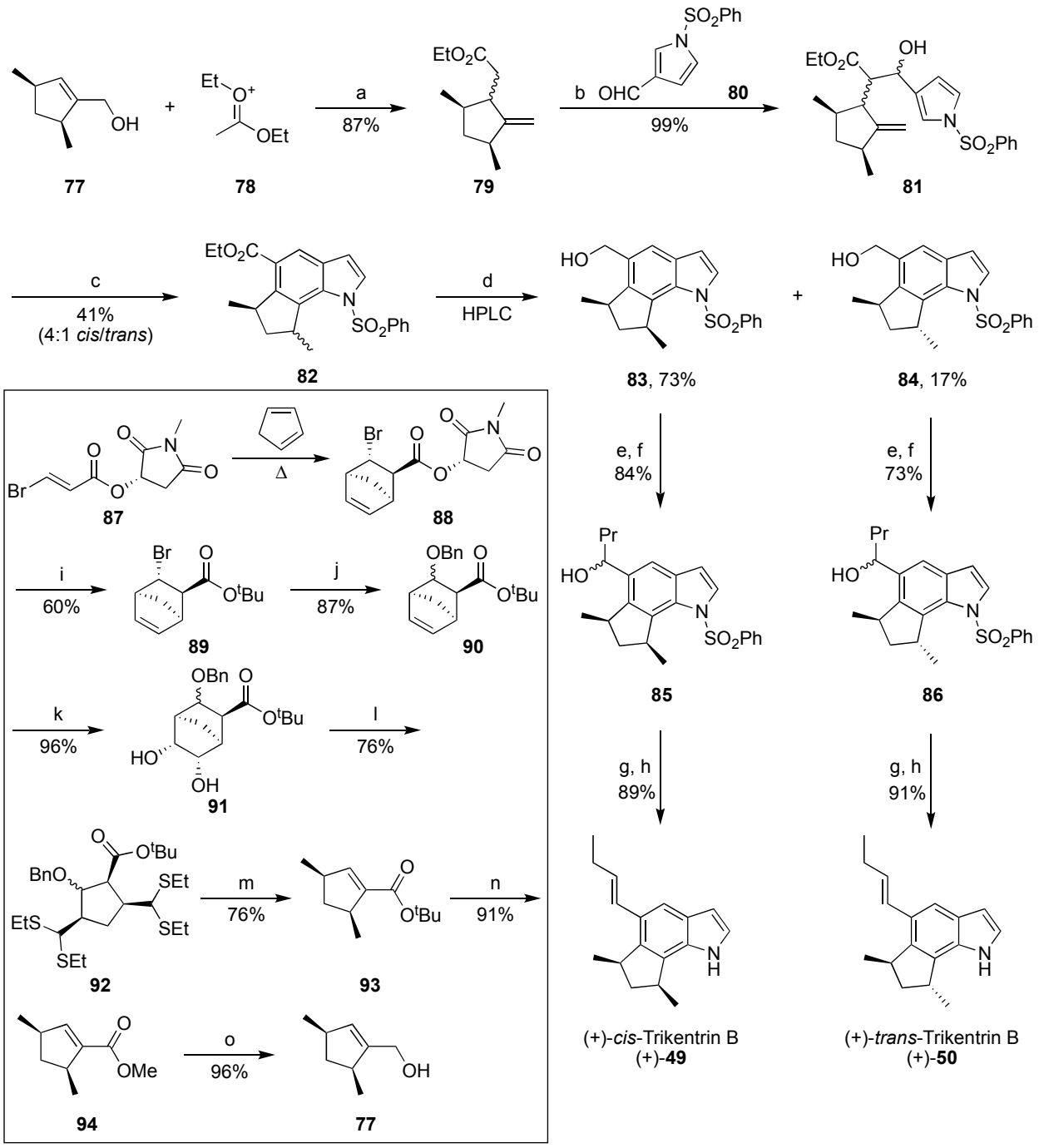
77
78
a
87%
79
b OHC
80
99%
81
c
41%
(4:1 cis/trans)
82
d
HPLC
83, 73%
84, 17%
e, f
84%
e, f
73%
85
86
g, h
89%
g, h
91%
(+)-cis-Trikentrin B
(+)-49
(+)-trans-Trikentrin B
(+)-50
87
88
i
60%
89
j
87%
90
k
96%
91
l
76%
92
m
76%
93
n
91%
94
o
96%
77

The synthesis of the *iso*-*trans*-trikentrin B followed a similar route as the synthesis of (+)-*cis*- and (+)-*trans*- trikentrin B as shown in Scheme 1.4. Oxidation of the secondary alcohol of **81** with MnO_2 followed by deethoxycarbonylation with dilute NaOH gave **95** in 66%. Addition of the phenylsulfonylmethyl group to yield **96** was achieved after reaction of **95** with phenylsulfonylmethyl lithium. Oxidative cleavage of the exocyclic double bond with catalytic OsO_4 in the presence of excess sodium metaperiodate furnished the ketone **97** that was subjected to an acid-catalyzed cyclization with *p*-toluenesulfonic acid to form the *cis*- and *trans*- indole derivatives **98** and **99** in 44% and 16%, respectively, after separation by HPLC. Treatment of the *trans*-**99** with allyltrimethylsilane elongated the carbon chain to give **100** in 91%. The final product (6*R*,8*R*)-*iso*-*trans*-trikentrin B was obtained after isomerization of the double bond of **100** with rhodium chloride and hydrolysis of the phenylsulfonyl group with KOH.

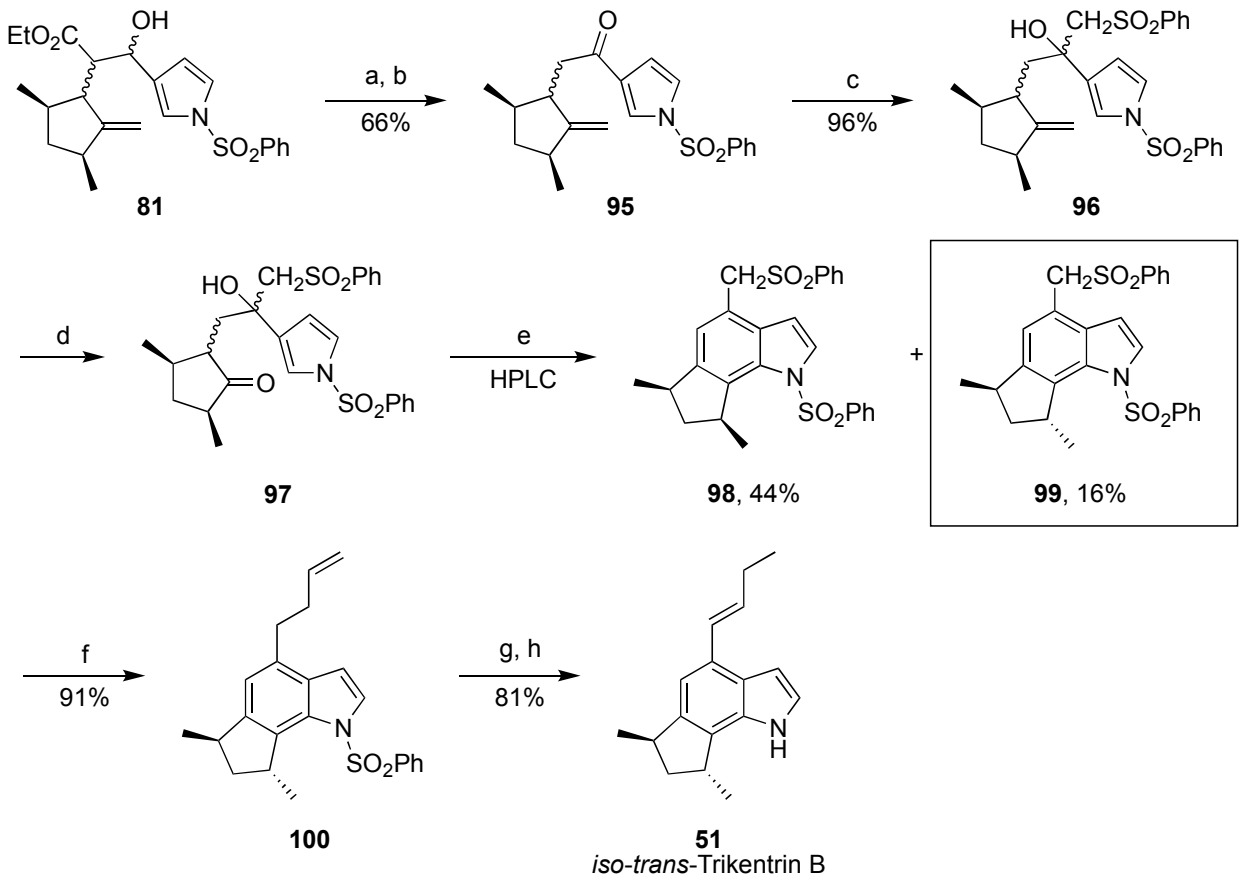

Scheme 1.4: The asymmetric synthesis of *iso-trans*-Trikentrin B [**51**] by Natsume and coworkers (1993). Reagents and conditions: (a) MnO_2, reflux, 2 hr.; (b) (i) NaOH, DME/MeOH/ H_2O (1:2:1), reflux, 3 hr.; (ii) $PhSO_2Cl$, THF, DMF, NaH, 0 ºC, 2 hr.; (c) $PhSO_2CH_2Li$, THF, BuLi, -73 ºC, 20 min. to -20 ºC, 30 min.; (d) OsO_4, $NaIO_4$, THF, H_2O, rt, 19 hr.; (e) $PhCH_2SH$, PTSA, reflux, 1.5 hr.; (f) allylTMS, $EtAlCl_2$, CH_2Cl_2, -20 ºC; (g) EtOH, $RhCl_3$, sealed tube, 100 ºC, 50 hr.; (h) KOH, DME/MeOH/H_2O (1:1:1), reflux, 3 hr.

The enantioselective synthesis of (+)-herbindoles A-C followed a parallel route as the trikentrin syntheses (Scheme 1.5). The intermediate **101** was obtained via Claisen condensation of **77** with **78**. As discussed previously, enolization and nucleophilic addition of **101** with the pyrrole **80** afforded the alcohol **102**. Oxidation of **102** with MnO_2, deexthoxycarbonylation of the resulting **103**, nucleophilic addition of phenylsulfonylmethyl to the carbonyl of **104** followed by oxidation of the exocyclic double bond of **105** with OsO_4 and excess sodium metaperiodate and acid-catalyzed cyclization and aromatization gave the indole intermediates **106** and **107** in 15% and 45% yield, respectively. Reduction of the phenyl sulfonyl and deprotection of the N-phenyl

sulfonyl of the *cis*-indole **107** was achieved in one step with metallic magnesium in the presence of ammonium chloride to produce (+)-herbindole A in 85% yield. (+)-Herbindole B was obtained after benzylic substitution to a methyl group with $AlMe_3$ and removal of the N-phenylsulfonyl protecting group. (+)-Herbindole C was obtained in 43% yield after three steps from the *cis*-**107** via alkylation with allyltrimethylsilane, isomerization of the double bond and deprotection.

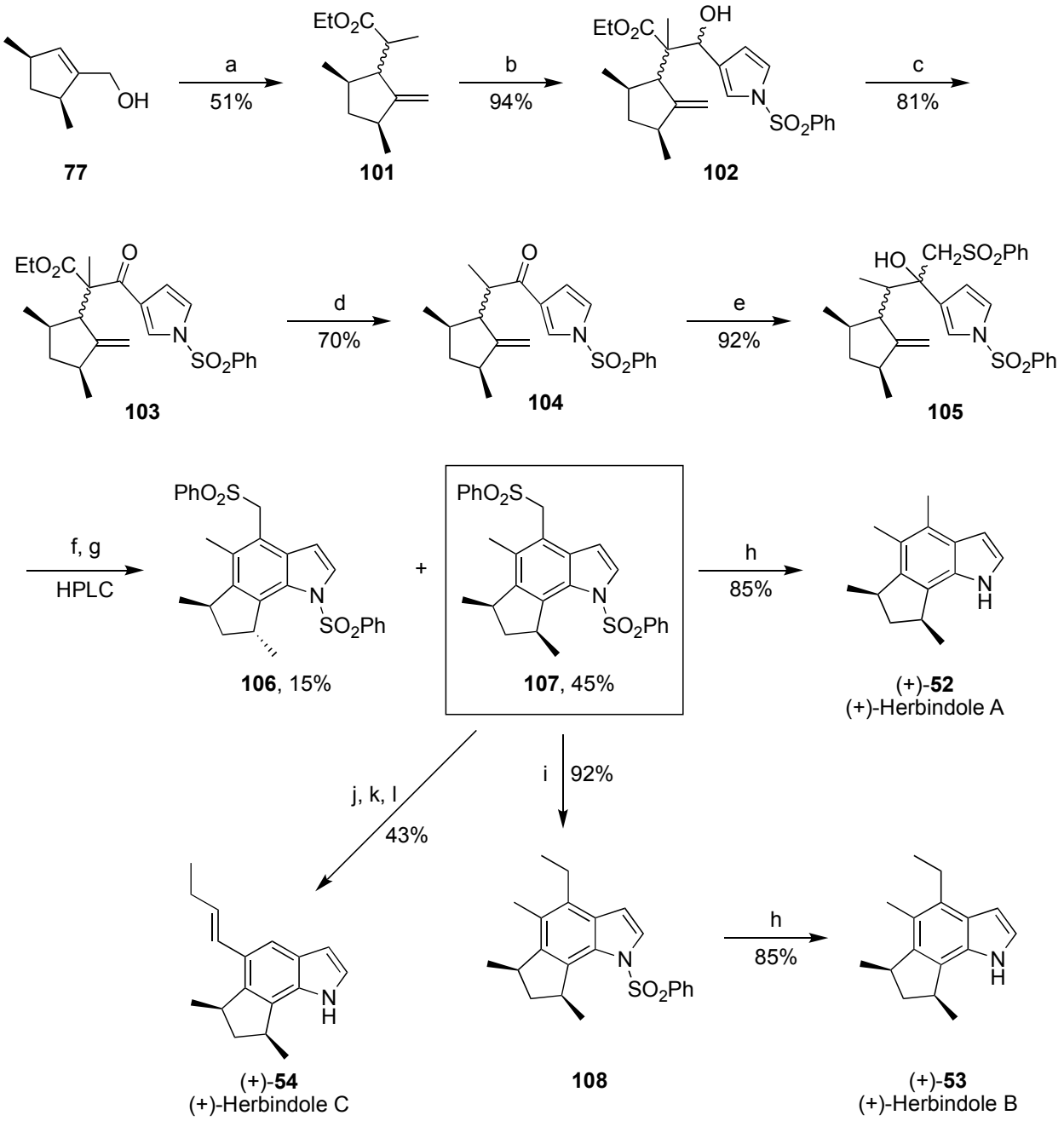

Scheme 1.5: The asymmetric synthesis of (+)-Herbindole A [(+)-**52**], (+)-Herbindole B [(+)-**53**] and (+)-Herbindole C [(+)-**54**] by Natsume and coworkers (1994). Reagents and conditions: (a) $EtC(OEt)_3$, *t*-BuCOOH, toluene, reflux, 3 hr.; (b) (i) LDA, THF, -65 ºC, 40 min.; (ii) **80**, -78 ºC, 40 min.; (c) MnO_2, CH_2Cl_2, rt, 1.5 hr.; (d) LiCl, HMPA/H_2O, 130 ºC, 24 hr.; (e) $PhSO_2CH_2Li$, THF, BuLi, -73 ºC, 20 min, -20 ºC, 30 min.; (f) OsO_4, $NaIO_4$, THF, H_2O, rt, 19 hr.; (g) PTSA, PhSH, toluene, reflux 5 hr.; (h) Mg, NH_4Cl, MeOH, rt, 2 hr.; (i) $AlMe_3$, CH_2Cl_2, 0 ºC, 1 hr.; (j) allyltrimethylsilane, $EtAlCl_2$, CH_2Cl_2, -20 ºC, 20 min.; (k) RhI_3, EtOH, 100 ºC, 50 hr.; (l) KOH, DME/MeOH/H_2O (1:1:1), reflux, 6 hr.

Natsume and coworkers also reported several other racemic syntheses of all the trikentrins

that are similar to the routes described above. Fundamentally, the enantioselective syntheses accomplished by Natsume were essential for the assignment of the absolute configuration of the trikentrins and herbindoles. Kanematsu and coworkers also achieved the synthesis of (+)-*cis*-trikentrin B via an intramolecular Diels-Alder reaction of the allenic dienamide to construct the tricyclic backbone.[39] Kanematsu first introduced the aforementioned strategy in his racemic synthesis of *cis*-trikentrin B, and further developed it for the asymmetric synthesis as illustrated in Scheme 1.6. The synthesis of (+)-*cis*-Trikentrin B was accomplished via Nucleophilic addition of *n*-propyl to **109**, oxidative cleavage and functional group transformation of **110** followed by a Diels-Alder cyclization and aromatization of **111** derived from the norbornene derivative **113**.

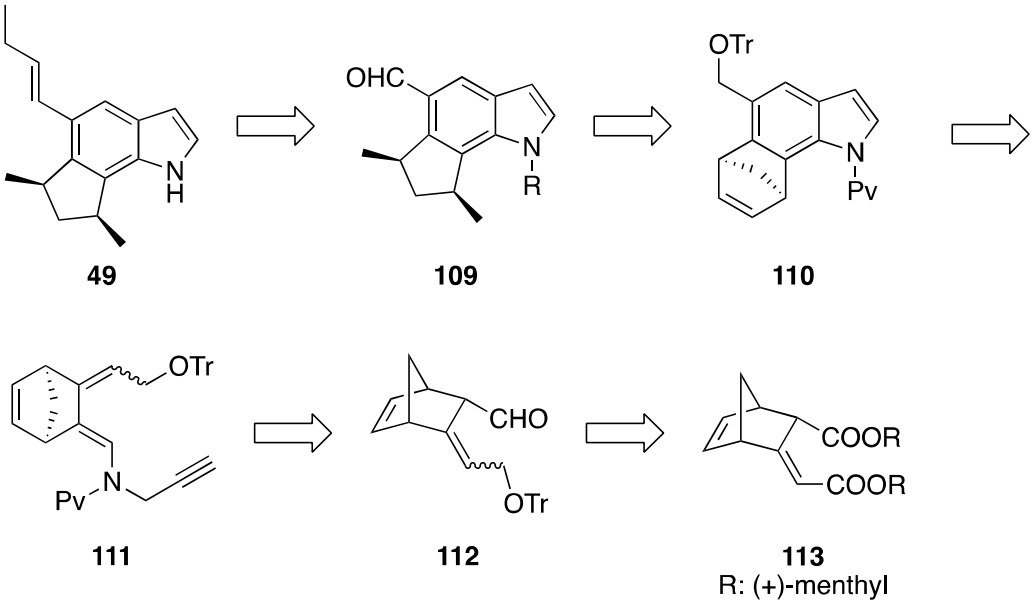

Scheme 1.6: The retrosynthesis of (+)-*cis*-Trikentrin B [(+)-**49**] via an intramolecular Diels-Alder reaction as described by Kanematsu and coworkers (1995).

The key intermediate **188** was synthesized from the norbornene synthon **113** that was prepared via a Diels-Alder reaction of cyclopentadiene with allene-1,3-dicarboxylate. Reduction of the synthon **113** gave the diol **114** in 93%. Selective oxidation of the allylic alcohol afforded the carboxylic acid that underwent an intramolecular cyclization to form the tricyclic lactone **115**.

Hydrolysis of the lactone with LiOH followed by esterification with Shioiri's reagent afforded the allylic carboxylic ester **116** in 54%. TBS-protection of the primary alcohol of **116** followed by DIBAL reduction gave **117** in 94%. Trityl-protection of the allylic alcohol of **117** followed by TBAF deprotection afforded the important intermediate **118** in 84%. Oxidation of the primary alcohol of **118** with PCC to the aldehyde, treatment of the aldehyde with proparglamine to the enamine that was immediately reacted with pivaloyl chloride in the presence of collidine formed the propargylic intermediate **111** in 41%. Crabbe homologation of **111** afforded the optically active allene **119** in 56%. Diels-Alder cyclization in refluxing toluene followed by aromatization gave the indole (+)-**110**. Dihydroxylation of (+)-**110** with catalytic OsO_4 in the presence of NMO followed by oxidation of the resulting secondary alcohols with sodium metaperiodate gave the corresponding dialdehyde in 88%. Reduction and pyrrole deprotection of **121** with $NaBH_4$, mesylate-protection of the primary alcohols followed by reduction of the dimesylate **122** gave the dimethyl intermediate (+)-**123**. N-acetate protection of the pyrrole, trityl-deprotection with camphorsulfonic acid and MnO_2 oxidation of the subsequent alcohol gave the aldehyde (+)-**124** in 65%. Nucleophilic addition of *n*-propylmagnesium bromide to the aldehyde, elimination of the resulting secondary alcohol with *p*-toluenesulfonic acid, and pyrrole-deprotection with $NaBH_4$ afforded (+)-*cis*-trikentrin B as identified by HR-MS, ^{1}H and ^{13}C NMR, IR and ECD.

Scheme 1.7: The asymmetric synthesis of (+)-*cis*-Trikentrin B [(+)-**49**] by Natsume and coworkers. Reagents and conditions: (a) DIBAL, CH_2Cl_2, -78 ºC to 0 ºC; (b) Ag_2CO_3, Celite, benzene, reflux; (c) LiOH, THF, H_2O; (d) $TMSCHN_2$, MeOH, benzene; (e) TBDMSCl, imidazole, DMAP, CH_2Cl_2; (f) DIBAL, CH_2Cl_2, -78 ºC; (g) TrCl, Et_3N, DMAP, CH_2Cl_2; (h) TBAF, THF; (i) PCC, CH_2Cl_2; (j) propargylamine, MS 4 Å, Et_2O; (k) pivaloyl chloride, 2,4,6-collidine, CH_2Cl_2, rt; (l) HCHO, i-Pr_2NH, CuBr, 1,4-dioxane, reflux; (m) toluene, 160 ºC; (n) MnO_2, CH_2Cl_2, rt; (o) OsO_4, NMO, pyridine, Et_2O, 1,4-dioxane; (p) $NaIO_4$, THF, H_2O, rt; (q) $NaBH_4$, MeOH, rt; (r) MsCl, Et_3N, Et_2O, 0 ºC; (s) Zn, NaI, DME, reflux; (t) CH_3COCl, NaH, 18-crown-6, THF, rt; (u) camphorsulfonic acid, MeOH, THF, rt; (v) MnO_2, CH_2Cl_2, rt; (w) n-PrMgBr, THF, 10 C; (x) p-TsOH, benzene, 50 ºC; (y) $NaBH_4$, MeOH, rt.

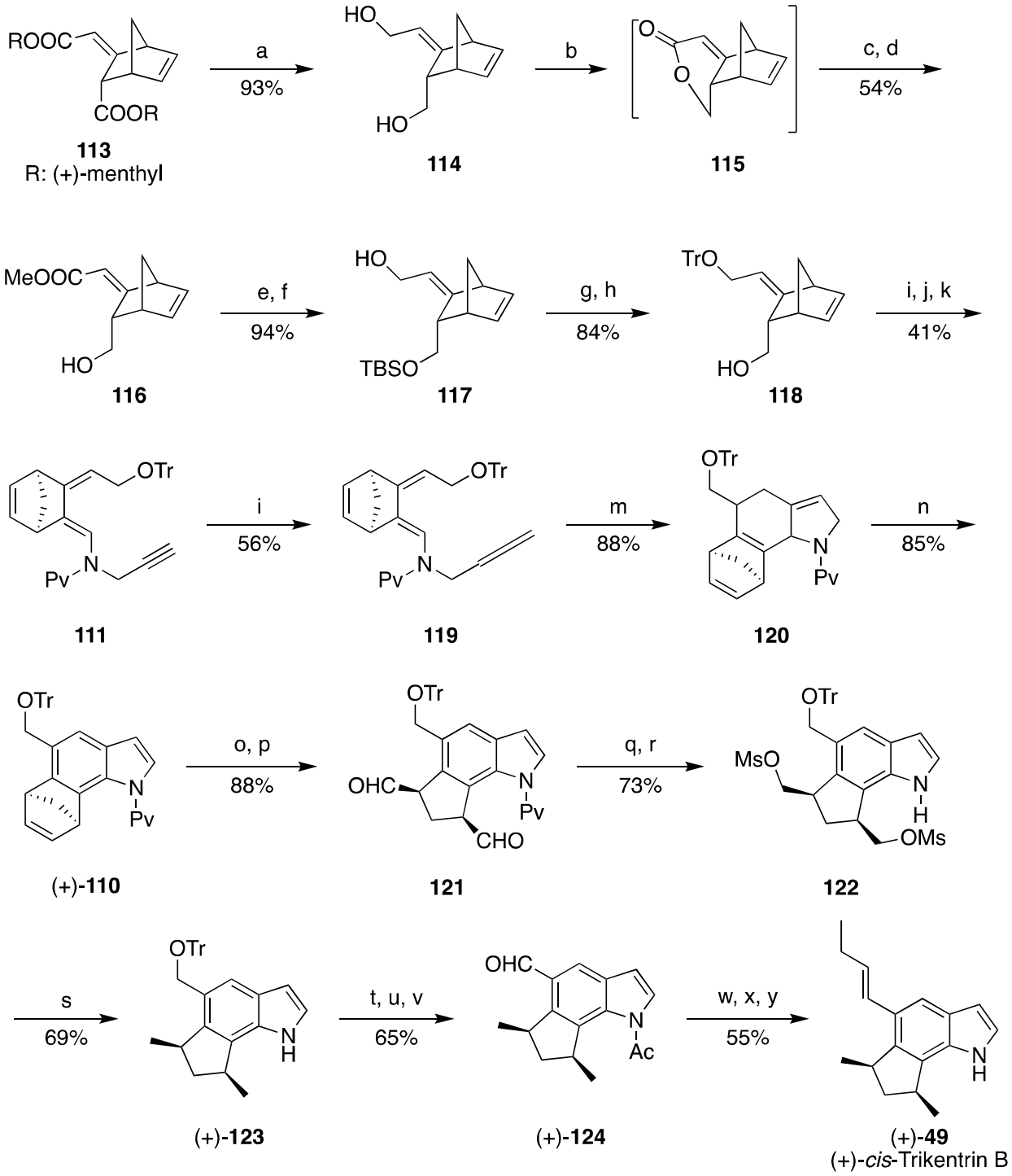
ROOC
COOR
a
93%
HO
HO
b
O
O
c, d
54%
113
R: (+)-menthyl
114
115
MeOOC
HO
e, f
94%
HO
TBSO
g, h
84%
TrO
HO
i, j, k
41%
116
117
118
OTr
Pv
N
i
56%
OTr
Pv
N
m
88%
OTr
N
Pv
n
85%
111
119
120
OTr
N
Pv
o, p
88%
OTr
OHC
N
Pv
CHO
q, r
73%
OTr
MsO
N
H
OMs
(+)-110
121
122
s
69%
OTr
N
H
t, u, v
65%
OHC
N
Ac
w, x, y
55%
N
H
(+)-123
(+)-124
(+)-49
(+)-cis-Trikentrin B

Additionally, Sato and coworkers published the first asymmetric synthesis of (–)-herbindoles A-C via a transition-metal catalyzed intramolecular [2+2+2] cyclization of two alkynes and an ynamide.[45] The retrosynthesis of (–)-herbindoles A-C is described in scheme 1.8. All three of the herbindoles were synthesized from the key indoline derivative **125** whose rings were constructed via [2+2+2] intramolecular cyclization of **126**. Synthesis of the dialkynylynamide **126** was achieved via C-N coupling of the bromoalkyne **127** with the corresponding ynamide **135**. The bromoalkyne **127** was obtained through a Corey-Fuchs synthesis starting with the chiral **128**.

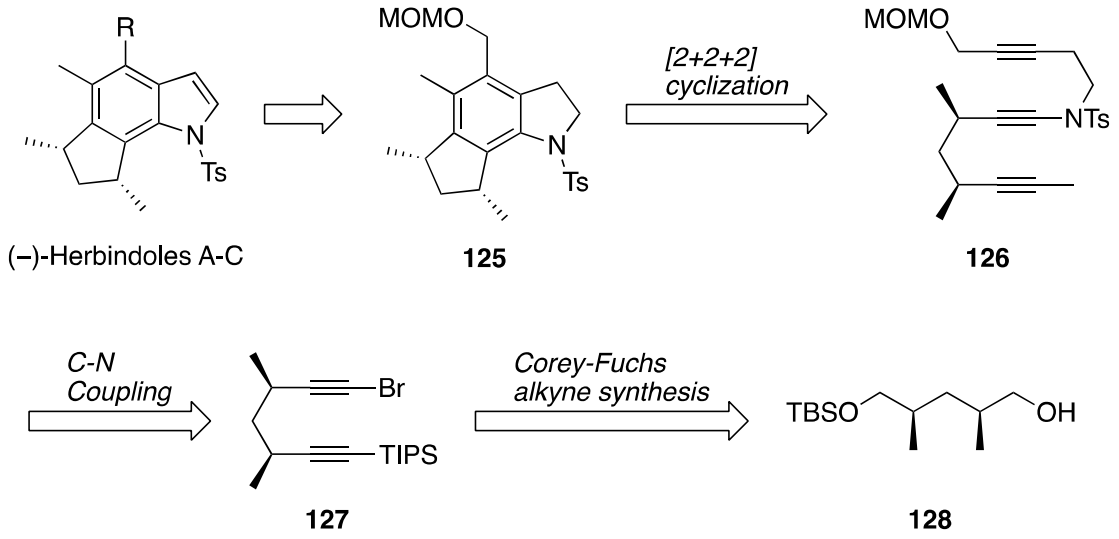

Scheme 1.8: The retrosynthesis of (–)-Herbindoles A-C [(–)-**52-54**] as described by Sato and coworkers (2012).

The total synthesis of (–)-herbindoles A-C is depicted in Schemes 1.9 and 1.10. Parikh-Doering oxidation of the alcohol **128** followed by bromination gave the dibromide **129**. Alkyne formation with *n*-BuLi and quenching with TIPSCl followed by TBS-deprotection gave the alcohol **130**. Oxidation of **130**, dibromination and treatment with another strong base LiHMDS gave the bromoalkyne **127** in 90% yield. The hydroxyl group of the known alkyne **134** was MOM-protected and the tosylamide was obtained after Boc-deprotection while heating. Further amidation

of the resulting ynamide **135** to the bromoalkyne **127** in the presence of catalytic $CuSO_4$ gave the dialkynylynamide **125** that was converted to the methyl-homologue **126** in 78%.

The [2+2+2] intramolecular cyclization of **126** was achieved in the presence of various transition metals catalysts as previously reported for inter- or intramolecular cyclizations (Table 1.1). The cyclization of **126** in the presence of Cp*RuCl(cod), $CpCo(CO)_2$, $RhCl(PPh_3)$ and Ni $(cod)_2$ catalyst proceeded to completion and gave the desired indoline **125** in good yield. In contrast, the oxidation with Pd(0)-PPh_3 returned the starting material uncyclized in 98%. Consequently, Sato and coworkers employed the Wilkinson's catalyst (run 3) to promote the cyclization of **126** in good yield in 5 hours.

Table 1.1: Reaction conditions for the transition-metal-catalyzed [2+2+2] cyclization of **126**.

Run	Catalyst (mol %)	Solvent	Temp (°C)	Time (hr.)	Yield (%)
1	Cp*RuCl(cod) (5)	Toluene	Rt	48	91
2	$CpCo(CO)_2$ (10)	*p*-xylene	140	24	95
3	$RhCl(PPh_3)$ (4)	Toluene	50	5	97
4	Ni $(cod)_2$ (5)	THF	50	24	80
5	Pd_2dba_3•$CHCl_3$ (2.5) PPh_3 (10)	toluene	50	24	-

Bromination of **125** gave the benzylic bromide intermediate **132** that underwent a radical reduction with *n*-Bu_3SnH in the presence of AIBN to give the (–)-herbindole A scaffold **133** in 92%. Tosyl deprotection with metallic Na followed by aromatization of the indoline with the cobalt (II) catalyst gave (–)-herbindole A in 49% overall yield over 15 steps starting from the optically active alcohol **128**.

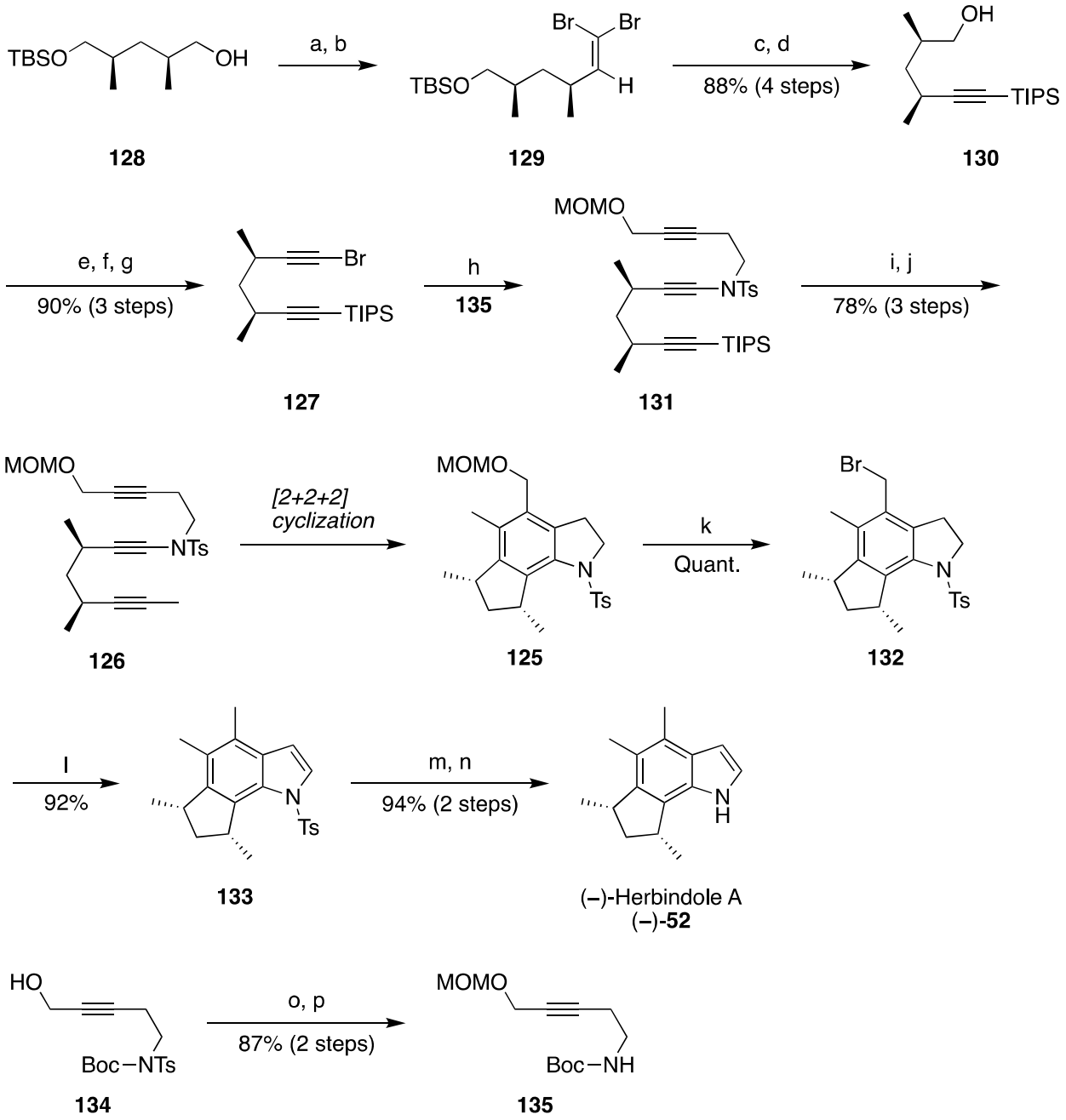

Scheme 1.9: The asymmetric synthesis of (–)-Herbindoles A [(–)-**52**] as described by Sato and coworkers (2012). Reagents and conditions: (a) SO_3•Pyr., DMSO, Et_3N, CH_2Cl_2, 0 ºC, 1.5 hr.; (b) CBr_4, PPh_3, CH_2Cl_2, 0 ºC, 2 hr.; (c) *n*-BuLi, THF, -78 ºC, 1 hr. then TIPSCl, rt, 10.5 hr.; (d) HCl, EtOH, rt, 17 hr. (e) SO_3•Pyr., DMSO, Et_3N, CH_2Cl_2, 0 ºC, 4 hr.; (f) CBr_4, PPh_3, CH_2Cl_2, 0 ºC, 2 hr.; (g) LiHMDS, THF, -78 ºC, min. to rt, 12 hr.; (h) $CuSO_4$•$5H_2O$, K_3PO_4, 1,10-phenanthroline, toluene, 60 ºC, 44 hr,; (i) TBAF, THF, rt, 1.5 hr.; (j) LiHMDS, THF, -78 ºC, 1 hr. then MeI, rt, 15 hr.; (k) BBr_3, CH_2Cl_2, -78 ºC, 2.5 hr.; (l) *n*-Bu_3SnH, AIBN, toluene, 100 ºC, 1 hr.; (m) Na, naphthalene, THF, -78 ºC, 2 hr.; (n) Co^{II}(salen), O_2, MeOH, rt, 2 hr.; (o) MOMCl, CH_2Cl_2, rt, 48 hr.; (p) neat, 185 ºC, 30 min.

The synthesis of (–)-herbindole B and C was also achieved from the key indoline intermediate **125**. Deprotection of the MOM-group of **125**, followed by Dess-Martin periodinane (DMP) oxidation of the primary alcohol to the aldehyde, Tebbe olefination to the corresponding alkene and Pd-C hydrogenation gave **137** in good yield. Tosyl-deprotection followed by aromatization with cobalt(II) catalyst gave (–)-herbindole B in 36% overall yield in 17 steps. DMP oxidation of **136** to the aldehyde, nucleophilic addition with *n*-propylmagnesium bromide to elongate the sidechain followed by dehydration afforded **138** in 91% yield. Again, tosyl deprotection and aromatization gave (–)-herbindole C in 44% overall yield in 17 steps. The (–)-herbindole A-C were identified according to the NMR data and negatively signed $[\alpha]_D$ values.

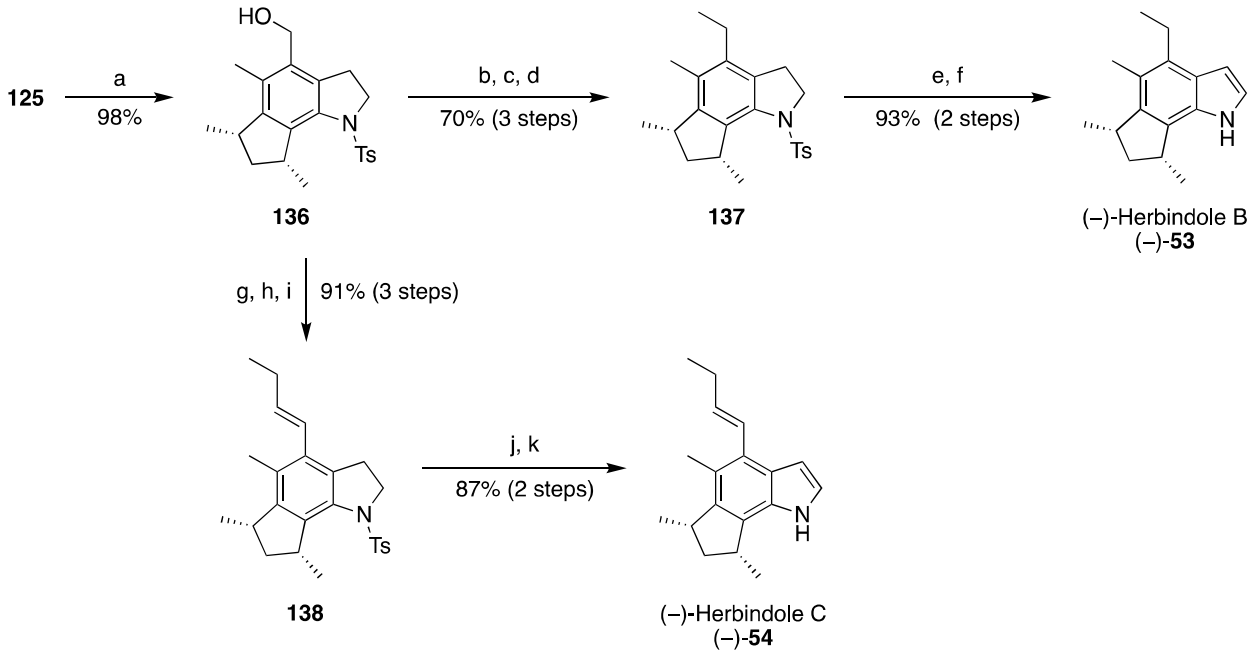

Scheme 1.10: The asymmetric synthesis of (–)-Herbindoles B-C [(–)-**53**-**54**] as described by Sato and coworkers (2012). Reagents and conditions: (a) HBF_4, CH_3CN/ H_2O, 60 ºC, 48 hr.; (b) DMP, CH_2Cl_2, rt, 3 hr.; (c) Tebbe reagent, THF, 0 ºC, 2 hr.; (d) H_2/ Pd-C, EtOAc, rt, 2 hr.; (e) Na, naphthalene, THF, -78 ºC, 1 hr.; (f) Co^{II}(salen), O_2, MeOH, rt, 1.5 hr.; (g) DMP, CH_2Cl_2, rt, 2 hr.; (h) *n*-PrMgBr, THF, 0 ºC, 3 hr.; (i) *p*-TsOH, benzene, 50 ºC, 20 hr.; (j) Na, naphthalene, THF, -78 ºC, 1 hr.; (k) Co^{II}(salen), O_2, MeOH, rt, 1.5 hr.

Although, the synthesis of the trikentramides A-D has not been achieved, there are many approaches reported in the literature for the construction of the indoline-2,3-dione backbone (**139**)

with some shown in Scheme 1.11.[46] Li and coworkers utilized a Cu-catalyzed intramolecular C-H oxidation of formyl *N*-arylformamide to construct the isatin backbone (path a) in which the two C-H's acted as the reactants and the O_2 served as the terminal oxidant of the Cu catalyst.[47] Cheng and coworkers employed $[CuI(bpy)]_2$ in the presence of an atmosphere of oxygen to form substituted *N*-alkylisatins via a Cu(I)-catalyzed intramolecular C-H oxidation of 2-aminoaryl methyl ketones (path b).[48a] Similarly, Ilangovan and Satish synthesized the isatin backbone via a C-H oxidation of the terminal ketone and dealkylative C-N annulation of secondary and tertiary amines in the presence of $Cu(OAc)_2 \bullet H_2O$ and NaOAc at slightly elevated temperatures (80 ºC, path b).[48b] Although, Cheng et. al. and Ilangovan and Satish accomplished the synthesis of the isatin backbone (**139**) from a similar starting reagent (**141**), the method of Cheng and coworkers required high temperatures (140 ºC), a high boiling point solvent (1,2-dichlorobenzene) and the presence of 2,2′-bipyridine ligand. Additionally, the latter group studied the cyclization of both 2′-*N*-aryl/alkylaminoacetophenones and 2′-*N,N*-dialkylaminoacetophenones as well as the role of the amine in the cyclization.

Lei and coworkers introduced the two adjacent carbonyl groups of the isatin derivatives via an oxidative Pd-catalyzed double carbonylation of the C-H/N-H of anilines under an atmosphere of CO and in the presence of $PdCl_2(PPh_3)_2$ and $Cu(OPiv)_2$ in DMSO/toluene at elevated temperature (100 ºC, path c).[49] In contrast, Wang and coworkers utilized the Pd-catalyst, $Pd(OAc)_2$, in the presence of K_2CO_3 to perform a double insertion of acetonitrile onto *N*-benzyl-2-iodoanilies (path d).[50] Ji and coworkers utilized *tert*-butyl hydroperoxide in the presence of iodine to successfully oxidize commercially available indoles into isatins as shown in path e.[51] Lee and workers utilized a copper-mediated ring contraction of 3-diazoquinoline-2,4-diones to form isatin derivatives as depicted in path f.[46]

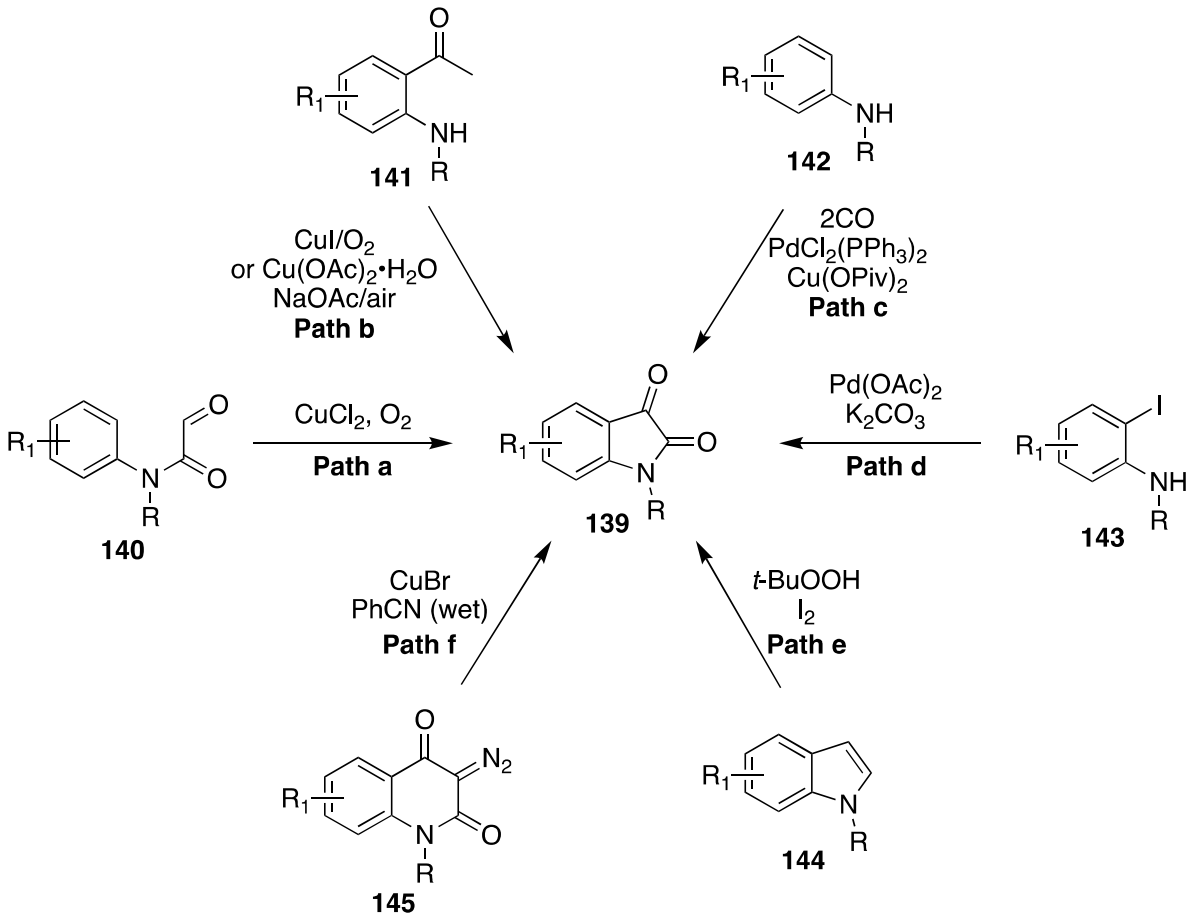

Scheme 1.11: Various approaches to the synthesis of the isatin backbone.

CHAPTER TWO. DISCOVERY OF ANTATOLLAMIDES A AND B

Abstract: Two dimerized cyclic hexapeptides, antatollamides A (**146**) and B (**147**), were isolated from the colonial ascidian *Didemnum molle* collected in Pohnpei. The amino acid compositions and sequences were determined by interpretation of MS and 1D and 2D NMR data. Raney Ni reduction of antatollamide A cleaved the dimer to the corresponding monomeric cyclic hexapeptide with replacement of Cys by Ala. The amino acid configuration of **146** was established, after total hydrolysis, by derivatization with a new chiral reagent, (5-fluoro-2,4-dinitrophenyl)-N^{α}-L-tryptophanamide (FDTA), prepared from L-Trp, followed by LCMS analysis; all amino acids were found to be L-configured except for D-Ala.

2.1 Isolation and Structure Elucidation of Antatollamides A and B

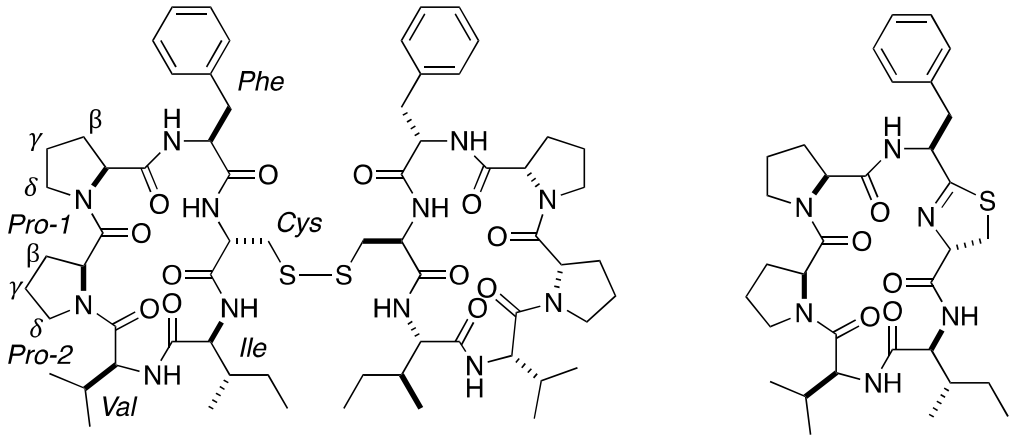

Figure 2.1: The structures of antatollamides A (**146**), B (**147**) and mollamide F (**14**).

Separation of the MeOH-soluble extract of lyophilized *D. molle* by solvent partitioning and reversed phase HPLC gave two new peptides, **146** and **147** (Figure 2.1). HRMS analysis of **146** showed two prominent sodium adduct molecular ions: $[M+Na]^+$ at m/z 1333.6433, and the reduced monomeric form at m/z 679.3250 $[M/2+H+Na]^{2+}$, corresponding to formulas $C_{66}H_{94}N_{12}O_{12}S_2$ and

$C_{33}H_{48}N_6O_6S$, respectively. Analysis of 1D and 2D NMR data of **146** - including the presence of four amide proton signals (δ 7.04 (d, 9), 8.43 (d, 6.6), 7.69 (d, 7.8) and 8.15 (d, 7.8), six α protons (δ 4.24 (t, 7.5), 4.50 (m), 4.39 (t, 8.4), 3.84 (t, 6.6), 4.46 (m) and 4.53 (m)), and six expected amide carbonyl ^{13}C NMR signals (δ 170.6, 170.4, 170.3, 170.2, 169.71 and 169.67) – supported a peptide structure. Exhaustive analysis of HSQC, HMBC, COSY, TOCSY and NOESY data identified six spin systems assigned to the amino acid residues as Cys, two Pro, Ile, Phe, and Val. Due to congestion of the ^{13}C NMR carbonyl signals, which hampered analysis of long-range heteronuclear correlations, the amino acid sequence was established from the NOESY data; specifically, observation of nOe crosspeaks (Figure 2.2) from the amide NH signals of each residue, i, to the adjacent CH_α proton signals of the adjacent residue, i–1.

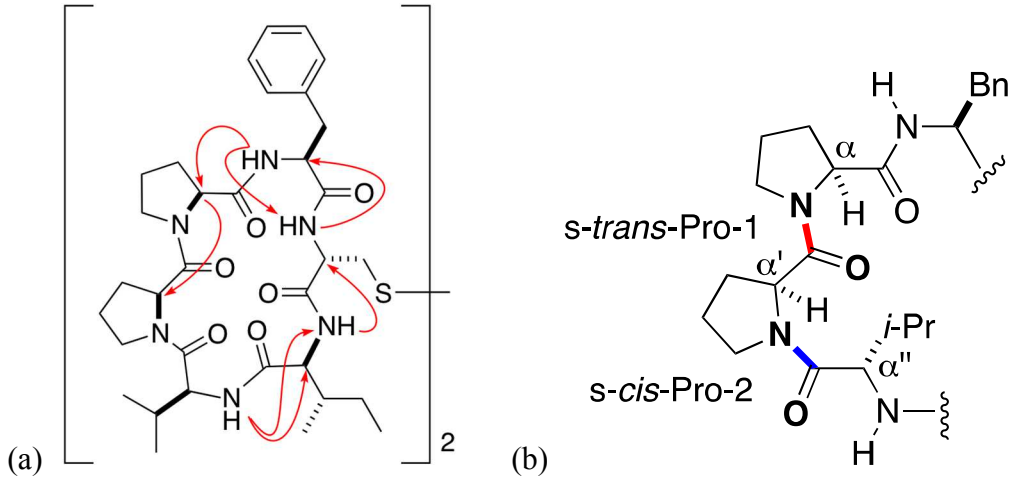

Figure 2.2: Antatollamide A (a) Summary of NOESY correlations observed for **146** (DMSO-d_6, 600 MHz, t_m = 500 mS) (b) 3D approximation of the s-*trans*-Pro-1–s-*cis*-Pro-2 element (amide bonds highlighted in color).

A second dimeric cyclohexapeptide **147**, isomeric with **146**, was separated from the latter by reversed phase HPLC. Analysis of the 1D and 2D NMR data for **147** (Table 2.1) revealed that both **146** and **147** shared the same amino acid sequence, but exhibited significant differences in the ^1H and ^{13}C NMR chemical shifts of the Pro residues. Pro residues, in particular those involved

in oligo-Pro sequences in conformationally restricted cyclic peptides, are known to exist in stable s-*cis* and s-*trans* configurations which interchange on slow time scales. The Pro amide bond configuration is empirically assigned from differences in the ^{13}C NMR chemical shifts ($\Delta\delta$) of their respective β-and γ-carbons.[52] Small and large chemical shift differences in the Pro-1 and Pro-2 residues of **146**, respectively ($\Delta\delta_{\beta\gamma}$ = 3.3 and 9.2 ppm), confirmed a *trans*-*cis* Pro-1–Pro-2 configuration. Conversely, **147** adopts the *cis*-*trans* Pro-1–Pro-2 configuration ($\Delta\delta_{\beta\gamma}$ = 9.5 and 4.2 ppm). The two diastereomers were stable; no interconversion between **146** and **147** or other isomers was observed over the time frame of these measurements (weeks).

Table 2.1: NMR data for **146** and **147** (600 MHz, DMSO-d_6).

		146			**147**		
	Position	δ_C [a]		δ_H [b], mult (*J*, Hz)	δ_C [a]		δ_H [b], mult (*J*, Hz)
Pro-1	C=O	170.3	C		169.9	C	
	α	58.7	CH	4.24, t (7.5)	58.7	CH	4.27, m
	β	28.3	CH_2	1.62, m	31.5	CH_2	1.30, m
				2.29, m			1.89, m
	γ	25.0	CH_2	1.83, m	22.0	CH_2	1.53, m
				1.98, m			1.59, m
	δ	47.5	CH_2	3.54, q (8.4)	46.7	CH_2	3.20, m
				3.79, m			3.27, m
Pro-2	C=O	170.6	C		170.2	C	
	α	60.5	CH	4.50, m	58.7	CH	4.16. dd (8.1, 5.1)
	β	30.6	CH_2	1.82, m	28.9	CH_2	1.66, m
				2.12, dd (12, 6.0)			2.19, m
	γ	21.4	CH_2	0.94, m	24.7	CH_2	1.82, m
				1.59, m			1.90, m
	δ	45.9	CH_2	2.90, t (9.9)	47.6	CH_2	3.49, m
				3.20, m			3.76, m
Val	C=O	169.67	C		171.2	C	
	α	54.8	CH	4.39, t (8.4)	56.0	CH	4.28, m
	β	30.3	CH	2.02, m	29.7	CH	1.91, m
	γ	18.0	CH_3	0.86, d (6.6)	19.0	CH_3	0.81, m
		19.2	CH_3	0.94, d (6.6)	19.5	CH_3	0.83, m
	NH			7.04, d (9.0)			7.08, d (9.6)
Ile	C=O	170.2	C		169.8	C	
	α	59.7	CH	3.84, t (6.6)	60.9	CH	3.70, t (6.3)
	β	35.2	CH	1.85, m	35.4	CH	1.76, m
	β-Me	15.6	CH_3	0.89, d (7.2)	15.9	CH_3	0.88, d (7.2)
	δ	25.0	CH_2	1.25, m	25.7	CH_2	1.23, m
				1.47, m			1.49, m
	δ	11.3	CH_3	0.85, t (7.2)	11.6	CH_3	0.84, m
	NH			8.43, d (6.6)			8.22, d (5.4)
Cys	C=O	169.71	C		170.9	C	
	α	54.8	CH	4.46, m	54.6	CH	4.57, m
	β	24.8	CH_2	2.48, m[c]	26.2	CH_2	2.69, m
							2.82, m
	NH			7.69, d (7.8)			7.26, m
Phe	C=O	170.4	C		171.6	C	
	α	55.0	CH	4.53, m	55.0	CH	4.42, m
	β	38.0	CH_2	3.00, dd (9.9, 3.6)	37.8	CH_2	2.89 dd (13.8, 10.8)
				3.12, dd (13.2, 6.0)			3.22, m
	γ	137.6	C		138.1	C	
	δ	129.2	CH	7.15, d (7.2)	129.6	CH	7.18, m
	ε	128.3	CH	7.25, m	128.6	CH	7.27, m
	ζ	126.4	C	7.19, m	126.8	C	7.19, m
	NH			8.15, d (7.8)			8.46, d (8.4)

a. 125 MHz Multiplicity determined from HSQC spectra. *b*, 600 MHz. *c*, 2H integration

The conformational changes introduced by s-*cis*/s-*trans* isomerism in **146** and **147** dramatically influenced their ECD spectra. The ECD spectrum of **146** (Figure 2.3) is dominated by three Cotton effects – one positive and two negative (λ 196 nm (Δε +18.7), 204 (–28.4), 221 (–24)) – that arise largely from π-π* exciton transitions of the amide carbonyl groups. In contrast, the signature features in the ECD spectrum of **147** are two considerably weaker positive Cotton effects (λ 196 nm (Δε +13.8), 204 (–5.5) 213 (+7.7)). We have noted earlier that similarly constrained medium ring peptide macrocycles, with embedded Pro residues – for example, styllisamides G and H from the Caribbean sponge, *Stylissa caribica*,[25c] and sanguinamides A and B from the Spanish dancer nudibranch, *Hexabranchus sanguineus*[53] – display ECD spectra that are exquisitely sensitive to s-*cis*/s-*trans* isomerism.

In theory, dimerism and Pro s-cis/s-trans isomerism in **146** and **147**, may generate up to 16 diastereomers, however, no evidence of isomers other than **146** and **147** were detected in the extracts of *D. molle*. From this we surmise that the **146** and **147** are not stereorandom isomers, but the consequence of a thermodynamically favorable "well" resulting from specific non-bonded constraints in the rigid hexapeptide motif.

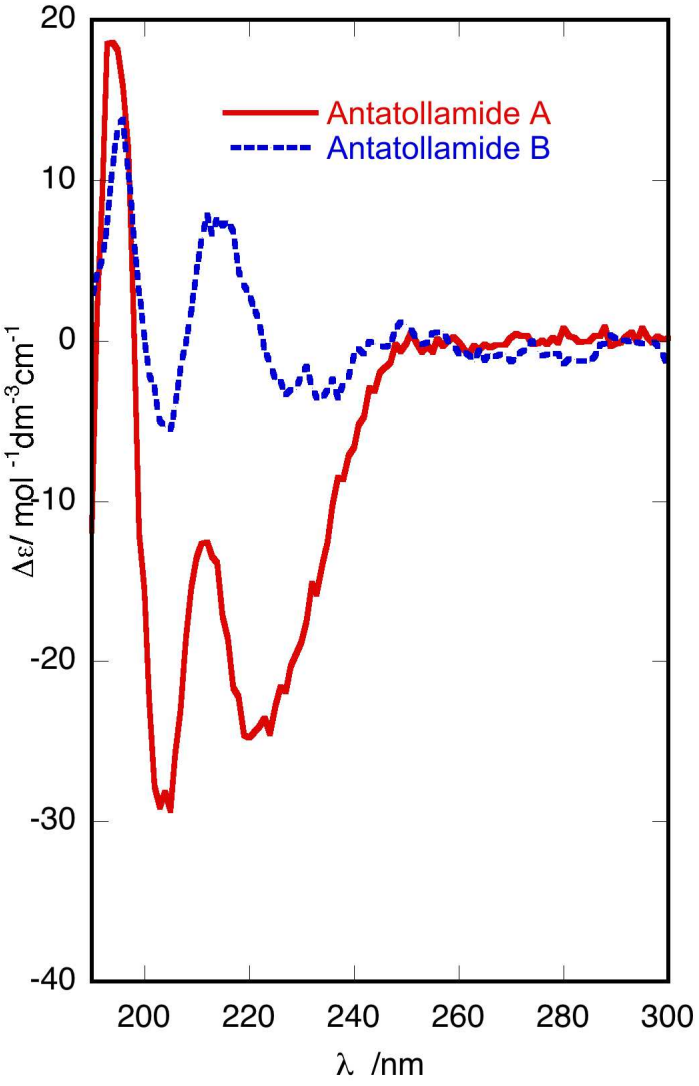

Figure 2.3: ECD Spectra of antatollamides A (**146**) and B (**147**) (CH_3CN, 23 ˚C).

2.2 Absolute Structural Assignment – Application of FDTA to Antatollamide A

The absolute configurations of all the individual amino acids of **146** were secured by Marfey's analysis[29] using a new variant of his eponymous reagent. Dimeric **146** was cleaved to the monomeric cyclic peptide **152** by desulfurization of the Cys-S-S-Cys unit to two D-Ala residues (Raney Ni, H2O-MeOH, 65 °C, Scheme 2.1). Inspection of the ^{1}H NMR spectrum of **152** revealed essentially the same signals as **146** with the appearance of a new methyl signal (δ 1.03,

d, J = 6.6 Hz, H_β, Ala). After hydrolysis of **152** (6 M HCl, 110 °C), the amino acid residues were derivatized with a versatile, new L-tryptophanamide variant of Marfey's reagent (see below) and their configurations assigned by comparative analysis by LCMS (reversed phase HPLC, H_2O (0.1% HCOOH)-CH_3CN gradient, see Experimental for details) along with standards. The following residues were identified: L-Pro, L-Val, L-Ile, D-Ala and L-Phe, and confirmed by co-injection with standards. It is notable that the latter conditions failed to separate L-Ile and L-*allo*-Ile DTA derivatives, however successful resolution (t_R) was obtained with salt buffered mobile phase (Zorbax SB-Aq, H_2O (NH_4OAc)-CH_3CN gradient: L-Ile (34.41), and L-*allo*-Ile (33.38). The configurations of the amino acid residues in **147** are presumed to be the same as those of **146**; too little sample remained available to analyze **147** independently.

The 5-fluoro-2,4-dinitrophenyl-N^{α}-L-tryptophanamide reagent, FDTA (**151**), was developed as an alternate reagent to the conventional Marfey's reagent, FDAA,[29] for the determination of the absolute configuration of amino acids. Compound **151** was synthesized using a variant of the literature method (Scheme 2.1).[29] L-Trp was converted to the corresponding methyl ester **149** that, in turn, was ammonialysed to the primary amide, L-Trp-NH_2 (**150**, NH_4OH, MeOH, quantitative). S_NAr coupling of **150** (1 equiv) with 1,5-difluoro-2,4-dinitrobenzene delivered FDTA (**151**, m.p. 220 – 222 °C). Reagent **151** was stable at room temperature in the dark with no detectable signs of decomposition after four months. The extinction coefficient of the long-wavelength UV-vis transition of **151** (λ_{max} 339 nm, ε log 4.12) is comparable to Marfey's reagent (λ_{max} 338 nm, ε log 4.18),[29] but the indole chromophore confers π-π* transitions to **151** of comparable intensity at shorter wavelength (e.g. λ_{max} 252, ε log 4.04) that may find utility in detection.

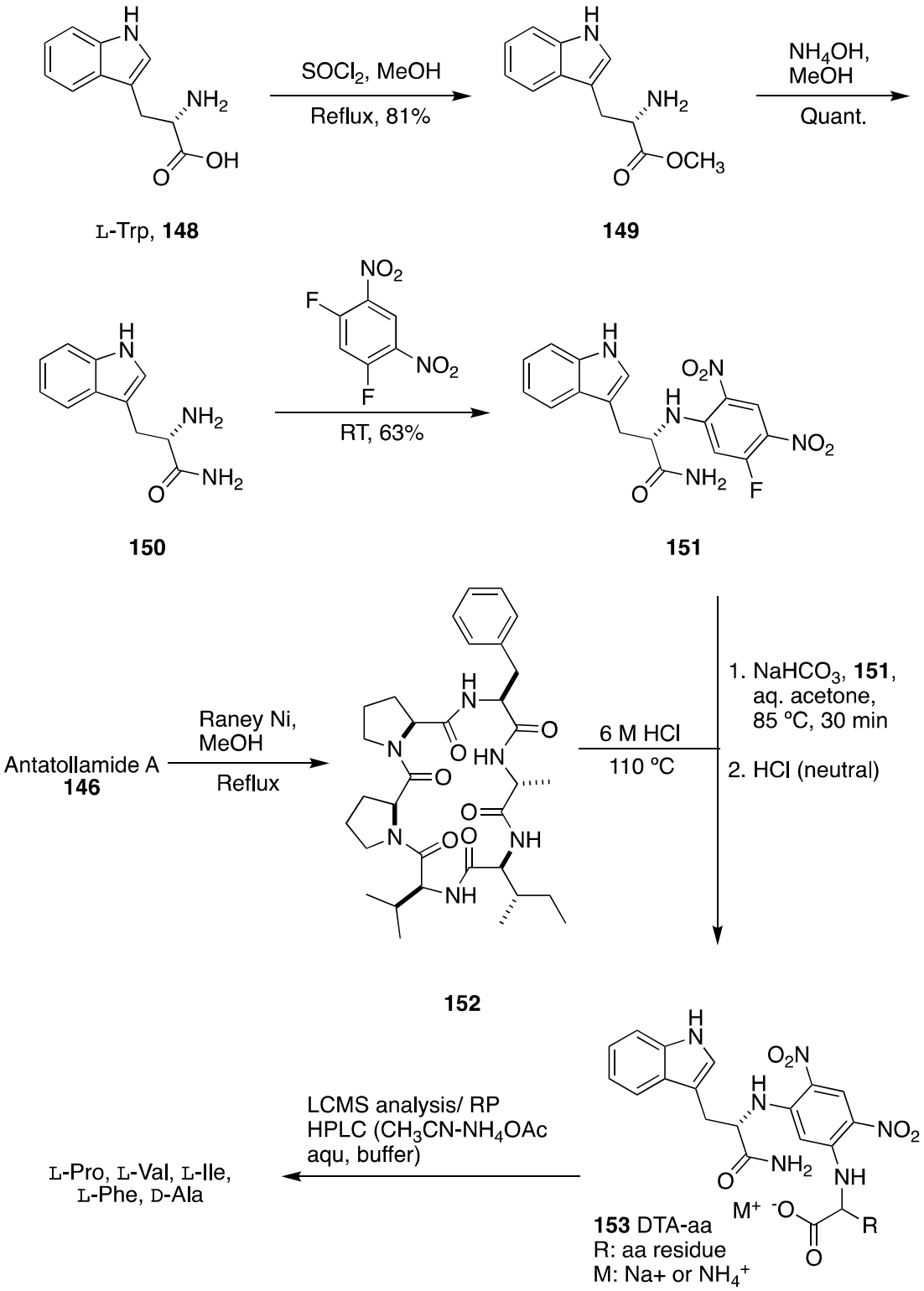

Scheme 2.1: The synthesis of FDTA (**151**) followed by the Raney Ni reduction of antatollamide A (**146**), hydrolysis and derivatization of the individual amino acids with **151**.

Among the cyanobactins, peptide **146** is most similar to mollamide F (**14**) reported by Ireland and coworkers from a *D. molle* collected from New Britain, Papua New Guinea.[16c] Both are cyclic peptides with two differences: **146** contains L-Phe and free D-Cys dimerically linked through a disulfide bridge while mollamide F is monomeric, containing D-Phe and an (*S*)-thiazoline residue (the latter presumably arises from D-Cys by cyclodehydration). The mechanism and gene clusters responsible for formation of thiazoline and oxazoline peptide residues in ascidians are now well known,[54] and it is clear that *Prochloron* in *D. molle* harbors the biosynthetic capacity for cyanobactin production. Mollamide F (**14**) appears to be formally related to **146** through heterocyclodehydration of D-Cys to the (*S*)-thiazoline residue and the epimerization of L-Phe to D-Phe. The unexpected D-thiazoline configuration of **14** – and by analogy, D-Cys in **146** – has drawn comment because the responsible biosynthetic gene cluster in *Prochloron*[9] from *D. molle* reveals, "absence of any apparent epimerase enzymes in the sequenced pathways".[16c]

Disulfide-linked peptides are among the more cytotoxic cyanobactins. Each of the structures of ulithiacyclamide (**33**)[22a] and ulithiacyclamide B (**34**)[22b] – highly cytotoxic cyanobactins from *Lissoclinum patella* (IC_{50} (KB cells) 35 and 17 and ng.mL^{-1}, respectively) – has two Cys residues linked by an intramolecular disulfide bond.[21d] To the best of our knowledge, **146** and **147** are the only cyanobactins that have intermolecular dimerization through Cys. In order to compare the antiproliferative properties of **146** and **33**, both were assayed against a chronic lymphocytic leukemia (CLL) primary cell line. While compound **33** was modestly potent (IC_{50} ~300 nM, or 400 ng.mL^{-1}), the open-disulfide dimeric analog **146** lacked substantial cell cytotoxicity (IC_{50} >10^4 nM).

2.3 Comparisons of Separations of aa-DTA and aa-DAA Derivatives

While Marfey's analysis using the conventional FDAA provides good resolution for differentiation of L- and D-enantiomers of non-polar amino acids, it notably performs poorly with some polar amino acids and fails entirely to discriminate certain *N*-Me amino acids (e.g. L- and D-*N*-Me-Ala, see Figure 2.4 and Table 2.2),[30,55] but the corresponding L-DTA derivatives are well-resolved. Other successful methods to overcome the resolution problems observed with Marfey's analysis are mentioned in Chapter One and include variants of the original reagent synthesized by replacements of the L-Ala-NH_2 group in FDAA with more non-polar amino acid amides (e.g. L-Val-NH_2 and L-Leu-NH_2),[26a,30] which increase the hydrophobic properties of the analytes, or conventional analysis using a C_3 reversed phase column under combined "C_3 and 2D C_3" HPLC conditions.[56] The FDTA reagent, **151**, was developed as an alternative reagent to Marfey's reagent, FDAA, for the determination of the stereochemistry of peptides or amino acid (aa) containing natural products. FDTA was applied to proteinogenic and non-proteinogenic amino acids and the behavior and mechanism of separation of the aa-derivatives were examined under various conditions.

The elution patterns of the amino acid diastereoisomers of –DAA and –DTA derivatizing reagents were obtained by reversed-phase LCMS. Elutions were completed with a linear gradient of 15–45% CH_3CN-H_2O containing 0.1% HCOOH as the mobile phase on a C_{18} column. The diastereoisomers were judged 'resolved' if they showed baseline separation, although partial separations were also considered diagnostic. Similar elution patterns were observed for both the –DAA and –DTA derivatives for most of the neutral amino acids. As previously observed with FDAA, the L-aa diastereomer eluted before the D-isomer. Conversely, the retention times of the aa-DTA derivatives were longer than the retention times of the corresponding aa-DAA derivatives as depicted in Figure 2.4. Additionally, a large spread was observed for the aa-DAA derivatives in

terms of the experimental retention times and the differences in the retention times of the L-aa- and D-aa- derivatives (Δt) that wasn't seen with the aa-DAA derivatives.

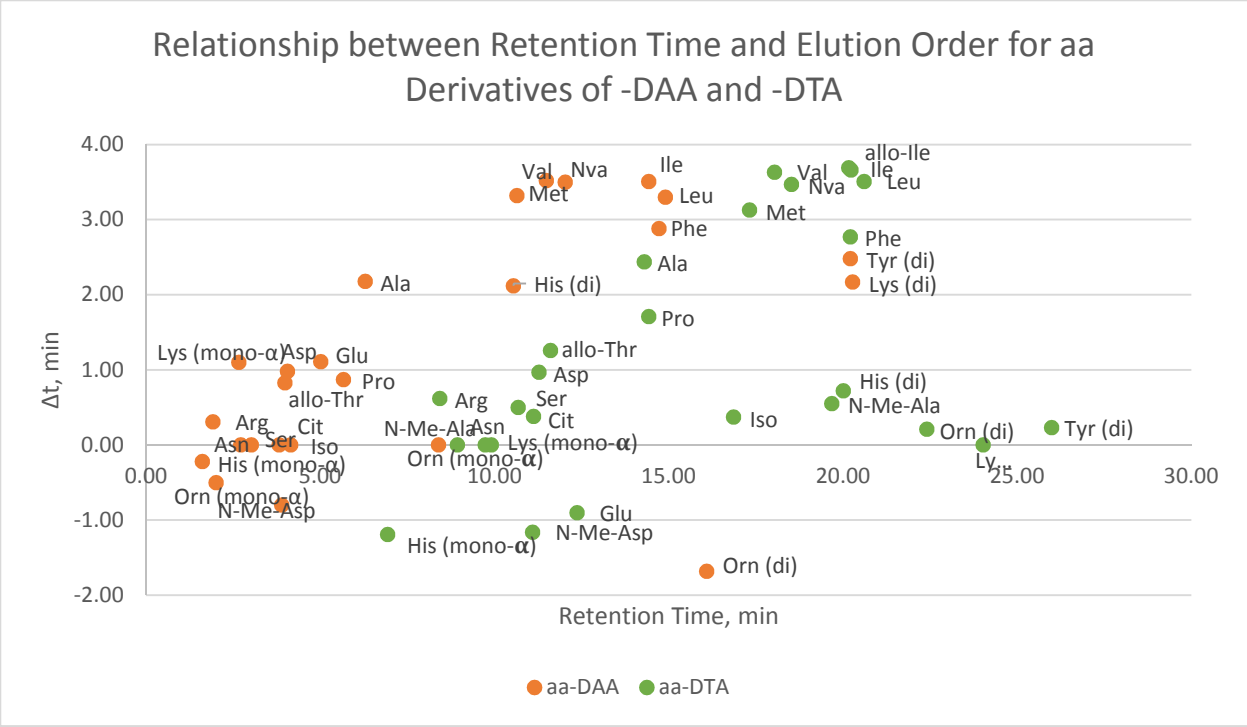

Figure 2.4: Comparison of the retention time and Δt ($t_{R,}$(D-aa) – $t_{R,}$(L-aa)) of the L-aa- and D-aa- derivatives of DAA and DTA.

Neither reagent resolved Asp while *only* FDTA resolved both DL-Cit and DL-Ser. Some major differences were observed for Glu and *N*-Me-Asp, where the D-diastereoisomer eluted first, and for the basic amino acids Lys, Orn and His (Table 2.2). Both the mono-α-*N* and di-*N*,*N*′- derivatives of all three basic amino acids were well-resolved with FDAA. In contrast, the –DTA derivatives showed poor resolution for the latter three amino acids as well as the Tyr derivatives despite increased retention times implying that there is change in the mechanism of separation of these derivatives. One other notable difference was the divergence of peaks and increase in retention times of the critical amino acid derivatives that are known to have a small Δ*t* under conventional Marfey's conditions. The *N*-Me-alanine derivative, which fails to resolve with the

conventional FDAA reagent, was separated into the L- and D- diastereoisomers with FDTA. Additionally, as mentioned above, derivatives of L-Ile and L-allo-Ile prepared from FDTA were resolved with a difference in t_R of more than 60 s.

Table 2.2: Comparative UHPLC Retention times (t_R, min) and Orders of Elution of L-DTA and L-DAA Derivatives of L- and D-Amino Acids.[a]

	DAA					DTA				
		t_R, min					t_R, min			
aa		L	D	Δt^b	α^c		L	D	Δt^b	α^c
Ala	L → D	5.20	7.38	2.18	1.42	L → D	13.08	15.52	2.44	1.19
Nva	L → D	10.28	13.78	3.50	1.34	L → D	16.79	20.26	3.47	1.21
Val	L → D	9.73	13.25	3.52	1.36	L → D	16.22	19.85	3.63	1.22
Leu	L → D	13.25	16.55	3.30	1.25	L → D	18.85	22.36	3.51	1.19
Ile	L → D	12.67	16.18	3.51	1.28	L → D	18.40	22.06	3.66	1.20
Met	L → D	8.98	12.30	3.32	1.37	L → D	15.75	18.88	3.13	1.20
Phe	L → D	13.28	16.16	2.88	1.22	L → D	18.83	21.60	2.77	1.15
Tyr (di)	L → D	18.97	21.45	2.48	1.13	L → D	25.87	26.10	0.23	1.01
Pro	L → D	5.23	6.10	0.87	1.17	L → D	13.57	15.28	1.71	1.13
Ser	L → D	3.02	3.02	0.00	1.00	L → D	10.43	10.93	0.50	1.05
allo-Thr	L → D	3.57	4.40	0.83	1.23	L → D	10.98	12.24	1.26	1.11
Asn	L → D	2.72	2.72	0.00	1.00	[d]	9.73	9.73	0.00	1.00
Glu	L → D	4.46	5.57	1.11	1.25	D → L	12.82	11.92	-0.90	1.08
Asp	L → D	3.57	4.55	0.98	1.27	L → D	10.79	11.76	0.97	1.09
Lys (mono-α)	L → D	2.11	3.21	1.10	1.52	[d]	9.91	9.91	0.00	1.00
Lys (di)	L → D	19.19	21.36	2.17	1.11	[d]	24.02	24.02	0.00	1.00
Orn (mono-α)	D → L	2.26	1.76	-0.50	1.28	[d]	8.93	8.93	0.00	1.00
Orn (di)	D → L	16.93	15.25	-1.68	1.11	L → D	22.30	22.51	0.21	1.01
His (mono-α)	D → L	1.72	1.50	-0.22	1.15	D → L	7.53	6.34	-1.19	1.19
His (di)	L → D	9.48	11.60	2.12	1.22	L → D	19.65	20.37	0.72	1.04
Arg	L → D	1.76	2.07	0.31	1.18	L → D	8.12	8.74	0.62	1.08
Cit[e]	D → L	4.15	4.15	0.00	1.00	D → L	10.93	11.31	0.38	1.03
N-Me-Ala	*d*	8.39	8.39	0.00	1.00	L → D	19.40	19.95	0.55	1.03
N-Me-Asp	D → L	3.49	4.29	0.80	1.23	D → L	11.67	10.51	-1.16	1.11
Iso-Ser[f]	*d*	3.82	3.82	0.00	1.00	L → D	16.67	17.04	0.37	1.02
Ile[g]	*n/a*					L → D	34.41			
allo-Ile[g]	*n/a*					L → D	33.38			

[a]Conditions: Reversed-Phase C_{18} column, 50 x 2.1 mm (1.9 µm), flow rate 0.50 mL min^{-1}; elution completed with a linear gradient of 15–45% CH_3CN/H_2O-0.1% HCOOH for 25 min, followed by 100% CH_3CN for 2 min and re-equilibration with 15% CH_3CN/H_2O-0.1% HCOOH for 3 min before the next measurement; void time t_M = 0.53 min. [b]$\Delta t = t_{R,}$(D-aa) – $t_{R,}$(L-aa); negative values indicate reversal of elution order. [c]$\alpha = [t_R(B) - t_M]/[t_R(A) - t_M]$, where A and B are the faster and slower eluting components, respectively. [d]Co-elution. [e]Citrulline. [f]3-Amino-2-hydroxypropanoic acid. [g]Conditions: Agilent Zorbex SB-Aq column, 4.6 X 250 mm (5 µm), stepped gradient, initial conditions 30–40% CH_3CN/H_2O/20 mM NH_4OAc-0.1% TFA, 40 min; 40–50% CH_3CN/H_2O/20 mM NH_4OAc-0.1% TFA, flow rate 0.7 mL min^{-1}.

2.4 Proposed Mechanism of Separation for L-Ala-DTA

To further study the separation of the critical amino acids with $\Delta t \leq 1.00$ minute, the effect of the NH_4OAc buffer on the elution and separation behavior of the diastereoisomeric derivatives of –DAA and –DTA was explored. Most literature variants of Marfey's method that include buffer in the mobile phase use either triethylammonium phosphate or NH_4OAc. In the present work, aqueous acetonitrile gradients (0.1% TFA or formic acid), without buffer, showed little or poor separation for some aa-DAA derivatives in contrast to the literature examples which were successful under the same solvent conditions. The latter observation suggests some dependency of separation on the stationary phase (e.g. particle homogeneity, proprietary differences in column chemistry, or simply column age). The presence of 20 mM NH_4OAc in the mobile phase improved the resolution for most of the amino acids including Lys, Orn, His, Asp and *N*-Me-Ala (Table 2.3). In contrast, aa-DAA-derivatives of both DL-Cit (neutral) and DL-Arg co-eluted as one peak. The largest improvement in separation occurred with DL-Lys, which failed to resolve in the absence of NH_4OAc but separated with a large gap (Δt = 10.11 min) in its presence. The origin of the dramatic effect of NH_4OAc, which buffers the mobile phase to approximately pH~4, upon retention times is unclear, but the generally longer retention times imply more hydrophobic mobile species than in the absence of the ammonium salt.

Table 2.3: Comparative HPLC Retention times (t_R, min) and Orders of Elution of select L-DTA and L-DAA Derivatives of L- and D-Amino Acids.[a]

	DAA				DTA			
	t_R, min				t_R, min			
aa	L	D	Δt^b	α^c	L	D	Δt^b	α^c
Tyr (di)	45.54	46.38	0.83	1.02	37.76	39.28	1.53	1.05
Ser	29.67	29.99	0.32	1.01	21.39	22.36	0.97	1.06
Asn	28.35	28.35	0.00	1.00	20.74	21.85	1.11	1.07
Glu	31.21	31.51	0.30	1.01	19.67	20.08	0.41	1.03
Lys (mono-α)	25.86	24.38	-1.48	1.08	22.04	22.04	0.00	1.00
Lys (di)	26.33	26.33	0.00	1.00	24.88	34.99	10.11	1.52
Orn (mono-α)	25.48	25.48	0.00	1.00	24.06	24.06	0.00	1.00
Orn (di)	41.98	41.98	0.00	1.00	33.81	32.98	-0.83	1.03
His (mono-α)	24.93	23.44	-1.49	1.08	22.34	21.80	-0.54	1.03
His (di)	34.34	34.69	0.35	1.01	32.42	32.99	0.57	1.02
Arg	26.61	25.17	-1.44	1.07	23.14	23.14	0.00	1.00
Cit[d]	29.23	28.12	-1.11	1.05	22.02	22.02	0.00	1.00
N-Me-Ala	34.32	34.88	0.57	1.02	24.26	25.53	1.28	1.07
N-Me-Asp	30.43	29.68	-0.74	1.03	18.99	18.54	-0.45	1.03
Iso-Ser[e]	29.70	29.98	0.28	1.01	23.28	23.28	0.00	1.00
allo-Ile	39.33	42.56	3.23	1.10	26.62	30.01	3.39	1.16
Ile	39.43	42.58	3.16	1.09	26.52	29.85	3.33	1.16

[a]Conditions: Reversed-Phase C_{18} column, 250 x 4.6 mm (1.9 μm), flow rate 0.70 mL min^{-1}; elution completed with a linear gradient of 15–65% CH_3CN/0.1 M NH_4OAc-H_2O-0.1% TFA for 40 min, followed by 100% CH_3CN for 5 min; void time t_M = 5.31 min. [b]$\Delta t = t_R$(D-aa) – t_R(L-aa). [c]$\alpha = [t_R(B) - t_M]/[t_R(A) - t_M]$, where A and B are the faster and slower eluting components, respectively. [d]Citrulline. [e]3-Amino-2-hydroxypropanoic acid.

To study the effect of the NH_4OAc buffer on FDTA, the ^1H NMR spectra of a sample of L-Ala-DTA in DMSO-d_6 were recorded as the solution was titrated with NH_4OAc in DMSO-d_6. The titration of the L-Ala-DTA with NH_4OAc (Figure 2.4a) showed an increasing NH_4^+ signal (1:1:1 triplet, J_{NH} = 34 Hz) at 0.1 – 1.0 equivalent that coalesced into one broad peak at higher concentration suggesting that the NH_4^+ may be involved in an intramolecular π-cation interaction as shown in Figure 2.4b. Evidence suggests that the molecular discrimination of –DTA derivatives is less to do with hydrogen bonding and more with hydrophobicity. One hypothesis is that a pronounced intramolecular π-cation interaction between the ammonium counterion and the electron rich indole ring presents a more compact, hydrophobic mobile species to the stationary

phase to enhance molecular discrimination between D- and L-amino acid derivatives. Such a π-cation interaction would, of course, be unlikely in traditional Marfey's derivatives obtained with FDAA where the only delocalized π-system available is the electron-deficient dinitroaryl ring. Additionally, H-5 appears at an unusually high field (5.63 ppm) for an aromatic proton in contrast to H-2 (8.92 ppm), implying that H-5 is shielded and lies above the indole ring.

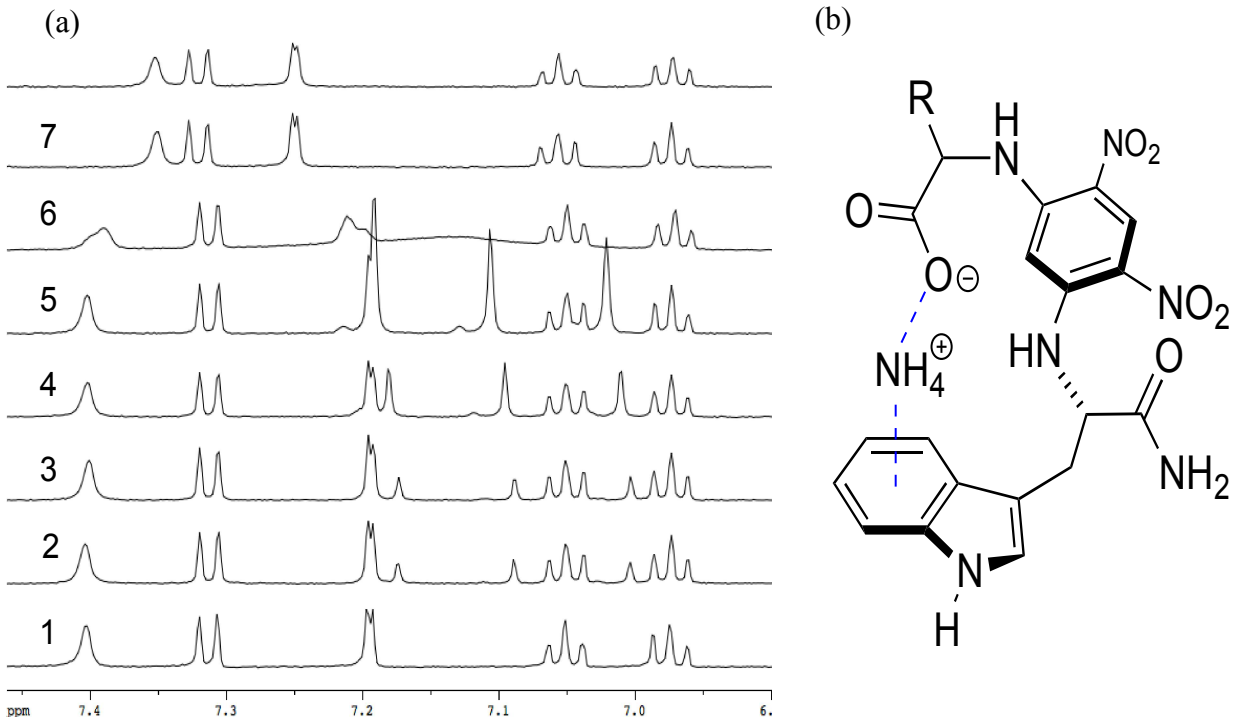

Figure 2.5: (a) The titration of L-Ala-DTA (600 MHz, DMSO-d_6) with no additive (1), 0.1% TFA and 0.1 equiv. (2), 0.2 equiv. (3), 0.5 equiv. (4), 1.0 equiv. (5), 2.0 equiv. (6), 5.0 equiv. (7), and 10.0 equiv. (8) of NH_4OAc. (b) Intramolecular p-cation interaction in L-aa-DTA derivatives.

In conclusion, two new dimeric hexapeptides, antatollamide A (**146**) and B (**147**) were isolated from the ascidian, *Didemnum molle* collected in Pohnpei, and characterized by NMR, chemical degradation to constituent amino acids, and derivatization with L-FDTA – a novel tryptophanamide variant of Marfey's reagent to give DTA-amino acid derivatives. NMR studies of the antatollamides revealed two configurations for the Pro-Pro dipeptide segment with the predominant natural product, **146**, bearing the *trans-cis* amide bond configuration. Under UHPLC

analysis, DTA-derivatives of critical amino acids show superior resolution compared to conventional Marfey's derivatives. Exploration of the mechanism of separation of FDTA derivatives, specifically L-Ala-DTA, in the presence of NH_4OAc revealed intramolecular π-cation interactions between the ammonium counterion and the indole of the tryptophan ring and indicated that the increased difference in hydrophobicity improves the resolution of the L- and D- amino acids.

Chapter 2, in part, is a reprint of the material as it appears in "Cyclic Hexapeptide Dimers, Antatollamides A and B, from the Ascidian *Didemnum Molle*. A Tryptophan-Derived Auxiliary for L- and D-Amino Acid Assignments" published in the Journal of Organic Chemistry, 2017, *82*, 10181-10187 by Salib, Mariam N.; Molinski, Tadeusz F. The thesis author was the primary investigator and author of this paper.

CHAPTER THREE. DISCOVERY OF *trans*-HERBINDOLE A AND TRIKENTRAMIDES E-I

Abstract: Six new cyclopenta[*g*]indoles were isolated from a West Australian sponge, *Trikentrion flabelliforme* Hentschel, 1912, and their structures elucidated by integrated spectroscopic analysis. The compounds are analogues of previously described trikentrins, herbindoles and trikentramides from related Axinellid sponges. The assignment of absolute configuration of the new compounds was carried out largely by comparative analysis of specific rotation, calculated and measured ECD, and exploiting van't Hoff's principle of optical superposition. Five of the new compounds were chemically interconverted to establish their stereochemical relationships, leading to a simple chiroptical mnemonic for assignment of this family of chiral indoles. The first biosynthetic hypothesis is advanced to explain the origin of the trikentrin—herbinole family and proposes a pyrrole—carboxylic thioester-initiated polyketide synthase mechanism.

3.1 Isolation and Structural Elucidation of *trans*-Herbindole A and Trikentramides E-I

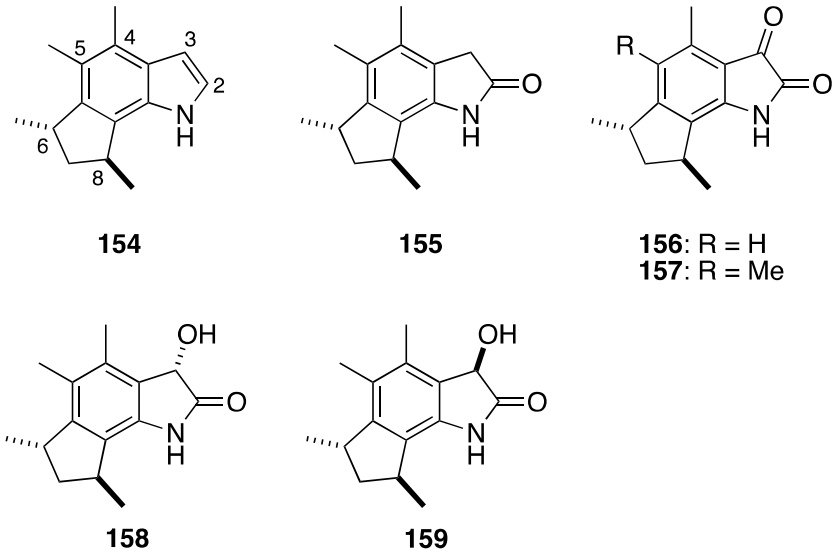

154 **155** **156**: R = H **157**: R = Me **158** **159**

Figure 3.1: The structures of *trans*-herbindole A (**154**) and trikentramides E-I (**155-159**).

The following chapter reports the structures of new trikentrin-like natural products, (+)-*trans*-herbindole A (**154**) and trikentramides E-I (**155-159**), from *T. flabelliforme* collected in Exmouth Gulf. The absolute configurations of **154-159** were assigned from chiroptical comparisons with trikentrins and herbindoles, and exploitation of van't Hoff's principle of optical superposition,[57] and chemical correlation to derive a new mnemonic for absolute stereostructure of this family of compounds. Surprisingly, the structures of **154-159** uniformly exhibit a *trans* configuration for the fused 1,3-dimethylcyclopentane ring, in contrast with the (–)-*cis*-herbindoles (**52**–**54**) obtained from a specimen of *T. flabelliforme* collected in the same vicinity,[35] and are enantiomorphic with the latter. A unifying hypothesis is proposed that rationalizes the biogenesis of trikentrins, herbindoles, trikentramides and two related sponge-derived indoles from West African *Trikentrion loeve*.

A MeOH extract of lyophilized *Trikentrion flabelliforme*, collected in Exmouth Gulf, Western Australia in 1993, was redissolved in MeOH-H_2O (9:1), and the solution was partitioned progressively against hexanes, CH_2Cl_2, and *n*-BuOH. The CH_2Cl_2-soluble "fraction B", enriched in indoles (TLC spots stained bright fuschia with vanillin-H_2SO_4), was separated by gel filtration chromatography (Sephadex LH-20) and further purified by reversed-phase HPLC (C_{18}) to obtain pure **154-159**.

The simplest of the new compounds, *trans*-herbindole A (**154**), $C_{15}H_{19}N$ (HRESITOFMS *m/z* 214.1592 $[M+H]^+$), when compared with *cis*-herbindole A (**52**), confirmed that **154** and **52** are constitutional isomers but diastereomeric in the 1,3-dimethylcyclopentane ring. Compound **154** displayed a relatively featureless ^1H NMR spectrum ($CDCl_3$) consisting of signals for a *trans*-1,3-dimethylcyclopentane ring: two methyl doublets (δ_H 1.21, 3H, d, J = 6.6 Hz and δ_H 1.49, 3H, d, J = 7.2 Hz), two methines (δ_H 3.46, 1H, quintet, J = 7.2 Hz and δ_H 3.71, 1H, qdd, J = 7.2, 7.5, 9.6

Hz) and H_2-7, a diastereotopic methylene group (H-7α δ_H 2.10, 1H, ddd, J = 1.2, 7.5, 12.1 Hz and H-7β, δ_H 1.97, 1H, ddd, J = 7.2, 9.6, 12.1 Hz). The relatively small separation in chemical shifts of the H_2-7 (Δε = 0.13 ppm) is characteristic of *pseudo*-enantiotopic methylene protons in *trans*-1,3-dimethylcyclopenta[*g*]indole ring (e.g. enantiotopic CH_2 in *trans*-1,3-dimethylindane, Figure 3.2a), as opposed to the larger signal separation ($\Delta\delta$ > 1.3 ppm) observed in the corresponding diastereotopic methylene of the *cis*-isomer.[36,40] A broad exchangeable singlet (δ 8.03, 1H, bs) was assigned to the indole NH. The remaining signals were pairs of aryl methyls (δ_H 2.35, 3H, s and δ_H 2.50, 3H, s), and pyrrole ring proton signals (δ_H 6.55, 1H, s and δ_H 7.14, 1H, s). Comparison of the HRMS, ^{1}H and ^{13}C NMR data of **154** to the published data of trikentramides A-D (**55**-**58**) and *cis*-herbindole A (**52**) further supported a 4,5-dimethylindole structure.

Trikentramide E, $C_{15}H_{19}NO$ (**155**), is an oxindole; the higher homolog of **58**. The ^{13}C chemical shifts of **155** at C-2 (δ_C 177.7 Cq) and C-3 (δ_C 35.7, CH_2) compare well with those of indolin-2-one,[58] but not indolin-3-one.[59] Again, the 1,3-dimethylindane ring is *trans*-substituted.

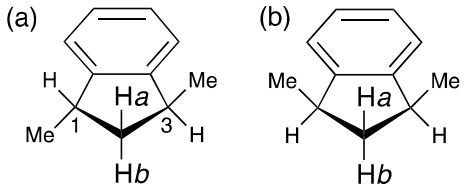

trans-***i*** *cis*-***ii***

Figure 3.2: Stereotopicity of the CH_2 group in *trans*- and *cis*-1,3-dimethylcyclopentanobenzene (1,3-dimethylindane). (a) enantiotopic (b) diastereotopic.

The formulas of trikentramides F (**156**, $C_{14}H_{15}NO_2$) and G (**157**, $C_{15}H_{17}NO_2$), with two oxygens, suggested homologous isatins, differing by substitution by Me at C-5 in **157**. The red-shifted long-wavelength band in the UV-vis spectrum of each compound [λ_{max} 326 (ε $\log_{10}$ 3.54)] was consistent with a substituted isatin (indolin-2,3-dione). The ^{13}C NMR spectra ($CDCl_3$) showed pairs of downfield signals attributed to the aryl ketone and lactam carbonyl groups, respectively

[e.g. **157**, δ183.2 (C-3), 160.2 (C-2)], matched those reported for the parent heterocycle, isatin (δ 184.5, 159.5, DMSO-d_6).[60] The ^{1}H NMR spectra of the two compounds appeared similar to those of **155** and supported the same *trans*-1,3-dimethylcyclopentano[*g*]indole ring. Full ^{1}H and ^{13}C NMR assignments (Tables 3.1 and 3.2) were secured through analysis of COSY, NOESY, HSQC and HMBC spectra (Figures 3.3 and 3.4).

The formula of isomeric dioxindoles (+)-trikentramides H (**158**) and (+)-I (**159**), $C_{15}H_{19}NO_2Na^+$ (HRESITOFMS *m/z* 268.1307 and *m/z* 268.1305, respectively $[M+Na]^+$) confirmed the two are formal reduction products of **157**. The ^{13}C chemical shifts of **159** at δ_C 178.9 (C-2) and 69.7 (C-3), which are consistent with those of 3-hydroxy-5-methylindolin-2-one,[61] verified the dioxindole arrangement of the keto and hydroxymethine groups at C-2 and C-3, respectively.

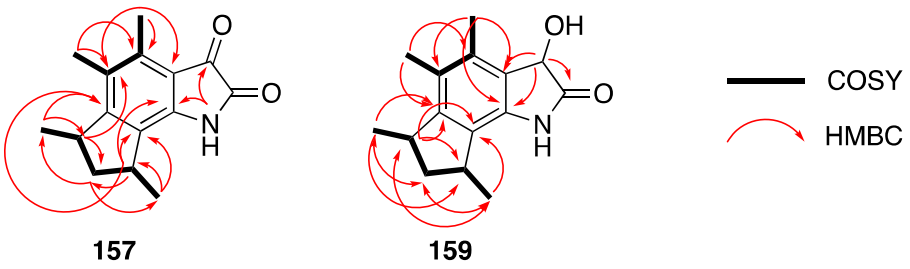

Figure 3.3: COSY and HMBC correlations of (–)-trikentramide G (**157**) and (+)-trikentramide I (**159**) (500 MHz, $CDCl_3$).

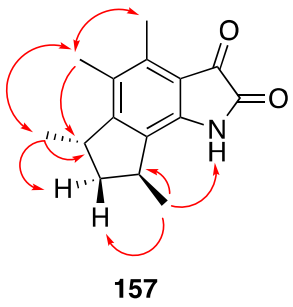

Figure 3.4: NOESY correlations of (–)-trikentramide G (**157**) (600 MHz, $CDCl_3$).

Table 3.1: ^{1}H NMR Data (δ,□mult)[a] for **154–159**.

#	**154**	**155**	**156**	**157**	**158**	**159**
NH	8.03, bs	7.97, bs	8.80, bs	8.96, bs	7.99, bs	8.21, bs
2	7.14, t, (2.4)					
3	6.55, dd (2.4, 3.0)	3.40, s			4.98, s	4.99, s
4						
5			6.68, s			
6	3.46, quin[b] (7.2)	3.31, quin[b] (7.2)	3.27, m[c]	3.29, quin[b] (7.2, 0.9)	3.27, quin[b] (7.2)	3.30, m[c]
7α	2.10, ddd, (1.2, 7.5, 12.1)	2.01, ddd, (1.2, 7.8, 12.3)	2.02, ddd, (3.0, 7.8, 12.6)	2.04, ddd, (1.5, 8.2, 12.6)	1.97, dd, (7.8, 12.6)	1.96, bdd[d], (7.8, 12.6)
7β	1.97, ddd, (7.2, 7.5, 9.6)	1.83, ddd, (7.2, 9.9, 12.3)	1.91, dt, (8.4, 12.6)	1.85, ddd, (7.2, 8.2, 9.6)	1.79, dt, (9.0, 12.6)	1.79, m
8	3.71, qdd, (7.2, 7.5, 9.6)	3.43, qdd, (6.6, 7.8, 9.9)	3.31, m[c]	3.44, qdd, (7.2, 8.2, 9.6)	3.37, m	3.40, m[c]
4-Me	2.50, s	2.18, s	2.55, s	2.49, s	2.28, s	2.28, s
5-Me	2.35, s	2.14, s		2.14, s	2.15, s	2.15, s
6-Me	1.21, d, (6.6)	1.13, d, (6.6)	1.26, d, (7.2)	1.14, d, (7.2)	1.12, d, (7.2)	1.07, d, (7.2)
8-Me	1.49, d, (7.2)	1.32, d, (6.6)	1.23, d, (6.6)	1.36, d, (7.2)	1.27, d, (6.0)	1.25, d, (6.6)

[a]600 MHz, $CDCl_3$. [b]quin = quintet. [c]overlap. [d]bdd = broad doublet of doublets.

Table 3.2: ^{13}C NMR Data (δ,□mult)[a] for **154–159** ($CDCl_3$, 125 MHz).

#	**154**	**155**	**156**	**157**	**158**	**159**
2	122.9, CH	177.7, C	160.3, C	160.2, C	178.5, C	178.9, C
3	101.6, CH	35.7, CH_2	[b]	183.2, C	69.7, CH	69.7, CH
3a	126.3, C	123.2, C	115.2, C	115.7, C	124.1, C	124.1, C
4	128.1, C	135.2, C	140.9, C	139.9, C	134.6, C	134.4, C
5	123.1, C	125.9, C	121.0, C	127.0, C	127.1, C	127.3, C
5a	125.7, C	148.7, C	161.4, C	160.6, C	150.9, C	150.8, C
6	38.4, CH	37.9, CH	38.5, CH	38.8, CH	37.9, CH	38.0, CH
7	43.9, CH_2	43.8, CH_2	43.0, CH_2	43.2, CH_2	43.8, CH_2	43.7, CH_2
8	36.5, CH	35.4, CH	34.6, CH	35.2, CH	35.6, CH	35.5, CH
8a	143.0, C	125.3, C	128.9, C	128.4, C	125.7, C	126.0, C
8b	130.8, C	131.5, C	144.5, C	142.8, C	134.3, C	134.1, C
4-Me	15.7, CH_3	16.1, CH_3	18.5, CH_3	14.5, CH_3	15.4, CH_3	15.4, CH_3
5-Me	15.2, CH_3	16.1, CH_3		13.4, CH_3	14.9, CH_3	14.9, CH_3
6-Me	20.4, CH_3	19.7, CH_3	19.3, CH_3	19.5, CH_3	19.8, CH_3	19.6, CH_3
8-Me	20.7, CH_3	20.1, CH_3	19.8, CH_3	19.6, CH_3	20.0, CH_3	19.9, CH_3

[a]Multiplicities determined from edited HSQC., or comparisons with **55-58**. [b]Signal not observed.

3.2 Absolute Assignment of *trans*-Herbindole A and Trikentramides F-I

Absolute configurations of **154–159** were assigned from analysis of the CD and $[\alpha]_D$ data, and comparisons with published chiroptical data of known compounds and DFT calculations of ECD. The simplest assignment, by comparisons of $[\alpha]_D$s (Table 3.3), is that of (+)-*trans*-

herbindole A (**154**, $[\alpha]_D$ +29.0) which follows from its structural similarity to (+)-*trans*-trikentrin A (**48**, $[\alpha]_D$ +23.3) and the relative invariance of $[\alpha]_D$ in trikentrins and herbindoles A and B, whether substituted at C-4 or C-5 by H, Me or Et (Table 3.3); therefore, both compounds bear the same (6*S*,8*S*) configuration (see below for more discussion). This is not necessarily true of **49**–**51**, and **54**; the conjugated *E*-butenyl chain, which constitutes a substituted styrenyl chromophore, adds complexity to the $[\alpha]_D$ of these indoles and abrogates simple chiroptical comparisons.

The specific rotations of oxidized indoline analogues, trikentramides A-I, do not follow a simple pattern; the magnitude and sign vary with substitution and electronic properties in a complex manner. For example, the two isatins **156** and **157** differ only in a single Me group at C-5, but show $[\alpha]_D$s ~0 and –43.4, respectively. These are confoundingly different from **154** and **155** (+29 and +19.0, respectively). Moreover, the $[\alpha]_D$ of highly dextrorotatory **159** (+232) appears to be largely influenced by the stereocenter at C-3. Consequently, in order to make the stereoassignments of **156** and **157**, we first chose to assign **158** and **159** by ECD and chemically correlate them to other family members.

Assignment of absolute configuration of trikentramides H (**158**) and I (**159**), which are epimeric dioxindoles, rested upon interpretation of their corresponding ECD spectra (Figure 3.5). The ECD spectra of oxidized indoles **155**-**157** exhibited relatively weak Cotton effects (CEs), not unlike Natsume's observations of indoles **47**-**49**.[38] In contrast, the ECDs of **158** [λ 243 ($\Delta\varepsilon$ –7.4), 221 (+8.6)] and **159** [λ 243 ($\Delta\varepsilon$ +5.0), 224 (–5.6)] are virtual mirror images dominated by relatively strong biphasic CEs that reveal a predominant influence of the C-3 stereocenter.

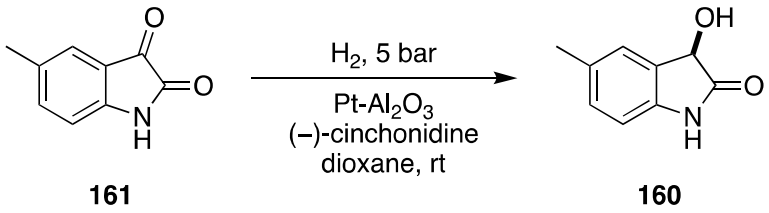

Scheme 3.1: Partial asymmetric hydrogenation of 5-methylisatin (**161**). See Ref.

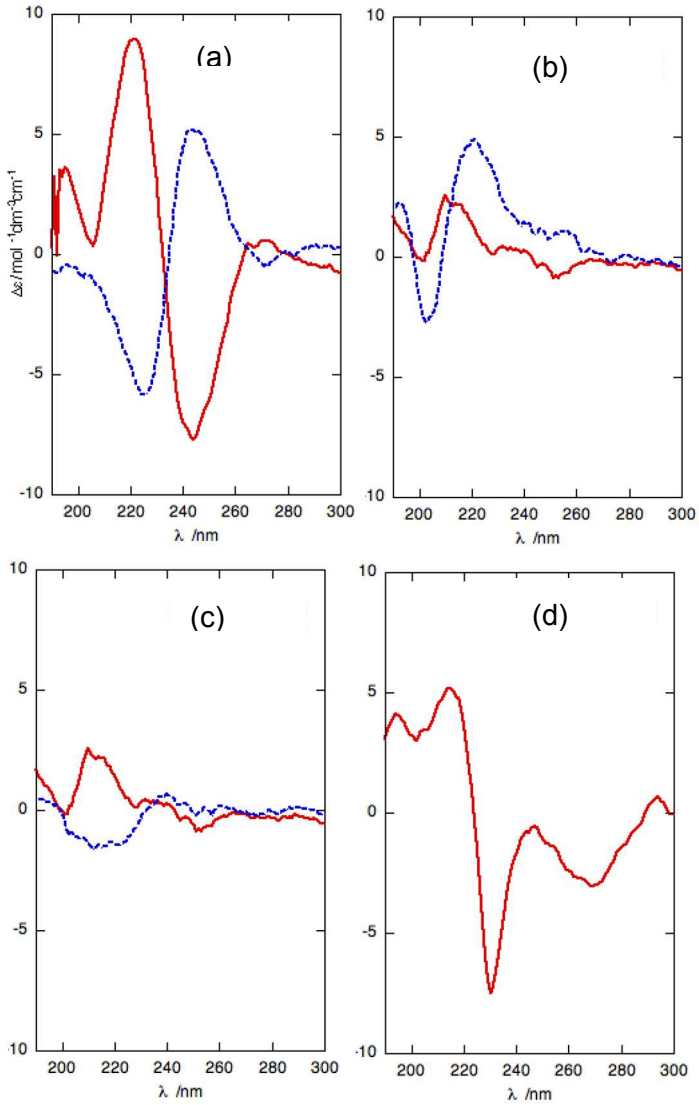

Figure 3.5: ECD spectra (CH_3CN, 23 ˚C) of (a) trikentramides H [(+)-**158**] and I [(+)-**159**], dash). (b) trikentramides F (**156**) and G [(–)-**157**, dash]. (c) trikentramides F (**156**) and E [(+)-**155**, dash]. (d) *trans*-herbindole A [(+)-**154**].

Asymmetric reductions of isatins to 3-hydroxoxindoles have been reported that provide comparison compounds for chiroptical assignments of **158** and **159**.[62,62,63] For example, isatin undergoes enzyme-catalyzed reduction in the presence of a carbonyl reductase derived from *Candida parapsilosis* to give (+)-(*R*)-dioxindole in 21% ee.[63] (*R*)-5-Methyldioxindole (**160**, 38.5% ee), prepared by Sonderegger and coworkers using partial asymmetric hydrogenation of **161** (H_2, Pt supported on Al_2O_3-(–)-cinchonidine, Scheme 3.1), exhibited an ECD spectrum dominated by a negative Cotton effect (CE) (λ 237 nm, –41, arbitrary units of ellipticity) and a second CE of opposite sign at longer wavelength (λ 264, +12.5).[61] The authors calculated the ECD spectrum of **160** using time dependent DFT (b3pw91 and 6-31G(d, p) basis set[64]) and assigned the latter the (R)-**160** configuration. We repeated the reduction of **161** under non-asymmetric conditions (EtOH, $NaBH_4$) and resolved the enantiomers of the product, (±)-**160**, by chiral phase HPLC (Phenomenex Lux 5U, Amylose 2) into (*S*)-**160** and (*R*)-**160** which, as expected, exhibit mirror image ECD spectra (see Supporting Information). The near identity of the ECD spectra of (*R*)-**160** and (+)-**159**, and the expected weaker dichroic contributions from the 1,3-dimethylcyclopentane in other trikentramides (Figure 3.5b,c), leads to the conclusion that the configuration of the natural products are (3*S*,6*S*,8*S*)-**158** and (3*R*,6*S*,8*S*)-**159**.

Reduction of **157** (Scheme 3.2, $NaBH_4$, EtOH, rt) gave the C-3 epimeric dioxindoles **158** and **159**, identical with the natural products by HPLC retention times, ^{1}H NMR, $[\alpha]_D$ and ECD. In addition, a minor product, from over-reduction of intermediate **158**/**159** at the benzylic carbon, was recovered and shown to match (+)-trikentramide E (**155)** by HPLC retention time, ^{1}H NMR and ECD. Finally, oxidation of the indole (+)-**154** under the selective conditions recently reported by Wang and coworkers (I_2, *t*-BuOOH, DMSO, 80 ˚C, Scheme 3.2),[65] gave a product identical with natural (–)-trikentramide G [(–)-**157**] by MS, ^{1}H NMR, ECD and HPLC retention time. Thus,

(+)-*trans*-herbindole A (**154**) is chemically correlated to (+)-**155**, (–)-**157**, (+)-**158** and (+)-**159** demonstrating that the dimethylcyclopentane ring is stereochemically uniform among these five natural products. Although we have no independent correlation of (+)-trikentramide E (**155**), it seems highly probable the configuration is the same as to its congeneric family members.[66]

The observed ECD spectra of **151** and **159** are the molar sum contributions of *independent* asymmetric perturbations to the benzenoid chromophore by the 1,3-dimethylcyclopentano group and the benzylic secondary OH group within their respective "first spheres of asymmetry". The latter is a formal corollary of van't Hoff's principle of optical superposition,[57] which has been applied both to configurational assignments through deconvolution of both molar rotation [*M*] and ECD ($\Delta\varepsilon$),[67] in combination with DFT calculations (e.g. CADPAC calculated $[\alpha]_D$ of (–)-1,3,5,7-tetramethyl-1,3-dihydroindol-2-one[37c]).

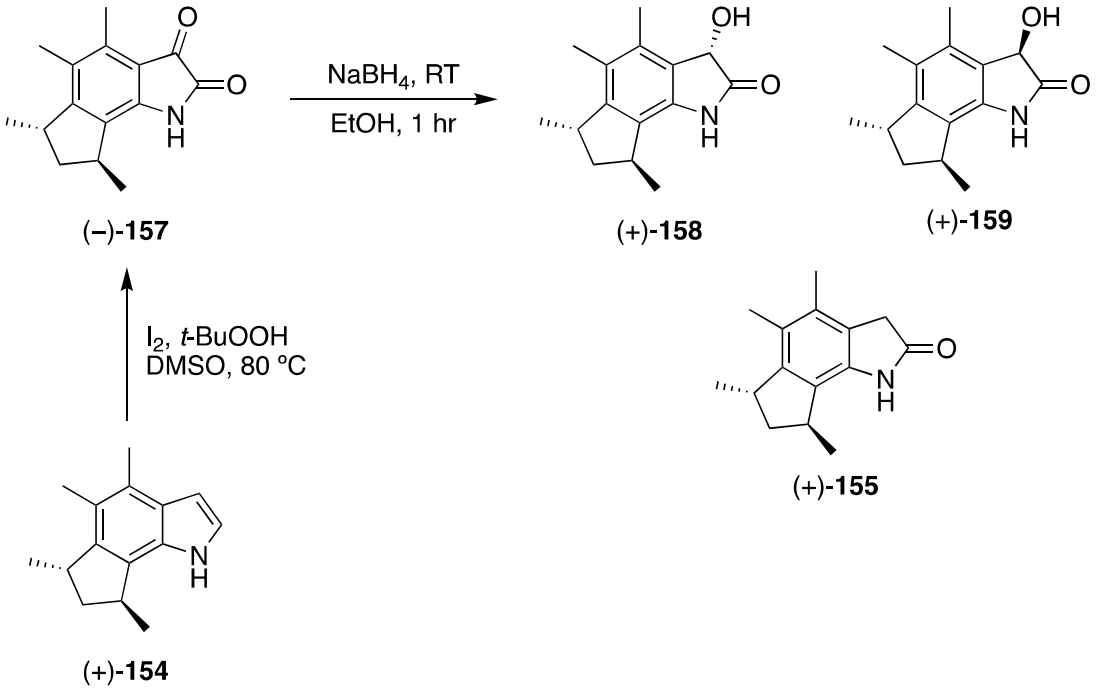

Scheme 3.2: Chemical interconversions of (+)-**154** with (+)-**155**, (–)-**157**, (+)-**158** and (+)-**159**.

Table 3.3: $[\alpha]_D$ for Natural and Synthetic Trikentrins, Herbindoles and Trikentramides.

Config.	Cmpd.	Source[a]	$[\alpha]_D$[b]	Ref.
	(+)-**47**	N	+48[c]	35
	(+)-**47**	S	+49	68
ent-	(–)-**47**	S	–68.6	37a,b
	(+)-**48**	N	+23.3[d]	35
	(+)-**48**	S	+24	37c
	(+)-**48**	S	+24	44b
ent-	(–)-**48**	S	–26.8	37a,b
	(+)-**49**	S	+102	37c
	(+)-**49**	S	+100.2	39
	(+)-**49**	S	+101	68
	(–)-**50**	N	–13[e]	35
ent-	(+)-**50**	S	+24	37c
	(?)-**51**	S	~0	37c
	(–)-**52**	N	–62	38
ent-	(+)-**52**	S	+56.9	38
ent-	(+)-**53**	S	+51.2	37a
ent-	(+)-**54**	S	+19.9	38
	(+)-**55**	N	+40.7	40
	(+)-**57**	N	+42.2	40
	(+)-**58**	N	+50.0	40
	(+)-**154**	N	+29.0	*f*
	(+)-**155**	N	+19.0	*f*
	(?)-**156**	N	~0	*f*
	(–)-**157**	N	–43.4	*f*
	(+)-**158**	N	+22.6	*f*
	(+)-**159**	N	+231.5	*f*

[a]N = natural; S = synthetic. [b]All measurements were made on solutions in $CHCl_3$ and, aside from the noted exceptions, within the concentration range *c*. ~0.027 – 0.50 g/100 cm^3. [c]*c* = 2.47. [d]*c* = 1.0. [e]*c* = 1.97. [f]This work.

The largest contribution to both the $[\alpha]_D$ and CD in *trans*- and *cis*-fused trikentrin-type indoles appears to be the C-8 stereocenter. For example, both (+)-*ent*-*cis*-**52** and (+)-*trans*-**154** have the same C-8 configuration and are dextrorotatory, although the magnitude of $[\alpha]_D$ of the former is almost twice that of the latter (Table 3.3). The presence of a C-5 Me group has little effect on $[\alpha]_D$; *trans*-(+)-**48** and (+)-**154** have almost the same specific rotation ($[\alpha]_D$ = +23.3 and +29.0, respectively). A brief conformational analysis of *cis* and *trans* herbindoles was carried out (MMFF94 and DFT) to derive their lowest energy conformations and frontier molecular orbitals.

The conformation of the cyclopentano[*g*]indole ring in **154** (Figure 3.6) is distorted from an idealized C_2 conformation by torsional strain and steric repulsion between the N-H bond and the methyl group, and between the Me groups at C-5 and C-6. For example, the C-5–C-5a–C-6–C-6(Me) dihedral angle is θ = 52.1˚, but the C-8b–C-8a–C-8–C-8(Me) dihedral angle is considerably larger, ψ = 72.3˚, however, the "unstrained" *trans*-1,3-dimethylindane ***i*** – Figure 3.1 – which freely inverts between the two C_2 degenerate conformers – displays θ = 40.1˚; ψ = 76.1˚. In contrast, the cyclopentane ring of (+)-*cis*-herbindole A (*ent*-**52**) has an almost symmetric envelope conformation (θ = –53.2˚, ψ = 48.3˚).

The major difference in frontier molecular orbitals of the delocalized π-system in 1,3-cyclopenta[*g*]indoles is the distortion of the LUMO by nonbonded interactions, particularly by the C-8 methyl group, which influences the rotational strength, and therefore ECD and $[\alpha]_D$, by altering molecular orbital symmetry properties. The influence of the C-8 stereocenter upon chiroptical properties is extrapolated into a simple stereochemical mnemonic (Figure 3.7): for trikentrin—herbindole-like indoles, the absolute configuration at C-8 determines the sign of $[\alpha]_D$, whether the 1,3-dimethylcyclopentane ring is *cis*- or *trans*-fused. The exceptions are butenyl-substituted compounds where contributions from the additional rotational strength of the styrenyl chromophore perturbs this simple rule. As the presence of C-4 or C-5 alkyl substituents (e. g. Me, Et) appear not to significantly change the relationship between sign of specific rotation and absolute configuration, we predict that hydrogenation of butenyl to an *n*-butyl group, prior to measuring the $[\alpha]_D$, will restore the relationship; the products should conform to the mnemonic and allow stereoassignment.

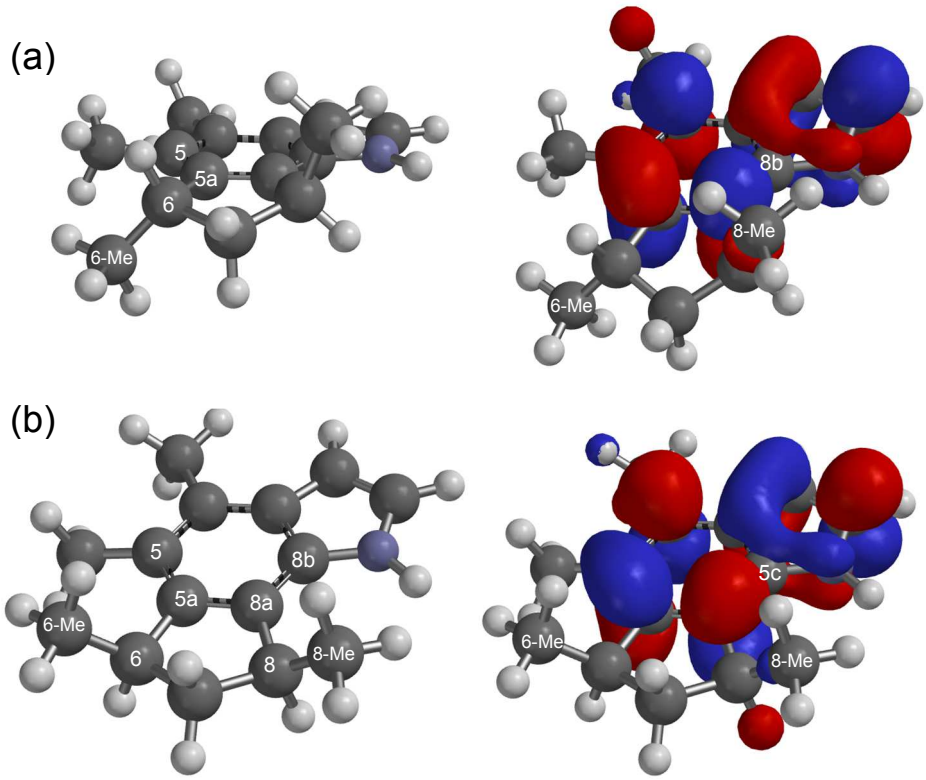

Figure 3.6. Energy minimized geometries (MMFF) and DFT calculated (ωB97X-D 6-31G*) LUMO of (a) (+)-*trans*-herbindole A (**154**) and (b) (+)-*cis*-herbindole A (*ent*-**52**).

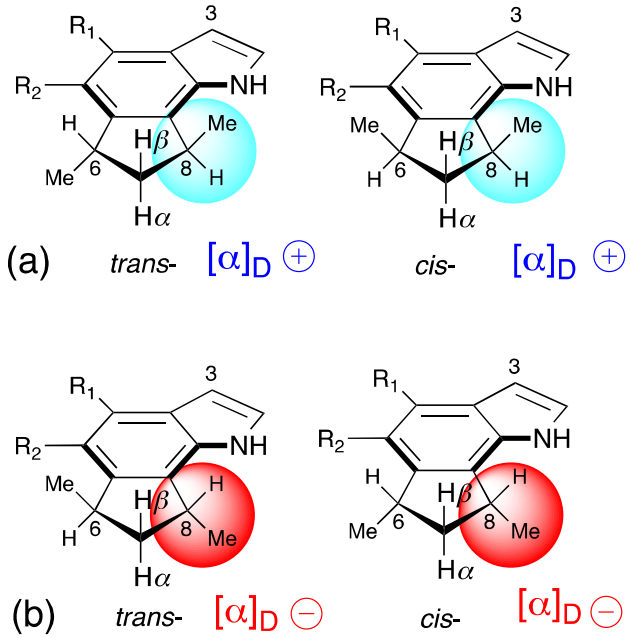

Figure 3.7. Chiroptical mnemonic for assignment of absolute stereostructures of trikentrins and herbindoles (a) *trans*- and *cis*-8*S* (b) *trans*- and *cis*-8*R* (R_1, R_2 = H, alkyl, but ≠ 1-alkenyl).

The biosynthesis of most natural product indoles follows familiar routes. Free indole is oxidatively liberated from Trp by the action of a tryptophanase (L-Trp indole lyase). Certain bacteria are known to harbor the enzyme and, in combination with oxidases, could give rise to polyhalogenated indoles in *Rhodophycae*. In considering possible biosynthetic pathways that generate **47**–**58** and **154-159**, degradation of Trp seems unlikely; not only does C-3 of the indole ring lack a carbon substituent, but the introduction of the fused carbocyclic ring at C-5a,b and additional carbon substituents at C-4 and C-5 necessitates unwieldy complexity in this putative biogenesis. Consequently, alternative pathways must be considered. Alignment of the structures of two C-2 substituted indenyl-pyrrole metabolites, trikentramine (**59**)[41a] and trikendiol (**60**)[41b] (Figure 3.8), both isolated from West African *Trikentrion loeve*, with *cis*-trikentrin A (**47**) suggest a hypothesis: the trikentrin-herbindole family are of polyketide origin. Proline is oxidatively modified to the hypothetical pyrrole-2-carboxylic thioester as a starter unit for ketide extensions by malonate (acetate) or methylmalonate (priopionate). In this scheme, the origin of the benzenoid ring differs slightly between two pathways, *a* and *b*. Because the C-C bond formation aligns carbons formally derived from the C=O group of the ketide extender units, it is unlikely that cyclization proceeds by aldol/Claissen condensations familiar from the biosynthesis of aromatic Type II polyketides. The indane ring of trikentramine (pathway *a*) is most likely assembled after partial reductions and polyene electrocyclization reactions, possibly involving oxidative single electron transfer (SET)[69], followed by aromatization to the benzenoid ring. For trikentrin-like secondary metabolites, (pathway *b*), similar reactions proceed, but for the fused indole ring we invoke a Friedel—Craft-type intramolecular alkylation at C-3 (pyrrole numbering) of the electron-rich pyrrole ring for construction of the C-3b–C-4 bond. Indeed, Natsume exploited a similar reaction for the indole ring closing steps of **48**, **50**, and **51**.[37]

The hypothesis succinctly accounts for the location of substituents at C-4 and C-5, namely H, Me, Et or butenyl, through chain extensions or termination of the polyketide chain by homologated malonate units. Subsequently, a manifold of oxidative reactions of the product indoles would generate **60** or conversely, the oxindole, isatin, and dihydroisatin scaffolds found in trikentramides A-D (**55-58**) and E-I (**154-159**).

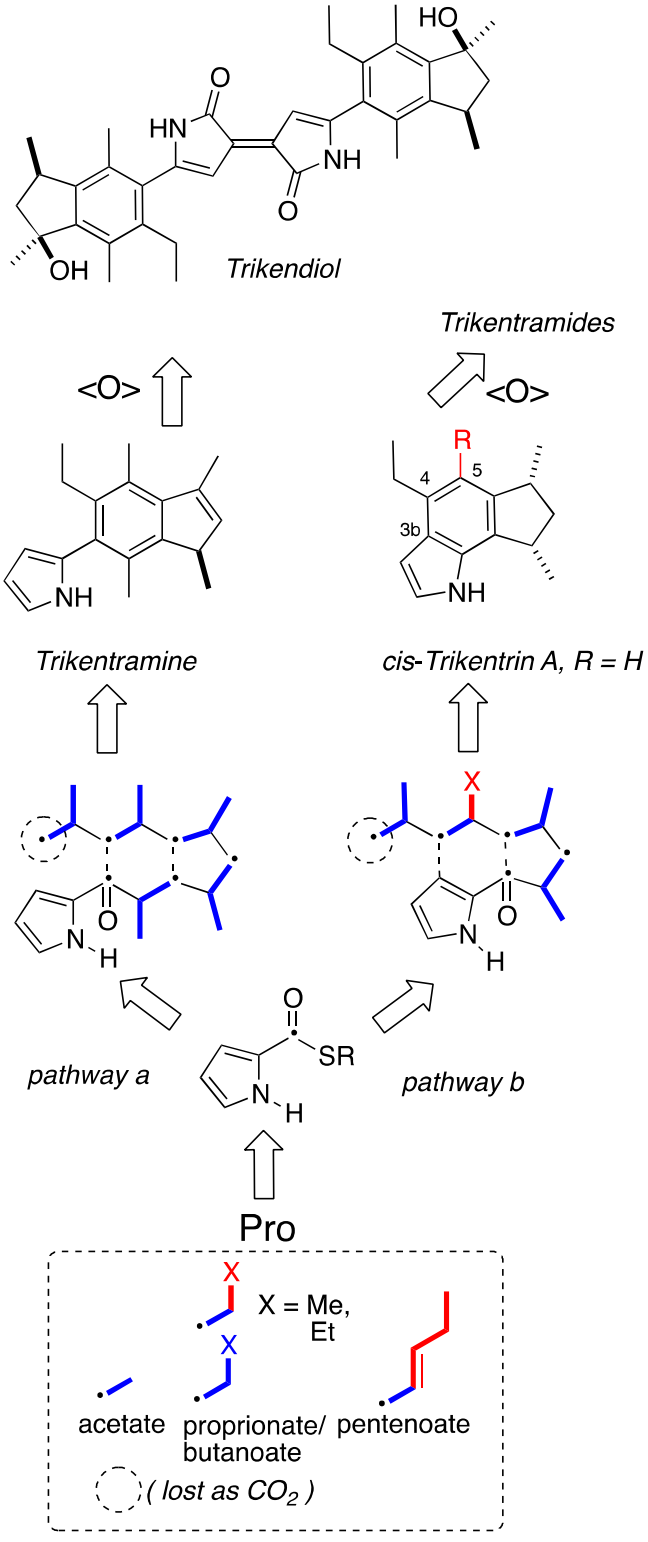

Figure 3.8: Hypothesis for the biogenesis of trikentrin-like natural products, including trikentramine (**59**), trikentramides A-I, and trikendiol (**60**).

In conclusion, six new cyclopenta[*g*]indole natural products – *trans*-herbindole A (**154**) and trikentramides E-I (**155**–**159**) – were isolated from the sponge *Trikentrion flabelliforme* and their absolute stereostructures solved by integrated analysis of MS, NMR and ECD studies, in combination with calculated DFT, and chemical correlation. A simple mnemonic emerged from analysis of the chiroptical data that allows easy identification of absolute configuration of indoles and dioxindoles within the series.

Chapter 3, in total, appears in "Six Trikentrin-like Cyclopentanoindoles from *Trikentrion flabelliforme*. Absolute Structural Assignment by NMR and ECD." The manuscript is published in the Journal of Organic Chemistry, 2018, *83*, 1278-1286 by Salib, Mariam N.; Molinski, Tadeusz F. The thesis author was the primary investigator and author of this paper.

EXPERIMENTAL

Biological Material. *Didemnum molle* (01-10-039) was collected in 2001 from a shallow reef near Ant Atoll, Pohnpei, Federated States of Micronesia (6˚ 53.963' N, 158˚ 20.525' E), using snorkel, at a depth of approximately –2 m. Voucher samples are archived in the Department of Chemistry and Biochemistry.

Extraction and Isolation. The *D. molle* tunicate was lyophilized (dry wt. 35.5 g) and extracted twice by homogenization with CH_2Cl_2/MeOH (1:1, 2 x 400 mL) and the filtered extracts were combined and concentrated under reduced pressure to yield the crude extract which was dissolved in MeOH-H_2O (9:1) and separated starting with progressive solvent partitioning as follows. The aqueous MeOH solution (400 mL) layer was repeatedly extracted with hexane (2 x 400 mL) to provide the hexane-soluble 'A' layer (0.6493 g). Water was added to the MeOH-H_2O layer (6:4 final ratio of MeOH-H_2O) and the mixture twice partitioned against CH_2Cl_2 (2 x 400 mL). The combined lower layers were concentrated to deliver the CH_2Cl_2-MeOH soluble 'B-layer' (1.50 g).

The B-layer was separated by flash chromatography (SiO_2, step gradient of MeOH in CH_2Cl_2), and the fraction eluted with 1:9 MeOH-CH_2Cl_2 (0.2163 g) was further partitioned by size-exclusion chromatography (Sephadex LH-20, MeOH) into nine fractions according to TLC (UV-activity, *p*-anisaldehyde staining). The third fraction (151.8 mg) containing **146** and **147** was separated by preparative reversed-phase HPLC (Phenomenex, Kinetex C_{18} column, 150 x 21.2 mm, linear gradient, initial conditions 90:10 H_2O-0.1% TFA-CH_3CN for three minutes to CH_3CN over 18 minutes for a total of 30 minutes, flow rate = 11 $mL \cdot min^{-1}$) to yield 22 fractions which included the known compounds *N*,*N*-diphenylurea and mollurea.[16c] The eighth fraction (6.2 mg) was purified by reversed-phase analytical HPLC (Luna Phenyl Hexyl column, 250 x 4.60 mm, step gradients, initial conditions 90:10 H_2O-0.1% TFA-CH_3CN for 3 minutes, 50: 50 for 15 min,

30:70 for 15 min to 100% CH_3CN for the last 5 min; flow rate = 0.700 mL·min^{-1}) to antatollamide A (**146**, 2.2 mg, t_R = 24.80 min) and antatollamide B (**147**, 0.1 mg, t_R = 23.32 min).

Antatollamide A (146): colorless solid; $[\alpha]^{23.5}_D$ –97 ± 1.6 (*c* 0.22, CH_3CN); UV (CH_3CN) λ□220 nm (ε□log$_{10}$ 4.19). ECD (CH_3CN, *c* 8.39 x 10^{-5} M, 23 ˚C) λ□196 nm (Δε +18.7), 204 (–28.4), 221 (–24); FTIR (ATR, ZnSe plate) ν 3484, 3300, 2965, 2877, 1653, 1520, 1456, 1318, 1205, 1139, 1027, 840, 802, 723 cm^{-1}; HRMS (ESI-TOF) *m/z*: Calcd for $C_{66}H_{94}N_{12}O_{12}S_2Na$ 1333.6454; Found 1333.6433. $[M/2+H+Na]^+$ Calcd for $C_{33}H_{48}N_6O_6SNa$ 679.3248; Found 679.3250; ^{1}H NMR and ^{13}C NMR. See Table 2.1.

Antatollamide B (147): colorless solid; $[\alpha]^{23.5}_D$ –22 ± 3 (*c* 0.080, CH_3CN); UV (CH_3CN) λ□219 nm (ε□log$_{10}$ 4.09). ECD (CH_3CN, *c* = 3.05 x 10^{-5} M, 23 ˚C) λ□196 nm (Δε +13.8), 204 (–5.5), 215 (+7.7); FTIR (ATR, ZnSe plate) ν 3445, 2968, 1678, 1633, 1523, 1440, 1331, 1204, 1138, 1028, 839, 802, 723 cm^{-1}; HRMS (ESI-TOF) *m/z*: $[M+Na]^+$ Calcd for 1333.6454; Found 1333.6448. $[M/2+H+Na]^+$ Calcd for $C_{33}H_{48}N_6O_6SNa$ 679.3248; Found 679.3248; ^{1}H NMR and ^{13}C NMR. See Table 2.1.

Desulfurization of Antatollamide A (146) – Desthio-antatollamide A (152). A suspension of Raney Ni (Raney® 2800 approx. 50 μL, 50% w/v H2O) was added to a solution of **146** (0.5 mg, 0.4 μmol) in MeOH (1.5 mL). The solution was purged with N_2 (5 min), then stirred at 65 ºC for 3 h while monitoring the disappearance of **146** (LC-MS). The mixture was cooled to room temperature, and passed onto an equilibrated SPE cartridge (C18) and eluted with MeOH to deliver desthioantatollamide A (**152**, 0.4 mg, 84%) as colorless solid that was used for acid hydrolysis (see below). An analytical sample of **152** was obtained by purification of an aliquot of crude compound (100 μg) by HPLC, using the same conditions for purification of **146** and **147**, and quantitated by QSCS (40 μg).[70] Colorless solid; ^{1}H NMR (600 MHz, DMSO-d_6) δ (ppm) 8.24

(d, J = 7.2 Hz, 1H), 8.22 (d, J = 8.4 Hz, 1H), 7.55 (d, J = 7.2 Hz, 1H), 7.25 (m, 2H), 7.19 (m, 1H), 7.13 (m, 2H), 4.50 (m, 2H), 4.42 (t, J = 7.2 Hz, 1H), 4.37 (t, J = 8.4 Hz, 1H), 4.20 (m, 2H), 3.81 (m, 1H), 3.79 (t, J = 6.3 Hz, 1H), 3.53 (q, J = 8.4 Hz, 1H), 3.20 (m, 1H), 3.10 (dd, J = 13.8, 6.0 Hz, 1H), 2.96 (dd, J = 13.2, 9.6 Hz, 1H), 2.89 (t, J = 9.6 Hz, 1H), 2.25 (m, 1H), 2.10 (m, 1H), 2.03 (m, 1H), 1.96 (m, 1H), 1.81 (m, 3H, 1.62 (m, 1H), 1.56 (m, 1H), 1.46 (m, 1H), 1.24 (m 2x 1H), 1.03 (d, J = 6.6 Hz, 3H), 0.93 (d, J = 7.2 Hz, 3H), 0.88 (d, J = 7.2 Hz, 3H), 0.86 (m, 6H).; HRMS (ESI-TOF) *m/z*: $[M+Na]^+$ Calcd for $C_{33}H_{48}N_6O_6Na^+$ 647.3528; Found 647.3528.

Acid Hydrolysis of Desthio-antatollamide A (152). Compound **152** (0.4 mg, 0.640 μmol) was dissolved in 6 M HCl (500 μL) and heated at 110 ºC with stirring for 12 h. The solution was cooled to 23 °C and extracted with EtOAc (3 X 500 μL). The combined organic layers were dried under a stream of N_2 and derivatized with (5-fluoro-2,4-dinitrophenyl)-N_α-L-tryptophanamide (FDTA, **151**) to yield the DTA-amino acid derivatives for LCMS analysis.

Synthesis of 2-((5-fluoro-2,4-dinitrophenyl)-*N*α-tryptophanamide (FDTA, 151). Thionyl chloride (3.6 mL, 49.7 mmol) was slowly added to a suspension of L-tryptophan (1.00 g, 4.90 mmol) in anhydrous MeOH (50 mL) at 0 °C. The solution was heated at reflux for 20 h, cooled, and the solvent removed under reduced pressure. The crude residue was dissolved in EtOAc, and the solution washed with saturated Na_2CO_3 followed by brine. The organic layer was dried over anhydrous Na_2SO_4, filtered and concentrated to yield methyl ester **149** (1.41 g, 81 %) as a pale yellow solid, identical by ^{1}H NMR and ESI-MS with literature values.[71] Concentrated aqueous ammonia (15 mL, 0.222 mol) was added dropwise to a solution of **149** (1.41 g, 6.47 mmol) in anhydrous MeOH (2 mL) at 0 °C, then the mixture warmed to room temperature with stirring until no **149** remained (TLC, ninhydrin). Removal of the solvent gave the primary amide **150** as an off-white solid (quantitative), identical by ^{1}H NMR and ESI-MS with literature values.[72]

Compound **151** was prepared according to a variation of the original protocol reported by Marfey.[29] Anhydrous $MgSO_4$ (1.25 g) was added to a stirred solution of **150** dissolved in NaOH (0.5 mL, 0.5 mmol) and acetone (10 mL). The solution was filtered, 1,5-difluoro-2,4-dinitrobenzene (0.10 g, 0.51 mmol) was added and the solution stirred for 0.5 h at room temperature. Standard workup gave **151** (0.122 g, 63 %); recrystallization from aqueous acetone delivered pure **151** as bright orange rosettes, m.p. 220 – 222 °C °C; $[\alpha]_D$ –230 (*c* 1.0, acetone); UV (MeOH) λ max 220 nm (ε log10 4.57), 252 (4.04), 266 (4.07), 339 (4.12); FTIR (ATR, ZnSe plate) ν 3416, 3330, 3196, 3114, 2925, 2253, 1682, 1630, 1579, 1542, 1520, 1457, 1421, 1367, 1329, 1287, 1126, 1099, 1050, 922, 834, 742, 707 cm^{-1}. ^1H NMR (600 MHz, DMSO-d_6, J_{HF} = ^1H-^{19}F coupling): δ 10.93 (bs, 1H), 8.94 (d, J = 7.8 Hz, 1H), 8.79 (d, J_{HF} = 8.4 Hz, 1H), 7.85 (bs, 1H), 7.57 (d, J = 7.8 Hz, 1H), 7.53 (bs, 1H), 7.30 (d, J = 8.4 Hz, 1H), 7.18 (s, 1H), 7.04 (t, J = 7.5 Hz, 1H), 6.94 (t, J = 7.5 Hz, 1H), 6.69 (d, J_{HF} = 14.4 Hz, 1H), 4.67 (m, 1H), 3.38 (dd, J = 14.4, 4.8 Hz, 1H), 3.27 (dd, J = 14.4, 7.2 Hz, 1H); ^{13}C NMR (125 MHz, DMSO-d_6, J_{CF} = ^{13}C-^{19}F coupling): δ 171.5 Cq, 158.7, Cq (J_{CF} = 265 Hz), 148.3 Cq (J_{CF} = 14.0 Hz), 136.2 Cq, 127.3 CH, 127.2 Cq, 127.1 Cq (br), 125.0 Cq (J_{CF} = 9.5 Hz), 124.6 CH, 121.2 CH, 118.6 CH, 118.4 CH, 111.4 CH, 108.4 Cq, 102.1 CH (J_{CF} = 27.4 Hz), 56.8 CH, 28.4 CH_2; HRMS (ESI-TOF) *m/z*: $[M+Na]^+$ Calcd for $C_{17}H_{14}N_5O_5FNa^+$ 410.0871; Found 410.0878.

Absolute Configuration of the Amino Acids of Desthio-antatollamide A (152) and Antatollamide A (146). The acid hydrolysate obtained from **152** (see above) was treated with FDTA (**151**, 2 mg, 5 μmol) in acetone (200 μL) and 1M $NaHCO_3$ (50 μL, 50 μmol), and the mixture heated at 85 ºC, with stirring, for 30 minutes. After cooling, the mixture was neutralized with 1M HCl (50 μL, 50 μmol) and concentrated under a stream of N_2. The residue was dissolved in H_2O (100 μL) and centrifuged to remove insoluble material before analysis by LCMS (Hypersil

Gold, C18 column, 50 x 2.1 mm, 1.9 μm, linear gradient, initial conditions 85:15 H_2O-0.1% HCOOH-CH_3CN to 55:45 over 25 minutes, flow rate = 0.50 mL·min^{-1}). The retention times (*t*R, min) for the standard amino acids DTA-amino acid derivatives were as follows: L-Ala (13.00), D-Ala (15.52), L-Pro (13.51), D-Pro (15.21), L-Val (16.24), D-Val (19.76), L-Ile and L-*allo*-Ile (co-elution, 18.30), D-Ile and D-*allo*-Ile (co-elution, 21.98), L-Phe (18.72), and D-Phe (21.53). LCMS analysis of DTA derivatives obtained from **152** showed the presence of L-Pro (13.57), D-Ala (15.47), L-Ile or L-*allo*-Ile (18.26), L-Phe (18.77), and L-Val (16.22). By correlation, **146** has the same absolute configuration.

As L-Ile and L-*allo*-Ile DTA derivatives co-eluted under the above conditions, they were resolved under a different combination of solid phase, solvent gradient and buffer (Agilent Zorbax SB-Aq column, 4.6 x 250 mm, 5 μm, step gradient, initial conditions 30–40% CH_3CN-20 mM NH_4OAc-0.1% TFA, 40 min; 40–50% CH_3CN-20 mM NH_4OAc-0.1% TFA, 5 min. Flow rate = 0.70 mL·min–1). The retention times for the standard amino acid DTA derivatives were as follows: L-Ile (t_R = 34.41 min), and L-*allo*-Ile (t_R = 33.38 min). The HPLC analysis of the DTA derivatives obtained from **152**, co-injected with L-Ile and L-*allo*-Ile, established the presence of L-Ile.

Cultured CLL Cytotoxicity Assay. Primary chronic lymphocytic leukemia (CLL) cells were seeded in RPMI 1640 with 10% of FBS (Fetal Bovine Serum) in 96-well plates (106 cells/well/100 μL) and treated with compounds at determined concentrations (0-10^4 nM). Cells were harvested after 48 h, washed and stained with PI (Propidium Iodide) and DioC6 (30 min, 37 ºC). After the incubation time, the cells were washed and run in a flow cytometer (FACS Calibur) with detection of fluorescence in channels 1 (DioC6) and 3 (PI). Cells that were positive by DioC6 were considered alive while cells that were positive by PI were considered dead.

Chromatography. LC-APCI-MS and LC-ESI-MS spectra were obtained using a Hypersil Gold C_{18} column, 50 x 2.1 mm, 1.9 μm, and 0.500 mL min^{-1} flow rate. Elution was completed with a linear gradient of 15–45% CH_3CN/H_2O-0.1% HCOOH for 25 minutes, followed by 100% CH_3CN for 2 minutes and re-equilibration with 15% CH_3CN / H_2O-0.1% HCOOH for 3 minutes before the next measurement. Analytical HPLC measurements were completed using a Luna C_{18} column, 250 x 4.60 mm, 5 μm, and 0.700 mL flow rate with UV detection (λ = 335 nm). Elution was completed with a step gradient of 15–65% CH_3CN/H_2O-0.1% TFA or CH_3CN/H_2O-0.1 M NH_4OAc-0.1% TFA for 40 minutes followed by a 5 minutes wash with 100% CH_3CN and re-equilibration, respectively.

Derivatization of the L- and D-amino acids. To a vial equipped with a stirrer was added DL-amino acid (10 mM, 250 μL, 2.5 μmol) in H_2O, FDTA (**151**, 140 μL, 1% in acetone) or FDAA (140 μL, 3.6 μmol, 1% in acetone), aqueous $NaHCO_3$ (1 M, 20 μL, 20 μmol) and acetone (200 μL) to improve solubility. The reactions were stirred at 85 °C for 30 minutes, cooled to room temperature and neutralized with HCl (1 M, 20 μL, 20 μmol). For LC-MS analysis, 20 μL aliquots of the derivatized amino acids were dissolved in 80 μL of MeOH, and 10 μL aliquots of each mixture were injected per run under described conditions. For HPLC analysis, 10 μL aliquots of undiluted samples were injected for each mixture. L-amino acids were prepared and analyzed in a similar manner.

Animal Material. The sponge *Trikentrion flabelliforme* (93-07-076) was collected in Exmouth Gulf (800 m south of Bundegi Beach), Western Australia, in 1993 at a depth of –9 m using scuba. The sponge was an orange, pliable, ear-shaped specimen with a smooth surface that, with pressure, emitted a red exudate. Spicule analysis revealed the presence of styles confirming

the sponge identity as *Trikentrion flabelliforme.* A voucher sample of the sponge is archived at UC San Diego.

Extraction of Sponge and Isolation of (+)-*trans*-Herbindole A (154) and Trikentramides E-I (155–159). Lyophilized *Trikentrion flabelliforme* (63.88 g dry wt) was extracted with CH_2Cl_2-MeOH (2 x 400 mL, 12 h), and the combined organic extracts were concentrated and dissolved in H_2O-MeOH (1:9, 400 mL) prior to repeated extraction with hexane (400 mL x 2). Concentration of the hexane-soluble layer gave Fraction A (1.4604 g). The aqueous-MeOH layer was adjusted to 2:3 H_2O-MeOH followed by extraction with CH_2Cl_2 (500 mL x 2) to yield Fraction B (0.6845 g). The aqueous layer was concentrated and extracted with *n*-BuOH (400 mL x 2) to yield the C layer (0.8460 g). The remaining aqueous layer was dried to yield Fraction D (1.7995 g). Fraction B, the TLC of which stained bright fuschia with vanillin-H_2SO_4, was separated further by size exclusion chromatography (Sephadex LH-20, elution with MeOH) to give 10 fractions, which were pooled according to TLC (10% MeOH-CH_2Cl_2), UV-activity and staining with vanillin-H_2SO_4 in EtOH. Fractions 4 (0.0698 g) and 6 (0.0357 g) were further purified by reversed-phase HPLC (Phenomenex, Kinetex C_{18} column, 150 x 21.2 mm, linear gradient, initial conditions 75:25 H_2O-0.1% TFA-CH_3CN for three minutes, 30:70 for 17 minutes to 100% CH_3CN for the last 6 minutes, flow rate = 12 mL·min^{-1}) to give *trans*-herbindole A (**154**, 4.7 mg, t_R = 25.26 min), trikentramides F (**156**, 2.4 mg, t_R = 18.21 min), G (**157**, 5.5 mg, t_R = 19.62 min), H (**158**, 1.6 mg, t_R = 15.12 mim) and I (**159**, 2.8 mg, t_R = 15.42 min). Pure trikentramide E (**155**, 1.8 mg, t_R = 21.32 min) was obtained after purification with slightly different reversed-phase HPLC conditions (Phenomenex, Kinetex C_{18} column, 150 x 21.2 mm, linear gradient, initial conditions 75:25 H_2O-0.1% TFA-CH_3CN for three minutes, 30:70 for 21 minutes to 100% CH_3CN for the last 2 minutes, flow rate = 12 mL·min^{-1}).

(+)-trans-*Herbindole A* (***154***)*:* Gray oil; UV (CH_3CN) λ_{max} 221 nm (ε $\log_{10}$ 4.53), 271 (3.86); $[\alpha]_D$ +29 (*c* 0.24, $CHCl_3$); ECD (CH_3CN) λ 214 (Δε +5.3), 230 –7.3), 269 (–3.0), 294 (+0.66; FTIR (ATR, ZnSe plate) ν 3439, 3431, 3421, 2953, 2924, 2866, 1481, 1451, 1403, 1393, 1375, 1133, 1132, 1109 and 727 cm^{-1}; ^1H NMR and ^{13}C NMR ($CDCl_3$), Tables 3.1 and 3.2; HRESITOFMS *m/z* 214.1592 $[M+H]^+$ (calcd for $C_{15}H_{20}N^+$ 214.1590).

(+)-Trikentramide E (***155***)*:* pale orange solid; UV (CH_3CN) λ_{max} 204 nm (ε $\log_{10}$ 4.10), 213 (4.08), 253 (3.63); $[\alpha]_D$ +19 (*c* 0.18, $CHCl_3$); ECD (CH_3CN) λ 215 (Δε –1.45); FTIR (ATR, ZnSe plate) ν 3206, 2948, 2871, 1670, 1626, 1456, 1449, 1307, 1295, 1256, 1206, 1143, 1137 and 711 cm^{-1}; ^1H NMR and ^{13}C NMR ($CDCl_3$), Tables 3.1 and 3.2; HRESITOFMS *m/z* 230.1534 $[M+H]^+$ (calcd for $C_{15}H_{20}NO^+$ 230.1539).

Trikentramide F (***156***)*:* Dark yellow solid; UV (CH_3CN) λ_{max} 199 nm (ε $\log_{10}$ 4.23), 218 (4.03), 245 (3.98), 326 (3.54); $[\alpha]_D$ ~0 (*c* 0.12, $CHCl_3$); ECD (CH_3CN) λ 210 (Δε +2.4), 214 (2.2), 252 (–0.7); FTIR (ATR, ZnSe plate) ν 3177, 2960, 2932, 2928, 2925, 2874, 1737, 1726, 1638, 1594, 1484, 1451, 1390, 1377, 1351, 1277, 1263, 1250 and 1178 cm^{-1}; ^1H NMR and ^{13}C NMR ($CDCl_3$), Tables 3.1 and 3.2; HRESITOFMS *m/z* 230.1173 $[M+H]^+$ (calcd for $C_{14}H_{16}NO_2^+$ 230.1176).

(–)-Trikentramide G (***157***)*:* Orange solid; UV (CH_3CN) λ_{max} 199 nm (ε $\log_{10}$ 4.36), 218 (4.14), 249 (4.14), 328 (3.70); $[\alpha]_D$ –43 (*c* 0.55, $CHCl_3$); ECD (CH_3CN) λ 192 (Δε –2.2), 203 (–2.6), 221 (+4.9), 255 (+1.1); FTIR (ATR, ZnSe plate) ν 3267, 3239, 2946, 2872, 1738, 1725, 1626, 1592, 1450, 1382, 1344, 1299, 1273 and 1250 cm^{-1}; ^1H NMR and ^{13}C NMR ($CDCl_3$), Tables 3.1 and 3.2; HRESITOFMS *m/z* 244.1331 $[M+H]^+$ (calcd for $C_{15}H_{18}NO_2^+$ 244.1332).

*(+)-Trikentramide H (**158**):* Pale yellow solid; UV (CH_3CN) λ_{max} 269 nm (ε $\log_{10}$ 3.97), 221 (4.17); $[\alpha]_D$ +22.6 (*c* 0.053, $CHCl_3$); ECD (CH_3CN) λ 221 (Δε +8.6), 243 (–7.4), 272 (+0.6); FTIR (ATR, ZnSe plate) ν 3311, 2957, 2928, 1715, 1704, 1633, 1456, 1203, 1184, 1139, 1100, 769, 762, 752 and 727 cm^{-1}; ^1H NMR and ^{13}C NMR ($CDCl_3$), Tables 3.1 and 3.2; HRESITOFMS *m/z* 268.1309 $[M+Na]^+$ (calcd for $C_{15}H_{19}NO_2Na^+$ 268.1308).

*(+)-Trikentramide I (**159**):* Tan solid; UV (CH_3CN) λ_{max} 221 nm (ε $\log_{10}$ 3.96), 252 (3.39); $[\alpha]_D$ +232 (*c* 0.093, $CHCl_3$); ECD (CH_3CN) λ 224 (Δε –5.6), 243 (+5.0); FTIR (ATR, ZnSe plate) ν 3397, 3235, 2958, 2925, 2870, 2856, 1681, 1633, 1447, 1204, 1189, 1138, 1104, 834, 801, 770, 761, 722 and 701 cm^{-1}; ^1H NMR and ^{13}C NMR ($CDCl_3$), Tables 3.1 and 3.2; HRESITOFMS *m/z* 268.1305 $[M+Na]^+$ (calcd for $C_{15}H_{19}NO_2Na^+$ 268.1308).

Reduction of 5-Methylisatin – Dioxindoles (*S*)-160 and (*R*)-160. Reduction of 5-methylisatin (**161**) with $NaBH_4$ was carried out according to the protocol described by Hara and coworkers[73] to provide (±)-5-methylisatin [(±)-**160**] as a colorless solid (50%). UV-vis (CH_3CN) λ_{max} 209 nm (ε $\log_{10}$ 4.11), 248 (3.65), 296 (2.88). LRMS *m/z* 164.20 $[M+H]^+$. The ^1H and ^{13}C NMR spectra of the product matched the literature values for (*R*)-**160**.[Error! Bookmark not defined.]

A sample of (±)-**160** (~100 μg) was resolved by chiral reverse-phased HPLC (Lux 5U Amylose-2 column, 250 x 4.60 mm, isocratic conditions 2.5% *i*-PrOH-CH_3OH, flow rate = 1.0 mL min^{-1}) to give the enantiomeric dioxindoles (*R*)-**160** (t_R = 4.68 min) and (*S*)-**160** (t_R = 5.52 min). (*S*)-**160**: ECD (2.5% *i*-PrOH-CH_3OH) λ□210 (Δε +54), 240 (-24.5), 267 (+7.4). (*R*)-**160**: λ 210 (Δε -54), 240 (+24.9), 267 (-7.0), [lit.[Error! Bookmark not defined.] 237 (–41), 264 (+12.5), arbitrary units of ellipticity].

Reduction of Trikentramide G (157). $NaBH_4$ (1.40 mg, 35.8 μmol) was added in portions to a solution of **157** (3.0 mg, 8.2 μmol) in anhydrous EtOH (1.0 mL) at room temperature. After 1

hr., the solution was diluted with H_2O (2.0 mL), acidified to pH ~ 6 with HCl (1N), and extracted with CH_2Cl_2 (2 x 2 mL). The organic layer was dried and the residue (5.2 mg) was purified by reversed-phase HPLC (Phenomenex, Kinetex C_{18} column, 150 x 21.2 mm, linear gradient, initial conditions 75:25 H_2O-0.1% TFA-CH_3CN for three minutes, 30:70 for 17 minutes to 100% CH_3CN for the last 6 minutes, flow rate = 12 mL min^{-1}) to give **155** (0.5 mg, t_R = 19.30 min), **158** (1.0 mg, t_R = 15.13 min) and **159** (1.2 mg, t_R = 15.43 min) with ECD and HPLC retention times identical with the natural products.

Oxidation of *trans*-Herbindole A [(+)-154] to Trikentramide G [(–)-157]. *trans*-Herbindole A was oxidized according to the procedure of Wang and coworkers.[65] A solution of (+)-**154** (1.0 mg, 4.7 μmol) in DMSO (0.05 mL) was treated with a solution of iodine (1.4 mg, 5.6 μmol) and *t*-butyl hydroperoxide (70% w/v solution in H_2O, 3.0 μL, 23.4 μmol) in DMSO (0.50 mL) and heated to 80 ˚C with stirring for 18 h. The solution was cooled, quenched with $Na_2S_2O_3$ (5%, 2.0 mL), extracted with EtOAc (3 x 1.0 mL) and purified by reversed-phase HPLC (Luna C_{18} column, 250 x 4.60 mm, linear gradient, initial conditions 65:35 H_2O-0.1% TFA-CH_3CN for three minutes, 30:70 for 20 minutes to 100% CH_3CN for the last 6 minutes, flow rate = 1.0 mL min^{-1}) to give a product, as a yellow glass (0.5 mg), that (–)-**157** was identical to natural trikentramide G [(–)-**157**] by MS, ^1H NMR, ECD and HPLC retention time.

REFERENCES

(1) (a) D'Ambrosio, M.; Guerriero, A.; Debitus, C.; Ribes, O.; Pusset, J.; Leroy, S.; Pietra, F. *J. Chem. Soc., Chem. Commun.* **1993**, 1305-1306. (b) D'Ambrosio, M.; Guerriero, A.; Chiasera, G.; Pietra, F. *Helv. Chim. Acta* **1994**, *7*, 1895-1902. (c) D'Ambrosio, M.; Guerriero, A.; Ripamonti, M.; Debitus, C.; Waikedre, J.; Pietra, F. *Helv. Chim. Acta* **1996**, *79*, 727-735.

(2) (a) Pettit, G. R.; Ducki, S.; Herald, D. L.; Doubek, D. L.; Schmidt, J. M.; Chapuis, *J. Oncol. Res.* **2005**, *15*, 11-20. (b) Tilvi, S.; Moriou, C.; Martin, M.; Gallard, J.; Sorres, J.; Patel, K.; Petek, S.; Debitus, C.; Ermolenko, L.; Al-Mourabit, A. *J. Nat. Prod.* **2010**, *73*, 720-723.

(3) Hong, T. W.; Jímenez, D. R.; Molinski, T. F. *J. Nat. Prod.* **1998**, *61*, 158-161.

(4) Li, Z.; Shigeoka, D.; Caulfield, T. R.; Kawachi, T.; Qiu, Y.; Kamon, T.; Arai, M.; Tun, H. W.; Yoshimitsu, T. *Med. Chem. Commun.* **2013**, *4*, 1093-1098. (b) Mason, C. K.; McFarlane, S.; Johnston, P. G.; Crowe, P.; Erwin, P. J.; Domostoj, M. M.; Campbell, F. C.; Manaviazar, S.; Hale, K. J.; El- Tanani, M. *Mol. Cancer Ther*. **2008**, *7*, 548-558.

(5) (a) Ocio, E. M.; Mateos, M.-V.; Prosper, F.; Martin, J.; Rocafiguera, A. O.; Jarque, I.; Iglesias, R.; Motlloo, C.; Sole, M.; Rodriguez-Otero, P.; Martinez, S.; Fernandez-Garcia, E.; Michot, J.-M.; Soto-Matos, A.; Rodriguez Diaz-Pavon, J.; Ribrag, V.; San Miguel, J. *J. Clin. Oncol.* **2016**, *34*, Suppl; Abstract 8006. (b) Broggini, M.; Marchini, S. V.; Galliera, E.; Borsotti, P.; Taraboletti, G.; Erba, E.; Sironi, M.; Jimeno, J.; Faircloth, G. T.; Giavazzi, R.; Dincalci, M. *Leukemia* **2003**, *17*, 52-59.

(6) Kong, D. X.; Jiang, Y. Y.; Zhang, H. Y. *Drug Discov. Today* **2010**, *15*, 844-886.

(7) (a) Manivasagan, P.; Venkatesan, J.; Sivakumar, K.; Kim, S.-K. *Microbiol. Res.* **2014**, *169*, 262-278. (b) Gauvin-Bialecki A. et al. (2016) Bioactive Molecules of Marine Invertebrates from South-West Indian Ocean: Status and Perspectives. In: Ramasami P., Gupta Bhowon M., Jhaumeer Laulloo S., Li Kam Wah H. (eds) Crystallizing Ideas – The Role of Chemistry. Springer, Cham

(8) Montaser, R.; Luesch, H. *Future Med. Chem.* **2011**, *3*, 1475-1489.

(9) Sivonen, K.; Leikowski, N.; Fewer, D. P.; Jokela, J. *Appl. Microbiol. Biotechnol.* **2010**, *86*, 1213-1225.

(10) Donia, M. S.; Hathaway, B. J.; Sudek, S.; Haygood, M. G.; Rosovitz, M. J.; Ravel, J.; Schmidt, E. W. *Nat. Chem. Biol.* **2006**, *2*, 729-735.

(11) (a) Tianero, M. D.; Pierce, E.; Raghuraman, S.; Sardar, D.; McIntosh, J. A.; Heemstra, J. R.; Schonrock, Z.; Covington, B. C.; Maschek, J. A.; Cox, J. E.; Bachmann, B. O.; Olivera,

B. M.; Ruffner, D. E.; Schmidt, E. W. *Proc. Natl. Acad. Sci.* **2016**, *113*, 1772-1777. (b) Fischbach, M.A.; Clardy, J. *Nat. Chem. Biol.* **2007**, *3*, 353-355.

(12) Lin, Z.; Torres, J. P.; Tianero, M. D.; Kwan, J. C.; Schmidt, E. W. *Appl. Environ. Microbiol.* **2016**, *82*, 3450–3460.

(13) Rudi, A.; Aknin, M.; Gaydou, E. M.; Kashman, Y. *Tetrahedron* **1998**, *54*, 13203-13210.

(14) Rudi, A.; Chill, L.; Aknin, M.; Kashman, Y. *J. Nat. Prod.* **2003**, *66*, 575-577.

(15) Toske, S. G.; Fenical, E. *Tetrahedron Lett.* **1995**, *36*, 8355-8358.

(16) (a) Carroll, A. R.; Bowden, B. F.; Coll, J. C.; Hockless, D. C. R.; Skelton, B. W.; White, A. H. *Aust. J. Chem.* **1994**, *47*, 61-69; (b) Donia, M. S.; Wang, B.; Dunbar, D. C.; Desai, P. V.; Patny, A.; Avery, M.; Hamann, M. T. *J. Nat. Prod.* **2008**, *71*, 941-945; (c) Lu, Z.; Harper, M. K.; Pond, C. D.; Barrows, L. R.; Ireland, C. M.; Wagoner, R. M. V. *J. Nat. Prod.* **2012**, *75*, 1436-1440.

(17) Boden, C. D. J.; Norely, M.; Pattenden, G. *J. Chem. Soc. Perkin Trans. 1* **2000**, 883-888.

(18) (*a*) W. Konigsberg, R. H. Hill and L. C. Craig, *J. Org. Chem.*, 1961, **26**, 3867; (*b*) Y. Hirotsi, T. Shiba and T. Kaneko, *Bull. Chem. Soc. Jpn.*, 1970, **43**, 1870; (*c*) K. Yonetani, Y. Hirotsu and T. Shiba, *Bull. Chem. Soc. Jpn.*, 1975, **48**, 3302.

(19) Wesson, K. J.; Hamann, M. T. *J. Nat. Prod.* **1996**, *59*, 629-631.

(20) (a) Degnan, B. M.; Hawkins, C. J.; Lavin, M. F.; McCaffrey, E.J.; Parry, D. L.; Brenk, A. L. v.d.; Watters, D. J. *J. Med. Chem.* **1989**, *32*, 1349-1354; (b) Schmitz, F. J.; Ksebati, M. B.; Chang, J. S.; Wang, J. L.; Hossain, M. B.; Helm, D. v.d.; Engel, M. H.; Serban, A.; Silfer, J. A. *J. Org. Chem.* **1989**, *54*, 3463-3472; (c) Sesin, D. F.; Gaskell, S. J.; Ireland, C. M. *Bull. Soc. Chim. Belg.* **1986**, *95*, 853-867; (d) Morris, L. A.; Bosch, J. J. K. v.d.; Versluis, K.; Thompson, G. S.; Jaspers, M. *Tetrahedron* **2000**, *56*, 8345-8353.

(21) (a) Ireland, C. M.; Durso, A. R.; Newman, R. A.; Hacker, M. P. *J. Org. Chem.* **1982**, *479*, 1807-1811; (b) McDonald, L. A.; Ireland, C. M. *J. Nat. Prod.* **1992**, *55*, 376-379; (c) Rashid, M. A.; Gustafson, K. R.; Cardellina, J. H. II; Boyd, M. R. *J. Nat. Prod.* **1995**, *58*, 594-597; (d) Fu, X.; Do, T.; Schmitz, F. J.; Andrusevich, V.; Engel, M. H. *J. Nat. Prod.* **1998**, *61*, 1547-1551.

(22) (a) Ireland, C.; Scheuer, P. J. *J. Am. Chem. Soc.* **1980**, *102*, 5688-5691. (b) Williams, D. E.; Moore, R. E. *J. Nat. Prod.* **1989**, *52*, 732-739.

(23) Schmidt, E. W.; Nelson, J. T.; Rasko, D. A.; Sudek, S.; Eisen, J. A.; Haygood, M. G.; Ravel, J. *Proc. Natl. Acad. Sci.* **2005**, *102*, 7315-7320.

(24) (a) Pettit, G. R.; Herald, C. L.; Boyd, M. R.; Leet, J. E.; Dufresne, C.; Doubek, D. L.; Schmidt, J. M.; Cerny, R. L.; Hooper, J. N. A.; Rützler, K. C. *J. Med. Chem.* **1991**, *34*, 3339-3340; (b) Pettit, G. R.; Gao, F.; Cerny, R. L.; Doubek, D. L.; Tackett, L. P.; Schmidt, J. M.; Chapuis, J.-C. *J. Med. Chem.* **1994**, *37*, 1165-1168; (c) Pettit, G. R.; Gao, F.; Cerny, R. *Heterocycles* **1993**, *35*, 711-718; (d) Pettit, G. R.; Gao, F.; Schmidt, J. M.; Chapuis, J.; Cerny, R. L. *Bioorg. Med. Chem. Lett.* **1994**, *4*, 2935-2940.

(25) (a) Schmidt, G.; Grube, A.; Kock, M. *Eur. J. Org. Chem.* **2007***, 24*, 4103-4110. (b) Cychon, C.; Köck, M. *J. Nat. Prod.* **2010**, *73*, 738-742. (c) Wang, X.; Morinaka, B. I.; Molinski, T. F. *J. Nat. Prod.* **2014**, *77*, 625-630.

(26) (a) Kobayashi, J.; Tsuda, M.; Nakamura, T.; Mikami, Y.; Shigemori, H. *Tetrahedron* **1993**, *49*, 2391-2402. (b) Tsuda, M.; Sasaki, T.; Kobayashi, J. *Tetrahedron* **1994**, *50*, 4667-4680. (c) Napolitano, A.; Bruno, I.; Rovero, P.; Lucas, R.; Peris, M. P.; Gomez-Paloma, L.; Riccio, R. *Tetrahedron* **2001**, *57*, 6249-6255. (d) Teruya, T.; Sasaki, H.; Suenaga, K. *Tetrahedron Lett.* **2008**, *49*, 5297-5299.

(27) Müller, W. E. G.; Maidhof, A.; Zahn, R. K.; Conrad, J.; Rose, T.; Uhlenbruck, G. *Biol. Cell.* **1984**, *51*, 381-388.

(28) Hawkins, C. J.; Lavin, M. F.; Marshall, K. A.; Brenk, A. L. v.d.; Watters, D. J. *J. Med. Chem.* **1990**, *33*, 1634-1638.

(29) Marfey, P. *Carlsberg Res. Commun.* **1984**, *49*, 591-596.

(30) (a) Bhusan, R.; Brückner, H. *Amino Acids* **2004**, *27*, 231-247. (b) Fujii, K.; Ikai, Y.; Mayumi, T.; Oka, H.; Suzuki, M.; Harada, K. *Anal. Chem.* **1997**, *69*, 3346-3352.

(31) (a) Brüchner, H.; Keller-Hoehl, C. *Chromatographia* **1990**, *30*, 621-629. (b) Harada, K.; Fujii, K.; Mayumi, T.; Hibino, Y.; Suzuki, M. *Tetrahedron Lett.* **1995**, *36*, 1515-1518.

(32) (a) Głowacki, E. D.; Voss, G.; Leonat, L.; Irimia-Vladu, M.; Bauer, S.; Sariciftci, N. S. *Isr. J. Chem*. **2012**, *52*, 1-12. (b) Benkendorff, K.; McIver, C. M.; Abbott, C. A. *Evid.-Based Complement Altern. Med.* **2011**, 1-12. doi:10.1093/ecam/nep042 (c) Baker, J. T. *Endeavour* **1974**, *33*, 11-17.

(33) (a) Susse, P.; Krampe, C. *Naturwissenschaften* **1979**, *66*, 110-110. (b) Larsen, S.; Watjen, F. *Acta Chem. Scand.* **1980**, *A34*, 171-176.

(34) Woolner, V. H.; Jones, C. M.; Field, J. J.; Fadzilah, N. H.; Munkacsi, A. B.; Miller, J. H.; Keyzers, R. A.; Northcote, P. T. *J. Nat. Prod.* **2016**, *79*, 463-469. (b) Brennan, M. R.; Erickson, K. L *Tetrahedron Lett.* **1978**, *19*, 1637-1640.

(35) Capon, R. J.; Macleod, J. K.; Scammells, P. J. *Tetrahedron* **1986**, *42*, 6545-6550.

(36) Herb, R.; Carroll, A. R.; Yoshida, W. Y.; Scheuer, P. J.; Paul, V. J. *Tetrahedron* **1990**, *46*,

3089-3092.

(37) (a) Muratake, H.; Natsume, M. *Tetrahedron Lett.* **1989**, *30*, 5771-5772. (b) Muratake, H.; Watanabe, M.; Goto, K.; Natsume, M. *Tetrahedron* **1990,** *46*, 4179-4192. (c) Muratake, H.; Seino, T.; Natsume, M. *Tetrahedron Lett.* **1993**, *34*, 4815-4818.

(38) Muratake, H.; Mikawa, A.; Natsume, M. *Tetrahedron Lett.* **1992**, *33*, 4595-4598.

(39) Lee, M.; Ikeda, I.; Kawabe, T.; Mori, S.; Kanematsu, K. *J. Org. Chem.* **1996**, *61*, 3406-3416.

(40) Khokhar, S.; Feng, Y.; Campitelli, M. R.; Quinn, R. J.; Hooper, J. N. A.; Ekins, M. G.; Davis, R. A. *J. Nat. Prod.* **2013**, *76*, 2100-2105.

(41) Aknin, M.; Miralles, J.; Kornprobst, J.-M.; Faure, R.; Gaydou, E.-M.; Boury-Esnault, J.; Kato, Y.; Clardy, J. *Tetrahedron Lett.* **1990**, *31*, 2979-2982.

(42) Loukaci, A.; Guyot, M. *Tetrahedron Lett.* **1994**, *35*, 6869-6872.

(43) (a) Ensley, B.; Ratzkin, B.; Osslund, T.; Simon, M.; Wackett, L.; Gibson, D. *Science* **1983**, *222*, 167-169. (b) Gil-Turnes, M.; Hay, M.; Fenical, W. *Science* **1989**, *246*, 116-118.

(44) (a) Silva, L. F. Jr.; Craveiro, M. V.; Tebeka, I. R. M. *Tetrahedron* **2010**, *66*, 3875-3895. (b) Tebeka, I. R. M.; Longato, G. B.; Craveiro, M. V.; de Carvalho, J. E.; Ruiz, A. L. T. G.; Silva, L. F. *Chem. Eur. J.* **2012**, *18*, 16890-16901.

(45) Saito, N.; Ichimaru, T.; Sato, Y. *Org. Lett.* **2012**, *14*, 1914-1917.

(46) Shrestha, R.; Lee, G. J.; Lee, Y. R. *RSC Adv.* **2016**, *6*, 63782-63787.

(47) Tang, B.-X.; Song, R.-J.; Wu, C.-Y.; Liu, Y.; Zhou, M.-B.; Wei, W.-T.; Deng, G.-B.; Yin, D.-L.; Li, J.-H. *J. Am. Chem. Soc.* **2010**, *132*, 8900-8902.

(48) (a) Huang, P.-C.; Gandeepan, P.; Cheng, C.-H. *Chem. Commun.* **2013**, *49*, 8540-8542. (b) Ilangovan, A.; Satish, G. *Org. Lett.* **2013**, *15*, 5726-5729.

(49) Li, W.; Duan, Z.; Zhang, X.; Zhang, H.; Wang, M.; Jiang, R.; Hongyao, Z.; Liu, C.; Lei, A. *Angew. Chem. Int. Ed.* **2015**, *54*, 1893-1896.

(50) Senadi, G. C.; Hu, W.-P.; Boominathan, S. S. K.; Wang, J.-J. *Chem. Eur. J.* **2015**, *21*, 998-1003.

(51) Zi, Y.; Cai, Z.-J.; Wang, S.-Y.; Ji, S.-J. *Org. Lett.* **2014**, *16*, 3094-3097.

(52) Siemion, I. Z.; Wieland, T.; Pook, K.-H. *Angew. Chem. Int. Ed.* **1975**, *14*, 702-703.

(53) Dalisay, D. S.; Rogers, E. W.; Edison, A.; Molinski, T. F. *J. Nat. Prod*. **2009**, *72*, 732–738.

(54) Czekster, C. M.; Ge, Y.; Naismith, J. H. *Curr. Opin. Chem. Biol.* **2016**, *35*, 80-88.

(55) MacMillan, J. B.; Trousdale, E. K.; Molinski, T. F. *Org. Lett.* **2000**, *2*, 2721-2723.

(56) Vijayasarathy, S.; Prasad, P.; Fremlin, L. J.; Ratnayake, R.; Salim, A. A.; Khalil, Z.; Capon, R. J. *J. Nat. Prod.* **2016**, *79*, 421-427.

(57) van't Hoff, J. H. *Die Lagerung der Atome im Raume*, Vieweg, Braunschweig **1908**, ch. 8, pp. 95–97.

(58) Gassman, P. G.; Gilbert, D. P.; Luh, T.-Y. *J. Org. Chem.* **1977**, *42*, 1340-1344.

(59) Gaywood, A. P.; McNab, H. *Synthesis* **2010**, *8*, 1361-1364.

(60) Panasenko, A. A.; Caprosh, A. F.; Radul, O. M.; Rekhter, M. A. *Russ. Chem. Bull.* **1994**, *43*, 60-63.

(61) Sonderegger, O. J.; Bürgi, T.; Limbach, L. K.; Baiker, A. *J. Mol. Catal. A-Chem.* **2004**, *217*, 93-101.

(62) Birolli, W. G.; Ferrreira, I. M.; Jimenez, D. E. Q.; Silva, B. N. M.; Silva, B. V.; Pinto, A. C.; Porto, A. L. M. *J. Braz. Chem. Soc*. **2017**, *28*, 1023-1029.

(63) Hata, H.; Shimizu, S.; Hattori, S.; Yamada, H. *J. Org. Chem.* **1990**, *55*, 4377.

(64) Frisch, M. J.; Trucks, G. W.; Schlegel, H. B.; Scuseria, G. E.; Robb, M. A.; Cheeseman, J. R.; Zakrzewski, V. G.; Montgomery, J. A.; Stratmann, R. E.; Burant, J. C.; Dapprich, S.; Millam, J. M.; Daniels, A. D.; Kudin, K. N.; Strain, M. C.; Farkas, O.; Tomasi, J.; Barone, V.; Cossi, M.; Cammi, R.; Mennucci, B.; Pomelli, C.; Adamo, C.; Clifford, S.; Ochterski, J.; Petersson, G.A.; Ayala, P.Y.; Cui, Q.; Morokuma, K.; Malick, D. K.; Rabuck, A.D.; Raghavachari, K.; Foresman, J.B.; Cioslowski, J.; Ortiz, J. V.; Baboul, A. G.; Stefanov, B. B.; Liu, G.; Liashenko, A.; Piskorz, P.; Komaromi, I.; Gomperts, R.; Martin, R.L.; Fox, D. J.; Keith, T.; Al-Laham, M. A.; Peng, C. Y.; Nanayakkara, A.; Gonzalez, C.; Challacombe, M.; Gill, P. M. W.; Johnson, B.; Chen, W.; Wong, M. W.; Andres, J. L.; Gonzalez, C.; Head-Gordon, M.; Replogle, E. S.; Pople, J. A. *Gaussian98*, A.7 Ed., Gaussian Inc., Pittsburgh, PA, 1998.

(65) Zi, Y.; Cai, Z.-J.; Wang, S.-Y.; Ji, S.-J. *Org. Lett.* **2014**, *16*, 3094-3097.

(66) Another interpretation of the near-zero $[\alpha]_D$ of **156** is that the compound is racemic rather than coincidentally non-rotatory at the D emission line of Na˚, and that the other members are partially racemic. Given that the matching magnitudes of the ECD spectra of semi-synthetic and natural **158** and **159**, this possibility appears highly unlikely. It is may be more than coincidental, that 5-penten-1'-yl-substituted iso-*trans*-trikentrin B (**51**), which

like **156**, has a *trans*-dimethylcyclopentane ring and lacks substitution at C-5, also exhibits an $[\alpha]_D$ ~0. See ref. 37c.

(67) (a) Perry, T. L.; Dickerson, A.; Khan, A. A.; Kondru, R. K.; Beratan, D. N.; Wipf, P.; Kelly, M.; Hamann, M. T. *Tetrahedron* **2001**, *57*, 1483-1487. (b) Kondru, R. K.; Wipf, P.; Beratan, D. N. *J. Phys. Chem. A* **1999**, *103*, 6603-6611. (c) Kondru, R. K.; Chen, C. H. T.; Curran, D. P.; Beratan, D. N.; Wipf, P. *Tetrahedron: Asymmetry* **1999**, *10*, 4143-4150. (d) Kondru, R. K.; Wipf, P.; Beratan, D. N. *Science* **1998**, *282*, 2247-2250. (e) Kondru, R. K.; Lim, S.; Wipf, P.; Beratan, D. N. *Chirality* **1997**, *9*, 469-477. (b) Stout, E. P.; Molinski, T. F. *Eur. Chem. J.* **2012***,* 5131-5135. (f) Molinski, T. F.; Biegelmeyer, R.; Stout, E. P.; Wang, X.; Frota, M. L. C.; Henriques, A. T. *J. Nat. Prod.* **2013**, *76*, 374-381.

(68) Liu, W.; Lim, H. J.; RajanBabu, T. V. *J. Am. Chem. Soc.* **2012**, *134*, 5496-5499.

(69) (a) Stout, E. P.; Wang, Y.-G.; Romo, D.; Molinski, T. F. *Angew. Chem. Intl. Ed.* **2012**, *51*, 4877-4881. (b) Stout, E. P.; Morinaka, B. I.; Wang, Y.-G.; Romo, D.; Molinski, T. F. *J. Nat. Prod.* **2012**, *75*, 527-530.

(70) Dalisay, D. S.; Molinski, T. F.; *J. Nat. Prod.* **2009**, *72*, 739-744.

(71) Peng, S.; Winterfeldt, E. *Liebigs Ann. Chem.* **1990**, 313-318.

(72) Lan, J.-S.; Xie, S.-S.; Li, S.-Y.; Pan, L.-F.; Wang, X.-B.; Kong, L.-Y. *Bioorg. Med. Chem.* **2014**, *22*, 6089-6104.

(73) Usami, N.; Kitahara, K.; Ishikura, S.; Nagano, M.; Sakai, S.; Hara, A. *Eur. J. Biochem.* **2001**, *268*, 5755-5763.